

2012

Investigation of torrefaction process parameters and characterization of torrefied biomass

Dorde Medic
Iowa State University

Follow this and additional works at: <http://lib.dr.iastate.edu/etd>



Part of the [Bioresource and Agricultural Engineering Commons](#), and the [Oil, Gas, and Energy Commons](#)

Recommended Citation

Medic, Dorde, "Investigation of torrefaction process parameters and characterization of torrefied biomass" (2012). *Graduate Theses and Dissertations*. 12403.

<http://lib.dr.iastate.edu/etd/12403>

This Dissertation is brought to you for free and open access by the Graduate College at Iowa State University Digital Repository. It has been accepted for inclusion in Graduate Theses and Dissertations by an authorized administrator of Iowa State University Digital Repository. For more information, please contact digirep@iastate.edu.

Investigation of torrefaction process parameters and characterization of torrefied biomass

by

Dorde Medic

A dissertation submitted to the graduate faculty
in partial fulfillment of the requirements for the degree of
DOCTOR OF PHILOSOPHY

Co-majors: Agricultural Engineering; Biorenewable Resources and Technology

Program of Study Committee:
Matthew J. Darr, Major Professor
Robert C. Brown
D. Raj Raman
Tae Hyun Kim
Thomas J. Brumm

Iowa State University

Ames, Iowa

2012

Copyright © Dorde Medic, 2012. All rights reserved

Table of Contents

List of Tables	iv
List of Figures	v
Acknowledgements	vii
Abstract	viii
Chapter 1. General introduction.....	1
Problem identification.....	1
Research objectives.....	3
Dissertation organization	4
References.....	5
Chapter 2. Literature review	6
Lignocellulosic biomass.....	6
Lignocellulosic biomass composition.....	8
Thermochemical biomass conversion technologies.....	11
Torrefaction for biorenewables production	13
Overview of biomass torrefaction process.....	13
Torrefaction mechanism	14
Torrefaction kinetics	18
Torrefaction product distribution and composition	22
Torrefaction reactors.....	26
Economics.....	28
Properties and applications of torrefied biomass	30
References.....	35
Chapter 3. Effects of torrefaction process parameters on biomass feedstock upgrading	44
Abstract.....	44
Introduction.....	45
Methods.....	49
Samples	49
Torrefaction Reactor	49
Gas Analysis	50
Liquids Analysis	51
Proximate Analysis	51
Ultimate Analysis.....	52
High Heating Value Determination	52
Design of Experiments.....	52
Results and Discussion	53
Conclusions.....	68
Acknowledgements.....	69
References.....	69
Chapter 4. Effect of torrefaction on water vapor adsorption properties and resistance to microbial degradation of corn stover	72
Abstract.....	72

Introduction.....	73
Methods.....	76
Sample preparation	76
Water vapor adsorption experiments	77
Adsorption modeling	78
Microbial degradation experiment.....	81
Fiber analysis	81
Results and discussion	81
Experimental results.....	81
Fitting sorption models to experimental results.....	85
Microbial degradation results	92
Fiber analysis results.....	93
Conclusion	94
Acknowledgements.....	95
References.....	95
Chapter 5. Effect of particle size, different corn stover components and gas residence time on torrefaction of corn stover.....	99
Abstract.....	99
Introduction.....	100
Materials and Methods.....	103
Corn stover samples	103
Torrefaction experiments	105
Chemical analysis of raw and torrefied biomass	108
Statistical analysis.....	109
Results and Discussion	109
Conclusions.....	119
Acknowledgments.....	120
References.....	120
Chapter 6. General conclusions and future work.....	124
Future work.....	126
References.....	128

List of Tables

Table 1. Yields of different biomass types torrefied for 1h.....	24
Table 2. Box Behnken experimental design matrix generated by JMP.....	53
Table 3. Total mass balance for torrefaction experiments.....	55
Table 4. Summary statistics for the mass loss response surface model with three predictors: moisture, temperature and time	58
Table 5. ANOVA for the mass loss response surface model with three predictors: moisture, temperature and time.....	58
Table 6. List of all terms used to obtain mass loss and energy yield models and their respective <i>p</i> -values	59
Table 7. Ultimate analysis and computed energy density of torrefied samples.....	64
Table 8. Summary statistics for the energy yield response surface model with three predictors: moisture, temperature and time	67
Table 9. ANOVA for the for the energy yield response surface model with three predictors: moisture, temperature, and time	67
Table 10. ERH of saturated solutions at four temperature levels	77
Table 11. EMC of raw and torrefied corn stover	84
Table 12. Water vapor adsorption parameters for the raw and torrefied corn stover	86
Table 13. Fiber analysis of raw and torrefied corn stover	94
Table 14. Sample designation and basic properties	105
Table 15. Proximate analysis of raw corn stover biomass.....	112
Table 16. Elemental analysis and HHV of biomass samples.....	115

List of Figures

Figure 1. Stages in the torrefaction process	15
Figure 2. Weight loss of the main biomass constituents.....	16
Figure 3. Changes in polysaccharides and lignin during torrefaction	17
Figure 4. Typical mass and energy yields in torrefaction of wood at two conditions	22
Figure 5. Composition of the torrefaction reaction products	23
Figure 6. Power consumption and mill capacity during raw and torrefied biomass size reduction	31
Figure 7. Particle size distribution of coal, raw and torrefied willow & miscanthus	32
Figure 8. Van Krevelen diagram showing change in the biomass O/C and O/H ratio after torrefaction.....	33
Figure 9. Position of four thermocouples (T5, T6, T7 and T8) utilized for controlling the temperature inside the reactor.....	50
Figure 10. Temperature profiles for four thermocouples and average temperature profile (denoted by dashed line) used to determine process temperature and time.....	54
Figure 11. The effect of untreated biomass moisture content on mass loss of torrefied samples.....	56
Figure 12. Surface plot of the effect of temperature and moisture content of raw biomass on predicted mass loss	60
Figure 13. Composition of condensable volatiles released during torrefaction.....	60
Figure 14. Change in permanent gas composition with process parameters and raw biomass moisture content.....	61
Figure 15. Proximate analysis of torrefied and raw corn stover	63
Figure 16. Effect of process parameters and raw biomass moisture content on energy density of torrefied material.....	65
Figure 17. Effect of process parameters and initial moisture content of untreated biomass on energy yield.....	66
Figure 18. Surface plot of the effect of temperature and moisture content of raw biomass on predicted energy yield.....	68
Figure 19. Residual plots of the water vapor adsorption isotherms for raw and torrefied corn stover.....	87
Figure 20. Experimental and isotherms predicted by Modified Oswin model of raw corn stover.....	89
Figure 21. Experimental and isotherms predicted by Modified Oswin model of corn stover torrefied at 200 °C.....	90
Figure 22. Experimental and isotherms predicted by Modified Oswin model of corn stover torrefied at 250 °C.....	90
Figure 23. Experimental and isotherms predicted by Modified Oswin model of corn stover torrefied at 300 °C.....	91

Figure 24. Comparison of raw and torrefied corn stover isotherms at 10 and 40 °C	92
Figure 25. Dry matter loss due to microbial degradation at 0.97 ERH and 30 °C	92
Figure 26. Different corn stover components	104
Figure 27. Temperature programs used to conduct torrefaction experiments in the TGA ...	105
Figure 28. Bench scale reactor setup used in torrefaction experiments.....	107
Figure 29. Temperature time profile of the bench scale reactor	107
Figure 30. Average dry matter loss of torrefied ground stover and whole stalk samples.....	111
Figure 31. Average dry matter loss of torrefied stalk shell, stalk pith, and cob shell.....	111
Figure 32. Average energy yield of torrefied ground stover and whole stalk samples	118
Figure 33. Average energy yield of torrefied stalk shell, stalk pith, and cob shell samples.	119

Acknowledgements

I would like to express my sincere appreciation to my major professor Matthew Darr, for giving me the opportunity to study at Iowa State University under his mentorship, for optimism and understanding even during the stressful and tough times, and for great expertise on the topics that extend the scope of this work. Without his patient guidance, my learning and working experience at ISU would not be as complete as it is now.

I would also like to thank other members of my committee, Dr. Robert Brown, Dr. Tae Hyun Kim, Dr. Thomas Brumm and Dr. Raj Raman for their interest in my work and valuable advice.

I also appreciate the help and assistance of my friends and colleagues, especially Ajay Shah, Benjamin Potter, Jeffrey Zimmerman, Sarah Rahn, and the rest of my research group. This work would not be accomplished without the technical assistance from the Center for Sustainable and Environmental Technologies (CSET) and Biocentury Research Farm staff, especially Patrick Johnston and Andy Suby, who generously shared their resources and expertise. I also acknowledge financial support from ConocoPhillips Company.

I would like to express my gratitude to my parents and extended family in Serbia for their support and encouragement. Finally, I would like to thank my wife Jelena for her unconditional support, patience, and company during our ISU years, and our son Luka for making me smile. I wish to dedicate this work to all of them.

Abstract

This study sought to better understand the torrefaction process, and more specifically, how torrefaction affects the physical and chemical properties of corn stover biomass. The work done to accomplish this was divided into three sections that map to three research objectives. First, effect of torrefaction residence time, temperature and untreated biomass moisture content on chemical properties of torrefied corn stover was addressed. Second, effect of torrefaction process condition on physical characteristics of torrefied biomass, namely hydrophobicity was assessed. In addition, resistance to microbial degradation as a result of torrefaction and increased hydrophobicity was investigated. Third, influence of gas residence time and biomass particle size on chemical characteristics of torrefied corn stover was studied.

Corn stover biomass at three moisture contents (30, 45, and 50% wet basis) was torrefied at three different temperatures (200, 250, and 300 °C), and at three reaction times (10, 20, and 30 min). In each of the 17 treatments elemental and proximate compositions of the torrefied stover was determined, along with the composition of released gaseous and liquid products. Using these data, the mass and energy balance of each torrefaction was quantified. The energy balance accounted only for energy contained in the biomass. As torrefaction process temperature increased, an overall increase (2-19%) in the energy density of torrefied biomass and decrease (3-45% and 1-35% respectively) in mass and energy yield was observed. At 200 °C, mass and energy losses increased with an increase in the initial biomass moisture content. The difference in both mass and energy losses between biomass of 22% and 41% initial moisture content was about 10 percentage points at 200 °C. The liquid phase condensed from the stream of volatiles was composed primarily of water, followed by

acetic acid, methanol, hydroxyacetone, and furfural. The yield of condensables increased with torrefaction temperature. Permanent gas released in the process was mainly composed of carbon dioxide and carbon monoxide, with traces of hydrogen and methane present only at 300 °C.

The equilibrium moisture content (EMC) of raw corn stover, along with corn stover thermally pretreated at three temperatures, was measured using the static gravimetric method at equilibrium relative humidity (ERH) and temperature ranging from 10 to 98% and from 10 to 40 °C, respectively. Five isotherms were fitted to the experimental data to obtain the prediction equation which best describes the relationship between the ERH and the EMC of lignocellulosic biomass. Microbial degradation of the samples was tested at 97% ERH and 30 °C for period of 30 days. Fiber analyses were conducted on all samples. In general, torrefied biomass showed an EMC lower than that of raw biomass, which implied an increase in hydrophobicity. The modified Oswin model performed best in describing the correlation between ERH and EMC. Corn stover torrefied at 250 and 300 °C had negligible dry matter mass loss due to microbial degradation. Fiber analysis showed a significant decrease in hemicellulose content with the increase in pretreatment temperature, which might be the reason for the hydrophobic nature of torrefied biomass. This is probably due to loss of polar hydroxyl groups that serves as binding sites for water molecules.

The effects of particle size and gas residence time on the torrefaction of corn stover were investigated via torrefaction of different stover fractions: stalk shell, pith, and corn cob shell, and particle sizes, in a form of whole corn stalk and ground corn stover. Three levels of the purge gas residence times (1.2, 12 and 60 sec) were employed to assess the effects of volatiles and torrefied biomass interaction. Elemental analyses of all the samples were done,

and the obtained data was used to estimate the energy contents and energy yields of different torrefied biomass samples. Particle densities, elemental composition, and fiber composition of raw biomass fractions were also determined. The dry matter losses, higher heating values, and energy yields for different torrefied corn stover fractions were significantly different. This was probably due to the differences in particle densities, hemicellulose quantities, and the chemical and physical properties of the original biomass samples. Gas residence time did not have a significant effect on the aforementioned parameters.

Chapter 1. General introduction

Problem identification

Alternative energy sources have gained significant interest recently due to uncertainty of remaining oil resources and their positive effect on the environment, rural development, diversification of the energy supply and national security. Moreover, biomass is the only source of renewable carbon, an element essential for production of chemicals and materials. Nowadays, the majority of biorenewables production falls under biofuels production, with grain ethanol and bio-diesel being produced in significant quantities. According to the Environmental Protection Agency, grain ethanol and diesel production, totaling 45.5 billion liters, will account for about 77% of all biorenewable fuels produced in 2012 [1].

Nevertheless, public concern exists in regards to grain derived fuels production due to their competition with food production, land use change, and controversial effect on fossil fuel displacement. These are the main reasons why the US congress limits grain derived fuel production and mandates production of non-food derived bio-fuels, through the Energy Independence and Security Act of 2007 (EISA of 2007) [2] and RFS2. As per EISA of 2007, about 60% of 136 billion liters of biorenewables produced in 2022 need to be from non-food sources, such as lignocellulosic biomass.

It has been estimated by researchers in Oak Ridge National Laboratory [3] that there is potentially about 370 million dry tons per year of forest resources, and about 350 million dry tons per year of agricultural resources available. With high yield increase and use of perennials, the agricultural resource quantity could ramp up to 1000 million dry tons per year. Corn stover might be an important lignocellulosic feedstock for the production of

advanced bio-fuels, especially in the short term, due to its immediate availability and abundance. Estimated corn stover resources based in the US are about 75 million dry tons per year, with the potential for a 2.5 to 3 fold increase due to advances in technology [3].

Obviously, large scale biofuel production will demand significant quantities of biomass feedstock to be stored, transported, and processed in an economic and sustainable manner.

Although, the lignocellulosic biomass is available in large quantities it possesses characteristics that make its utilization complex and expensive. For example it has high moisture content, susceptibility to microbial degradation, low bulk density, low energy density, recalcitrance, high oxygen content, heterogeneity, and dispersed nature.

Torrefaction can be incorporated in a biorenewables production chain to significantly reduce the cost of biomass feedstock storage, transportation, and downstream processing, through the enhancement of biomass hydrophobicity, resistance to microbial degradation, energy density, homogeneity, brittleness, and chemical characteristics important for thermochemical downstream processing [4, 5]. Torrefaction is a thermochemical process carried out in a temperature range between 200 and 300 °C, under an inert atmosphere, and the heating rate below 50 °/min. There have been several studies on torrefaction of different woody biomasses, either as agricultural residues or herbaceous energy crops, including oak, willow, pine, birch, larch, wheat straw, miscanthus, and bagasse. The majority of studies investigated torrefaction of dry, ground material under relatively high purge gas flow rates [6-8]. Torrefaction of corn stover biomass has not been investigated yet, although it may be an important near term feedstock for biorenewables production. However, benefits gained through torrefaction of lignocellulosic biomass could be captured only if the process is positioned early in the supply chain, to utilize the feedstock without excessive pretreatment,

i.e. drying and size reduction, which are both energy intensive processes. Utilization of low purge gas flow rates might be important for reduction of capital and operating costs, and for minimizing dilution of volatiles that may be combusted to reduce energy cost and eliminate waste streams. The main physical characteristic of interest, in the majority of torrefaction studies, was the grindability of torrefied lignocellulosic biomass [8, 9]. While this is certainly an important property for downstream processing, hydrophobicity and susceptibility to microbial degradation represent characteristics crucial for safe and economic long term storage.

Research objectives

Specific objectives have been identified to help better characterize and understand the torrefaction process in general, and torrefaction of corn stover, a prevalent biomass source in the Midwest, in particular. The objective of the first study was to investigate the influence of reaction temperature, residence time, and raw biomass moisture content on specific energy, energy yield, mass yield, and chemical properties of both torrefied corn stover, and the condensable and permanent gases. The outcomes of this study can be used to establish mass and energy balances for the torrefaction process and serve as a foundation for its further optimization. The objective of the second study was to assess the effect of torrefaction on biomass physical property, such as hydrophobicity, and resistance against microbial degradation. Results of the work completed as a part of the second study, along with outcomes of the first study, could be utilized for process optimization in a way that will maximize the beneficial change in the biomass physical and chemical properties, while minimizing mass and energy losses. The objective of the third study was to determine the

influence of the volatiles residence time and biomass particle size on specific energy, energy and mass yield, and chemical properties of torrefied corn stover. Findings from the third study could help design and optimize continuous flow reactors in order to lower the cost and enhance the properties of the torrefied lignocellulosic biomass.

Dissertation organization

This dissertation is organized into six chapters. This first consists of problem identification, description of objectives, and dissertation organization. The second chapter provides a comprehensive literature review of lignocellulosic biomass feedstock and the torrefaction process. The third chapter deals with understanding the effects of basic torrefaction parameters (temperature and residence time), as well as the effects of untreated feedstock moisture content, on the chemical properties of torrefied biomass, mass yield, and energy yield. It is presented in the form of a research article that has been published in *Fuel*, under the title “Effects of torrefaction process parameters on biomass feedstock upgrading”. The fourth chapter covers the study of physical changes induced by torrefaction of lignocellulosic biomass. It is presented in the form of a manuscript submitted to *Energy & Fuel*, under the title “Effect of torrefaction on water vapor adsorption properties and resistance to microbial degradation of thermally treated corn stover”. The fifth chapter is related to understanding the effects of feedstock particle size and purge gas residence time on torrefied biomass chemical properties, mass yield, and energy yield. It is presented in the form of a manuscript submitted to *Energies*, under the name “Effect of particle size, different corn stover components and gas residence time on torrefaction of corn stover”. General conclusions and suggestions for future work are given in the sixth chapter.

References

1. Environmental Protection Agency. Regulation of Fuels and Fuel Additives: 2012 Renewable Fuel Standards. *Fed. Regist.* **2012**, 76, 1320-1358.
2. The Energy Independence and Security Act of 2007, Pub. L. No. 110-40 H.R. 6, 121 Stat. 1492, 2007.
3. Perlack R.D., Wright L.L., Turhollow A.F., Graham R.L., Stokes B.J., Erbach D.C. Biomass as feedstock for bioenergy and bioproducts industry: the technical feasibility of a billion-ton annual supply. DOE/GO-102995-2135 and ORNL/TM-2005/66. NTIS, Springfield, VA, 2005.
4. Uslu A., Faaij A., Bergman P. Pre-treatment technologies, and their effect on international bioenergy supply chain logistics. Techno-economic evaluation of torrefaction, fast pyrolysis and pelletisation. *Energy* 2008, 33, 1206 –1223.
5. Van der Stelt M.J.C., Gerhauser H., Kiel J.H.A., Ptasinski K.J. Biomass upgrading by torrefaction for the production of biofuels: A review. *Biomass Bioenerg.* 2011, 35, 3748-3762.
6. Ciolkosz D., Wallace R. A review of torrefaction for bioenergy feedstock production. *Biofuels, Bioprod. Biorefin.* 2011, 5, 317-329.
7. Prins M.J., Ptasinski K.J., Jansen F.J.J.G. Torrefaction of wood. Part 2. Analysis of products. *J. Anal. Appl. Pyrolysis* 2006, 77, 35-40.
8. Bridgeman T.G., Jones, J.M., Shield, I., Williams, P.T. Torrefaction of reed canary grass, wheat straw and willow to enhance solid fuel qualities and combustion properties. *Fuel* 2008, 87, 844–856.
9. Bridgeman T.G., Jones, I., Williams, P.T., Waldron D.J. An investigation of the grindability of two torrefied energy crops. *Fuel* 2010, 89, 3911-3918.
10. Arias B, Pevida C., Feroso J., Plaza M.G., Rubiera F., Pis J.J Influence of the torrefaction on grindability and reactivity of woody biomass. *Fuel Process. Technol.* 2008, 89, 169-175.

Chapter 2. Literature review

Lignocellulosic biomass

Biomass is defined as an organic, non-fossilized material derived from plants, animals and microorganisms [1]. In general, the term biorenewable resources refers to either dedicated energy crops or wastes [2]. Both of these categories can be further subdivided into the following three classes according to chemical characteristics of the source: lignocellulosic, starch- or sugar-derived, and triglyceride-based biomass [3].

Even though the expression *dedicated energy crops* may imply that the end use is exclusively for the production of energy and fuels, these crops are also grown for the production of chemicals and materials [4]. Dedicated energy crops are planted and harvested either annually (annuals) or on a three- to ten-year cycle (perennials). The relatively short production cycle of dedicated energy crops guarantees that the resource is used in a sustainable manner. These crops are composed of sugars, lipids, proteins, and fibers in various proportions, depending on species, geological origin, and growing season. However, maximizing the yield of the lignocellulosic, fibrous portion of the plant, while reducing simple sugars and lipids, seems to be the most promising route for fuels and chemicals production. This is mainly due to the higher energy yield ($\text{MJ ha}^{-1} \text{ yr}^{-1}$) of plants that have a larger fraction of vegetative (fibrous) parts [4].

Dedicated energy crops can be divided into two groups: herbaceous energy crops and short-rotation woody crops. Herbaceous energy crops are plants with little or no woody material. Herbaceous perennials are preferred over annuals as energy crops because they require less weed control, are more drought resistant, and are less likely to cause soil erosion,

and can reestablish themselves by vegetative reproduction. Herbaceous energy crops include switchgrass, wheatgrass, napiergrass, energy and sugar cane, sorghum, miscanthus, reed canary grass, big bluestem, and eastern gamagrass [4]. Short rotation woody crops are fast growing trees that are harvested on three- to ten-years cycles. They are grouped into two categories: hardwood and softwood. The advantages of hardwood species are that they can sprout from stumps after harvest and have lower ash content than softwood. Softwoods, on the other hand, have higher carbon content, energy density, and are available in significant quantities as manufacturing and logging residues. Short rotation woody crops include species such as hybrid poplar, eucalyptus, silver maple, sweetgum, sycamore, black locust, and willow [4, 5, 6].

Wastes are materials of low or no value, originating from manufacturing processes, agricultural activities, and households. Therefore, wastes include a wide range of materials such as agricultural and forestry residues (corn stover, manure, sugar cane bagasse, wood loggings, branches, bark, and rice hulls), municipal solid waste (food residues, paper, plastic bottles, and containers) and food processing residues (frying grease, organic solutions and suspensions, low grade meat, vegetables, and fruits). The main advantage of waste materials is their low cost. Nevertheless, the large variability of properties, compositional complexity, and uncertainty of supply are some of the disadvantages of using this type of feedstock [1, 2].

Corn stover belongs to the *agricultural residues* feedstock group. It represents the above-ground segment of the corn plant, with the exception of grain. It is comprised of leaves, husks (including silk), stalk (including tassel), and cobs [7]. Corn stover is composed of 38-40% cellulose, 28% hemicellulose, 7-21% lignin, and 3-7% ash, on average [8, 9]. It can be an important feedstock for bioenergy and biorenewable production due to its

availability, and proximity to existing biorefineries [10]. According to Kadam and McMillan [11], about 70% of corn stover produced on no-till farms, and 35% produced on the farms with conventional tilling means can be collected. This means that on average, 40% of all available corn stover produced can be harvested in a sustainable manner. At the 40% theoretical level of collection there is about 82 million dry metric tons of corn stover available in the US per year. This is in agreement with the quantity of corn stover available for collection (about 75 million metric tons per year) predicted by USDA and DOE [12]. The production of corn stover at levels of 75-82 dry Mt/y could yield about 4.8-5.5 billion G/y of cellulosic ethanol at conversion of 190 g EtOH/kg of biomass [13]. The current ethanol production from grain ethanol is about 13.5 billion G/y. Thus, cellulosic ethanol produced from corn stover could increase the total amount of ethanol available in the system by 40-50%, without increase in land area or change in agricultural practices already employed. Despite significant amounts of corn stover available for biorenewables production, its economical utilization may be hindered by factors characteristic for biomass feedstock in general: environmental concerns because of soil erosion and nutrient removal, high transportation cost due to dispersed areas of collection, low energy, low bulk density, high storage cost due to mass loss (respiration and microbial degradation) and low bulk density, and issues with upgrading due to high moisture content, recalcitrance, and heterogeneity [14, 15].

Lignocellulosic biomass composition

Lignocellulosic biomass is made of three major polymers: cellulose, hemicellulose, and lignin. Cellulose chains form elementary fibrils that further associate to form cellulose

crystallites. Cellulose crystallites are bundled together by hemicelluloses and enclosed in a matrix of hemicellulose and lignin [16]. Ratio and composition of these constituents depends on plant species, nutrient availability and exposure to environmental conditions during plant growth, and plant age [17, 18, 19].

Cellulose is the most abundant organic compound on the Earth. It is located primarily in the secondary cell wall, and accounts for 30-50% of the dry matter of different plant species [20]. Cellulose is a homopolymer composed of β -D-glucopyranose units (six carbon monosaccharide) connected via β -(1-4)-glycosidic bonds. It has a high degree of polymerization (about 10,000) and large molecular weight (about 500,000) [21]. The strong tendency to form intra-molecular hydrogen bonds between hydroxyl groups of glucose monomers results in a planar structure of the macromolecule. Planar structures possess fewer steric hindrances and enable easy intermolecular connections to form the crystalline regions responsible for inertness toward chemicals and solvents, as well as high tensile strength [18]. Fewer macromolecule interconnections result in lower density regions known as amorphous cellulose.

Hemicellulose is a heteropolysaccharide composed of several different monomers. It accounts for about 15-35% of dry matter of most plants. Unlike cellulose, a hemicellulose molecule has a low degree of polymerization (about 200). It is a highly branched molecule, which prevents the formation of hydrogen bonds between polymer chains. Thus, hemicellulose has an amorphous macromolecular structure with little strength which is responsible for its relatively easy hydrolysis by weak acids and bases [22]. The composition and structure of hemicellulose varies between softwood and hardwood, with significant differences even between branches, stems, and roots [18, 20]. Hemicellulose monomers

include hexoses (D-glucose, D-mannose, D-galactose), pentoses (D-xylose, L-arabinose, L-rhamnose), and small amounts of uronic acids (D-glucuronic, 4-O-methyl-D-glucuronic, and D-galacturonic acid) [23]. Softwood hemicelluloses consist mainly of galactoglucomannans, arabinoglucuronoxylan, and arabinogalactan. Hardwood hemicellulose consists of glucuronoxylan and glucomannan. Nevertheless, the most important hemicelluloses are xylans and glucomannans [24]. Cellulose and hemicellulose macromolecules connect through hydrogen bonds and van der Waals forces. Hemicellulose is able to bind to lignin by covalent chemical bonds [18].

Lignin is a distinct plant polymer due to its highly amorphous structure, heterogeneity, and aromatic nature. In addition, contrary to other macromolecules found in plants, there are no plant enzymes capable of lignin degradation [25]. It accounts for about 15-35% of dry matter of biomass, and represents the most abundant natural aromatic compound [26, 27]. Lignin is a highly branched, complex, hydrophobic polymer composed of phenylpropanoid units generated by the oxidative polymerization of one or more of the three hydroxycinnamyl alcohol precursors [28]. These alcohol monomers or monolignols are: *p*-coumaryl, coniferyl, and sinapyl alcohol. They form *p*-hydroxyphenyl, guaiacyl, and syringyl moieties, respectively, upon incorporation into lignin matrix via radical coupling at several sites with each other, or within the growing lignin oligomer. Softwood lignin contains mainly guaiacyl and a smaller fraction of *p*-hydroxyphenyl residues. Hardwood lignin is composed primarily of syringyl and guaiacyl residues, with fewer amounts of *p*-hydroxyphenyl residuals [29, 30]. Grass lignin has a similar composition to hardwood lignin with the exception of higher quantities of *p*-hydroxyphenyl residue [31, 32]. There have been at least 20 different bond classes identified in the lignin macromolecule, with more than two

thirds belonging to ether bonds and the rest being carbon-carbon bonds [18, 33]. Lignin is physically and chemically attached to other plant polymers, such as hemicellulose and proteins. Lignin-carbohydrate and lignin-protein complexes are formed via covalent benzyl ether, benzyl ester, glycosidic, and acetal type bonds, as well as hydroxycinnamic acid bridges [34, 35]. These complexes are of great importance for plant growth and existence due to their irreplaceable role in water conduction process through plant tissues, enhancing fiber strength, and protection from pathogens, insects, and herbivores [35, 36]. In addition, they obstruct hydrolysis of carbohydrates and limit carbohydrate availability to microorganisms and animals [37, 38]. Although lignin might be a low value by-product in biochemical pathways for biorenewables production, it may be well suited for thermochemical pathways as a significant source of heat energy, and liquid transportation fuels and chemicals [39].

Biomass contains, although only in minute proportions, another fraction composed of a wide variety of chemical compounds, known as extractives. Average content of extractives in biomass is 1-15%; however, some trees may have about 30% of the extractives known as tannins. The highly heterogeneous extractive fraction includes resin acids, fats, terpenes, flavonoids, lignans, stilbenes, carbohydrates, tannins, and inorganic salts. They can have a protective role against microorganisms, while some can serve as an energy reserve [40].

Thermochemical biomass conversion technologies

Thermochemical biomass conversion technology represents the process of exposing organic material to elevated temperatures under an oxygen depleted atmosphere. The aim of such a process is to thermally break down lignocellulosic material into smaller compounds that can be utilized directly or more easily upgraded into value-added products [41].

Burning biomass in an oxidative environment is the oldest conversion process practiced by man. Combustion, however, does not intend to produce value-added products in the form of fuels, chemicals or materials, as other thermochemical conversion technologies, but only heat energy [20].

Pyrolysis has been used for producing charcoal for the past 38,000 years for a wide variety of uses, such as heating, cooking, art-making, metallurgy, chemical industry, purification, soil amelioration, and medicine. Pyrolysis is a thermochemical conversion of biological material into solid (char), liquid (pyrolysis/bio-oil), and permanent gases, under an inert atmosphere. Fast pyrolysis has been developed relatively lately. It is different from traditional pyrolysis where charcoal is product of interest, mainly because it is aimed to produce liquid fuel that can be used as a substitute for crude oil. It utilizes high heating rates and short vapor reactor residence time. Bio-oil cannot be utilized directly in internal combustion engines and thus has to be upgraded in order to be used as a replacement for gasoline or diesel fuel [42-46].

Gasification is a thermochemical conversion process where the primary goal is to produce a high yield of hydrogen and carbon monoxide, the gas mixture typically recognized as syngas. This process is different from pyrolysis, as it uses higher process temperatures and a partially oxidizing atmosphere [46]. Gasification has been used for over 70 years to produce a low energy, density gas known as “producer gas” [47]. Syngas can be converted into oxygenated fuels, hydrogen, alkanes by means of catalysts, and into a broad range of chemicals through intermediate products, such as methanol [46].

The specificity of hydrothermal processing (HTP) that makes it different from other thermochemical conversion technologies is the liquid reaction environment. High air

temperatures (250-350 °C and 4-17 MPa) or supercritical water temperatures (above 374 °C and 22 MPa) are usually utilized in this process. Under such conditions water serves as a solvent, reactant, and catalyst to assist in decomposition of lignocellulosic material into bio-crude (similar to bio-oil) or gaseous products (similar to syngas), depending on temperature and pressure [48]. It was developed in the mid-1970's at the Massachusetts Institute of Technology as a waste treatment technology [20]. The advantage of HTP is a relatively high efficiency for high moisture biomass conversion, which, however, comes at the expense of high capital and operating cost.

Torrefaction also belongs to the group of thermochemical biomass upgrading technologies. This process is conducted in a temperature range of 200-300 °C, at atmospheric pressure, and under an inert atmosphere for duration of generally less than 1 hour.

Torrefaction for biorenewables production

Overview of biomass torrefaction process

Torrefaction is sometimes also referred to as roasting, slow- and mild-pyrolysis, wood cooking and high-temperature drying. The link between torrefaction and drying might be established due to relatively limited changes in biomass properties in 200-230 °C temperature regime. Such material resembles biomass that has only been dried. However, more intensive torrefaction conditions induce decomposition reactions in biomass that are also part of the pyrolysis process. The term torrefaction has its origin in French, where it means *roasting*. Moreover, this name is used to designate the process of roasting coffee beans that is conducted at lower temperatures and in an oxidative environment. The purpose

of torrefaction of coffee beans is, however, similar to one of the goals of biomass torrefaction: the enhancement of its brittleness [41, 49, 50].

The attempt to utilize the beneficial effect of torrefaction on biomass properties was first reported in 1930's in France, in a trial to improve woody biomass properties for application as gasifier fuel. Until lately, the only industrial application of the torrefaction process was in France in 1980's, under the name the Pechiney process, in which wood feedstock was torrefied to be used as a reducing agent in the metallurgical industry; the torrefied wood was used as a coke substitute in the production of silicone. At the same site, two additional batch plants were built for the production of barbecue fuel and firelighters [51]. However, this demonstration plant was dismantled a decade later. Pioneering work on torrefaction at two temperatures and two tropical wood species was conducted and published in the 1980's by Bourgois and Doat [52]. Comprehensive work in the field of torrefaction started about 10 years ago as a part of the effort to develop better feedstock for biorenewables production, specifically thermochemical conversion technologies. Even though there is still no existing commercial torrefaction facility, *Enviva LP* and *ConocoPhillips* have created the new company *ECo Biomass Technologies* in 2011 to produce and market torrefied wood pellets [53]. The torrefaction facility is scheduled to be on-line in 2013 and sell products to large power generating facilities.

Torrefaction mechanism

The overall torrefaction process is separated into five stages according to temperature-time profile, as proposed by Bergman et al. [51]. Stage 1 is the initial heating stage, during which biomass temperature increases until it reaches 100 °C and water starts to

evaporate (Figure 1). Biomass temperature does not change significantly until all free water evaporates during stage 2. This is the pre-drying phase. Stage 3 corresponds to post-drying and intermediate heating stage that occurs between 100 and 200 °C. During this phase physically bound water is released. In addition, some dry matter loss occurs due to evaporation of light organic fractions.

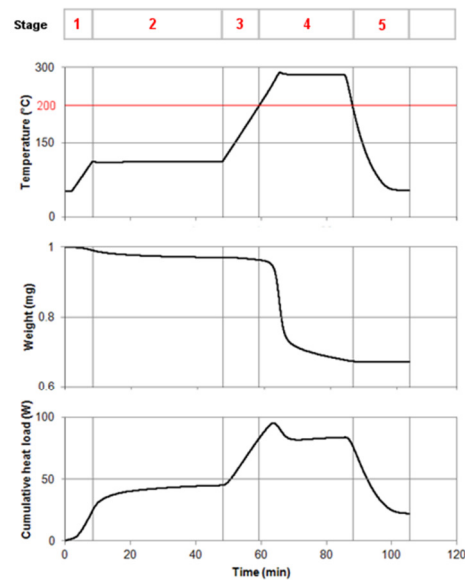


Figure 1. Stages in the torrefaction process (data taken from author's experiment; a 40 min drying phase was employed to eliminate the influence of moisture absorbed from the atmosphere on DML)

Stage 4 or the torrefaction phase, during which the decomposition reaction takes place, starts once the biomass temperature reaches 200 °C. The end of the torrefaction phase is considered to be in the moment when the temperature drops below 200 °C, even though a very limited mass loss occurs when the temperature falls below the maximum torrefaction temperature. The temperature of the torrefaction reaction is defined as the maximum biomass temperature. The stage 4 is responsible for the largest dry matter loss over the course of the

whole process. In the stage 5, cooling of the solid, torrefied biomass down to room temperature takes place.

Hemicellulose is a more reactive polymer in the torrefaction temperature range than lignin and cellulose. Most of the dry matter loss of biomass comes from hemicellulose, and to a much smaller extent, devolatilization of the other two polymers (Figure 2). Since it is hard to obtain pure hemicellulose in its native state, xylan is routinely used in experiments as it is the major hemicellulose monomer.

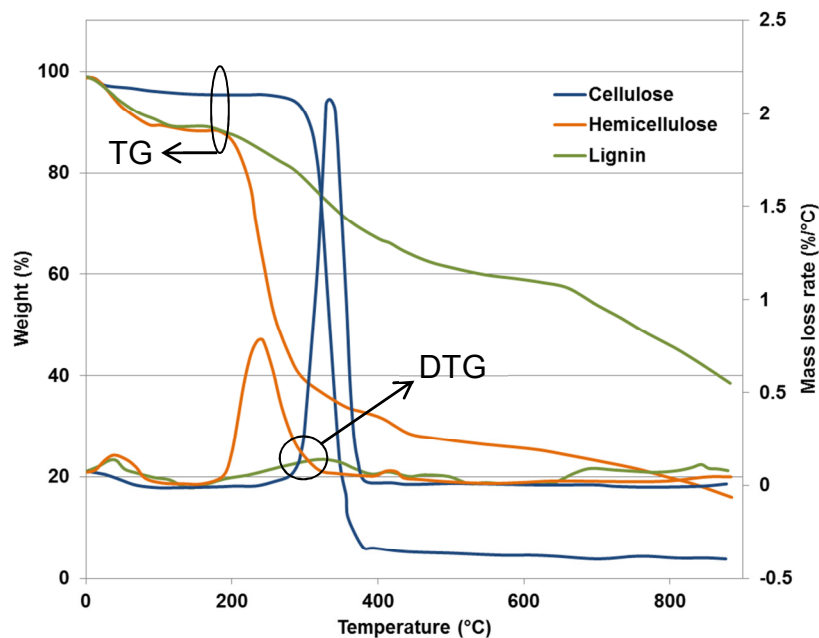


Figure 2. Weight loss of the main biomass constituents [54]

Xylan shows a peak mass loss rate at about 250 °C, and significant mass loss at the end of the torrefaction temperature range. Its decomposition can be represented by a two-step mechanism [55]. The first, fast step takes place in the low temperature regime (below 250 °C) comprised mainly of depolymerization reactions that yield a distorted solid intermediate (Figure 2). The second, slow stage takes place in the range between 250-300 °C and consists

of reactions that produce char and volatiles. Hardwood hemicellulose is more reactive because it contains mainly 4-O-methyl glucuronoxylan, whereas softwood contains less reactive glucomannan and arabinogalactan [56]. Lignin decomposes at a much slower rate, not only in the torrefaction temperature regime, but also over a much wider range, as justified by the absence of any significant peak on the mass loss rate curve (DTG, i.e. differential thermogravimetric signal in Figure 2). It shows a modest mass loss at the end of the torrefaction stage. Moreover, hardwood lignin is more reactive than softwood lignin [57]. Cellulose is most stable of all three macromolecules in the given temperature range, and the change in its weight at the end of the torrefaction process is very limited. Major reactions below 250 °C are depolymerization reactions. Above this temperature some mass loss in form of permanent gases and condensables may occur (figure 3).

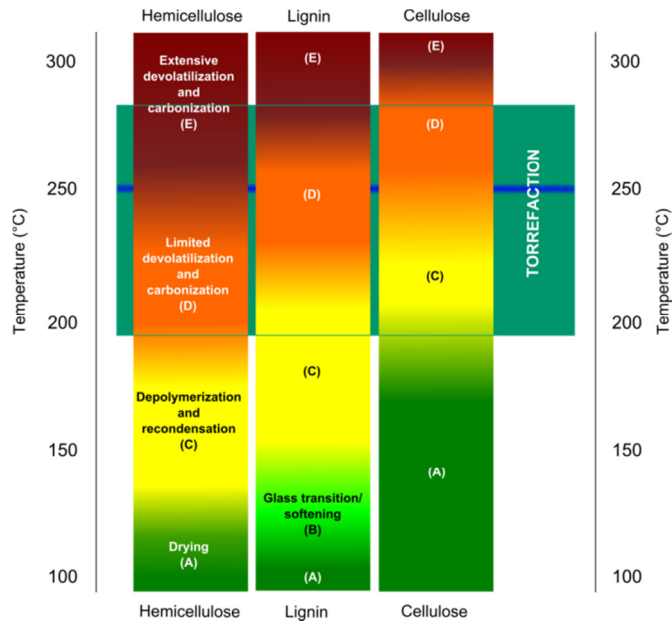


Figure 3. Changes in polysaccharides and lignin during torrefaction [51]

Torrefaction kinetics

Chemical kinetics is the study of the rate of chemical reactions, factors affecting the reaction rates, and the reaction mechanisms. Knowledge of chemical kinetics is necessary for the proper reactor design, as well as its safe, optimal, and economical operation. Kinetic models applied to biomass torrefaction have their origins in the field of pyrolysis [58]. The majority of these studies have investigated the pyrolysis of cellulose, hemicellulose (xylan) and lignin separately for the sake of simplicity. In addition, products of a pyrolysis reaction are lumped together into three broad categories: solid (char), permanent gases, and condensables (liquid bio-oil). As previously mentioned, torrefaction includes the same decomposition reactions that occur in the first stages of the pyrolysis process, making attempts to apply pyrolysis kinetics models to torrefaction a logical step.

A simple kinetics model has been applied to the torrefaction of wood model by Repellin et al. [59], although Orfao et al. [60] described such model as inappropriate for studying the pyrolysis of hemicellulose (xylan). It is represented by a one-step reaction (Eq. 1) with only two parameters, k_{OM1} and E_{AM1} .



Starting woody biomass, volatiles and char are denoted by A, V and C, respectively. Three species in the reaction are pseudo components whose compositions are not well defined. Since the molar masses of these pseudo components are not known, an additional parameter was introduced in the model to account for experimental yields of char and volatiles. This parameter f (Eq. 2) is defined as the ratio of molar mass of the pseudo chemical species, volatiles (M_V), and it has to be optimized.

solid products in the reactions (y_1 and y_2) are assumed to be constant and temperature-independent, meaning that the model neglects changes in the final char yield with temperature.

This kinetic model (Eq. 5), comprising of a two-step mechanism with parallel reactions, was suggested by Di Blasi and Lanzetta [55].



The yield of the solid products is given by Eq. 6 and Eq. 7.

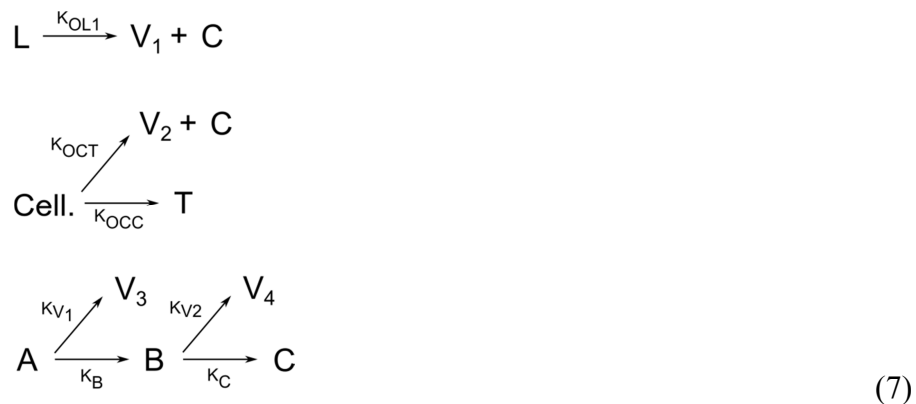
$$f_B = \frac{k_B}{k_B + k_{V1}} \quad (5)$$

$$f_C = \frac{k_C}{k_C + k_{V2}} \quad (6)$$

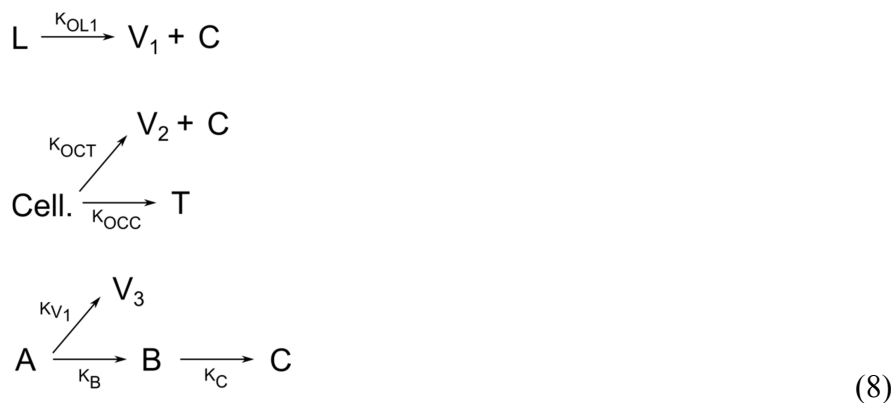
The fact that the ratio of volatile and solid products increases with an increase in temperature was incorporated in this model by the inclusion of a distinct reaction for formation of these two product classes. Even though this might not be correct from the standpoint of analytical chemistry, Prins et al. obtained a good correlation of the model and experimental data [56].

Rousett et al. [63] developed the model (system of Eq. 7) that treats wood thermal decomposition as a superimposition of the decomposition of its main components: lignin (L), cellulose (Cell.) and hemicellulose (A). According to the model, cellulose decomposes into tar (T), volatiles, and char in two parallel reactions. Lignin decomposes into char and

volatiles according to a simple one step mechanism. Hemicellulose decomposition proceeds, according to the Di Blasi-Lanzetta model, via two consecutive and two parallel reactions.



The ratio of molar masses of volatiles to char needs to be defined both for cellulose (f_L and f_{CC}) and lignin [59]. Nevertheless, Repellin et al. [59] had to reformulate the model due to nonphysical values obtained for the model parameters (system of Eq. 8).



Adjusted, Rousset's model performed well in regards to fitting experimental data. However, according to the model, beech (hardwood) has a higher reactivity than spruce (softwood), which is contrary to experimental data available in the literature [51, 56, 66]. In addition, hypotheses made to adjust the model compromised the Rousset model and the hypothesis of superimposition. Aforementioned, rendered the Rousset's model inapplicable in torrefaction process.

Torrefaction product distribution and composition

Major products of biomass torrefaction are generally grouped into solid torrefied biomass and volatiles (Figure 4). Volatiles are further subdivided into permanent gases and condensables, according to their state at room temperature.

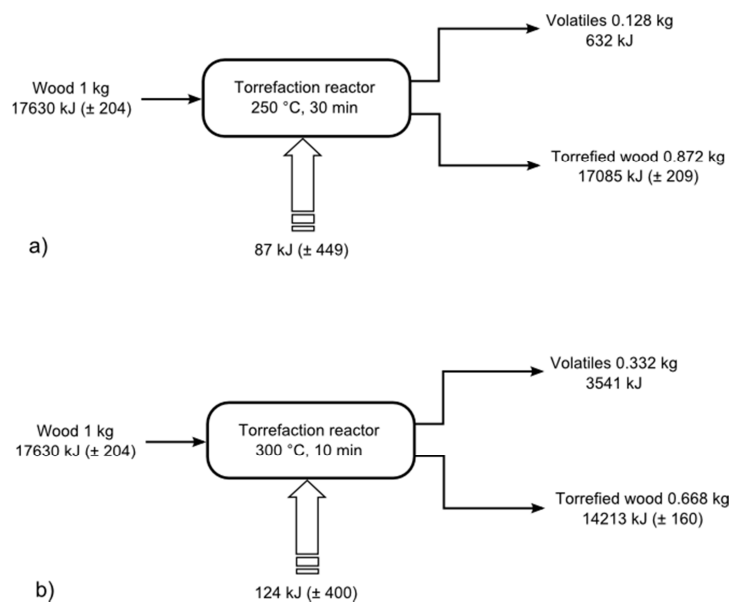


Figure 4. Typical mass and energy yields in torrefaction of wood at two conditions [64]

The composition and yield of products depend on torrefaction temperature, time, and biomass physical and chemical properties. Although volatiles can account for up to 30-40% of the initial biomass weight, they contain only about 10-15% of the energy of the initial material. This is mainly due to the high oxygen and low energy content of this product stream. The end result is an increase of energy density of torrefied biomass.

The solid product consists of intact polymers from fractions that are less reactive at the torrefaction conditions and various products of the reaction (Figure 5). The latter include oligomers formed via depolymerization and recondensation reactions, short chain organics

condensed in the matrix of torrefied biomass, carbonized char-like structures, and mineral matter present in the original biomass [51, 66].

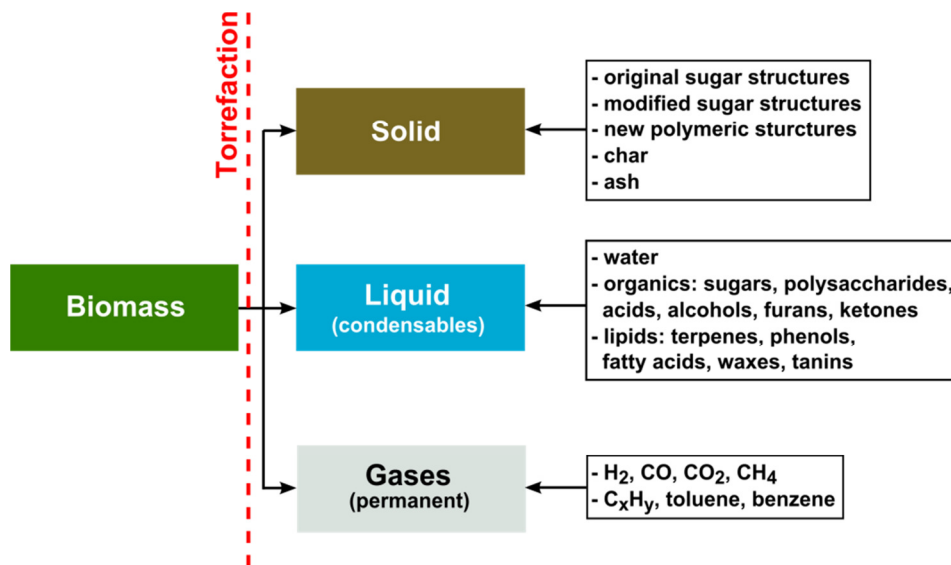


Figure 5. Composition of the torrefaction reaction products [51]

Permanent gases are generally referred to as the volatile fraction that is in a gas phase at the room temperature. It includes CO₂, CO, and smaller amount of H₂, CH₄ and other light C₂ hydrocarbons [65, 66]. Carbon dioxide represents the largest fraction of permanent gases. It is probably formed through decarboxylation reactions of organic acid moieties of the biomass. CO is the second most abundant permanent gas product. Since it cannot be formed in decarboxylation and dehydration reactions, its generation is assumed to be via a reaction between CO₂ and water molecules, catalyzed by carbonized torrefied biomass. The liquid fraction condensed from the stream of volatiles comprise numerous compounds such as water, acetic, acid, formic acid, methanol, lactic acid, furfural, hydroxyl acetone, and trace amounts of other organics [66]. Water vapor is generated by evaporation of free and physically bound water, as well as water produced during the thermal breakdown of biomass. Acetic acid and methanol originate from acid and alcohol groups attached to hemicellulose

chains. In general, water, acetic acid, and methanol are the major constituents of the liquid fraction.

The yield of solid product decreases with an increase in torrefaction temperature (Table 1) due to the extensive devolatilization of hemicellulose, and cellulose and lignin to a lesser extent, at temperatures close to 300 °C. The amount of liquids increases more significantly with the increase in temperature than the amount of permanent gases. It has been confirmed that temperature has most significant influence on product yield and composition [67, 68, 69].

Table 1. Yields of different biomass types torrefied for 1h* [42]

Biomass	Temp. (°C)	Gas (%)	Liquid (%)	Solid (%)	Solids composition (%)			% energy retained
					C	H	O	
Pine	230	0.6	7.0	92.4	49.7	5.9	44.3	96.5
Pine	250	1.0	10.8	88.2	50.9	5.8	43.2	94.4
Pine	280	2.1	19.8	78.1	56.4	5.5	38.0	93.9
Bagasse	230	2.6	9.9	87.5	48.6	5.6	45.5	96.4
Bagasse	250	10.4	10.7	78.9	50.6	5.6	43.5	92.0
Bagasse	280	12.9	18.5	68.6	52.8	5.3	41.5	82.9
Birch	250	1.7	12.8	85.5	51.5	5.8	42.5	97.9
Birch	230	0.8	6.0	93.2	48.2	5.9	45.7	93.8
Birch	250	1.2	10.8	88.0	49.5	5.7	44.7	90.0
Birch	280	2.0	19.0	79.0	51.3	5.6	43.0	84.3
Salix	230	1.0	8.0	91.0	45.6	5.9	48.2	94.4
Salix	250	1.5	13.0	85.5	45.8	5.8	48.1	88.4
Salix	280	3.0	18.0	79.0	46.3	5.6	47.7	81.8
Miscanthus	230	1.0	10.0	89.0	44.4	6.1	48.7	87.7
Miscanthus	250	2.0	15.0	83.0	47.4	5.8	46.1	87.7
Miscanthus	280	7.0	24.0	69.0	51.3	5.7	42.4	80.0
Straw Pellets	230	0.1	5.0	95.0	47.8	6.3	45.2	95.1
Straw Pellets	250	0.3	9.8	90.0	49.0	6.1	44.1	91.6
Straw Pellets	280	1.0	19.1	79.9	52.8	6.1	40.3	89.8
Wood Pellets	230	0.06	6.5	96.5	49.8	6.3	43.8	97.5
Wood Pellets	250	0.15	5.5	94.4	50.7	6.2	43.0	96.9
Wood Pellets	280	0.6	10	89.4	52.5	6.2	41.3	96.0

*solids composition expressed on a dry ash-free basis

As can be seen in the Table 1, the yield of solids can drop from above 90% to about 70-75% when the reaction temperature increases from 230 to 280 °C. The yield of permanent gases increases significantly, but its absolute amount still represents the smallest fraction of

all three. Condensables make a significant portion of the mass balance at 280 °C (about 20%).

Residence time is another parameter that affects product yield. Several studies investigated the influence of this factor on torrefaction of lignocellulosic biomass. Nevertheless, torrefaction time was less significant than temperature in all conducted experiments [70, 71, 72]. Residence time is the important parameter when it comes to reactor design since it determines the reactor volume necessary to achieve the projected capacity. Minimum residence time can vary depending on torrefaction temperature, biomass type, its physical and chemical properties, and intended end use. However, there is a maximum after which any further increase in residence time does not affect biomass properties significantly. According to Repellin et al. [60] there is an increase of only 1-5% in average weight loss when residence time increases from 20 to 40 min. Arias et al. [73] concluded that there was little improvement in biomass grindability at 240 °C, if the residence time was longer than 30 min. In their work Bergman et al. [51] concluded that torrefaction should be conducted for 17 min at 280 °C for co-firing applications.

Particle size also affects the torrefaction reaction, but to a lesser extent than temperature and residence time. Particle size did not have a significant effect on the torrefaction of willow in the 0-50mm range [51]. Another study confirmed this finding for willow and miscanthus [74]. Bergaman et al. [51] speculated that this is the consequence of a slow, kinetically controlled torrefaction reaction, as characterized by the absence of heat and mass transfer hindrances. The torrefaction reaction can be endothermic (below 275 °C) and exothermic (above 275 °C) [75, 76]. In spite of being relatively small, energy released in exothermic reaction still can cause problems in process control due to runaway reactions.

Particle size can affect the nature of a torrefaction reaction and cause excessive dry matter loss [77].

It has been found that high moisture content of raw biomass increases dry matter loss (DML), especially in the temperature regime below 250 °C. The difference in DML between 3 and 22% moisture content corn stover could be up to 10% if torrefaction is conducted at a temperature between 200 and 250 °C [78]. This is probably due to higher heat capacity and better heat conduction properties of water/water vapor than nitrogen, which accelerates torrefaction. In addition, higher availability of water molecules in high moisture content biomass increases rate of hydrolysis during torrefaction.

Torrefaction reactors

The correct choice of the reactor suitable for torrefaction may be very important given that each reactor has its distinct properties, and cannot equally process all biomass types with a wide variety of physical and chemical characteristics.

The first and only commercial torrefaction reactor, employed in the Pechiny process in 1980's (France) was an auger reactor. It consisted of a horizontal shell and concentrically placed auger. The heat was supplied to the process by conduction through both the shell and auger via thermal oil. Thus, this was an indirectly heated reactor. The biomass plug flow through the reactor was maintained by the auger. The reactor had accurate temperature control due to limited heat transfer, but it required a long residence time (60-90 min). Free-flowing material was necessary for this reactor to operate properly. The biomass fill ratio for this type of reactor was 60-70% [51].

A rotating drum reactor design was experimentally tested for torrefaction by Bergman et al. [51]. This technology is relatively simple and employs a rotating cylinder with metal bars along its circumference to help tumble the biomass. The rotating drum reactor can be heated directly and indirectly. In the directly heated reactor heating medium, usually nitrogen is in a direct contact with biomass. However, in the indirectly heated system heat is supplied to the biomass through the reactor wall. A directly heated reactor has good heat transfer characteristics due to the permanent mixing of biomass; however, directly heated reactor performs worse than the auger reactor due to lower heat transfer coefficient and longer solids residence time. Its fill ratio is only about 10-15%, which significantly decreases the reactor throughput.

A moving bed reactor may be vertical or horizontal. Its advantage is simple, compact design and high fill ratio (100%). It can also be directly or indirectly heated. In the former case, very high heat transfer coefficients can be achieved, which translates into short residence times. A pressure drop in vertical reactor can be significant. Non-free flowing biomass can be processed in this type of reactor [51].

A fluidized bed reactor has been widely used in the thermochemical conversion of biomass feedstock, such as pyrolysis, gasification, and combustion. In these reactors the fluidizing medium (usually gas) is passed through a bed of solid, granular, inert material (sand) at high velocity, causing the solid to behave as a fluid. The advantages of this technology are the high heating rate and heat transfer coefficient, as well as the stable and uniform temperature due to the vigorous mixing, large surface area, and thermal mass of the heat carrier. Nonetheless, attrition of sand particles makes it hard to separate torrefied

biomass from sand, which can increase ash content. Moreover, biomass can be hard to fluidize due to its irregular shape [80].

Microwave radiation is electromagnetic radiation in the frequency range 0.3-300GHz. Specialized “microwave chemistry” reactors utilize radiation whose frequency is 2.4GHz. The same frequency can be used to thermally process biomass. This frequency forces polar molecules of biomass to oscillate at the resonant frequency and induces friction and heating. Since the heating is generated in the entire volume of biomass at once, this phenomenon is known as a volumetric heating. The advantage of microwave torrefaction is the uniform biomass heating, shorter heating time, small footprint, and accurate control [81, 82].

Wet torrefaction does not refer to any specific reactor design, but to the liquid environment in which the torrefaction reaction is conducted. This makes it fundamentally different from dry torrefaction in that there is no biomass drying phase (stage 1 in Figure 1); the material is processed wet. In this process biomass is treated in hot pressurized water without phase change of the medium. Product characteristics and distribution do not differ significantly from common, *dry* torrefaction. The same effect that *dry* torrefaction has on biomass can be achieved at a lower temperature in the wet torrefaction process. The advantages of this process include a completely inert atmosphere, the high heat capacity of water, the high heat transfer coefficient between solid and liquid, and the ability to process high moisture content biomass [83, 84, 85].

Economics

Torrefaction unquestionably has a unique potential to improve the physical and chemical properties of biomass feedstock, such as grindability, storage stability, and energy

density, in a relatively simple manner. However, the implementation of any new technology might be justified only if its overall economics can be competitive on the market. In order to determine whether or not the cost of adding an extra unit operation to the production chain can be offset by the gains in biomass properties, techno-economic analysis is frequently conducted. Techno-economic analysis of the torrefaction process is hindered by the fact that there is no commercially proven system available, thus requiring many assumption to be made.

It has been claimed in the literature that torrefaction can have a significant, positive effect on biomass transportation, logistics, and utilization. Uslu et al. [86] analyzed an overseas biomass supply chain for energy and fuel production, and concluded that, on the basis of overall energy efficiency, torrefaction combined with pelletizing performs better than pelletizing only, for about 4-16% depending on the end use. In another study it was found that torrefaction is a more cost effective and environmentally friendly pre-treatment technology for Fischer-Tropsch production than rotating-cone and fluidized-bed pyrolysis [87]. Zwart et al. [88] have obtained similar findings from their assessment of overseas biomass supply chains. They have reported that pre-treatment at the front-end significantly reduces the production cost, with torrefaction being the most promising technology when compared to pyrolysis and traditional pelletizing. In addition, overseas, centralized facility that utilizes low-temperature circulating fluidized bed gasification technology had better economics than torrefaction, but such large facility would fail from the transportation point of view, due to an unrealistic number of trucks required to supply feedstock. Bergman et al. [51] analyzed several potential torrefaction reactor designs and concluded that the moving bed could be economically attractive. In another study Bergman et al. [88] have found that

torrefaction combined with pelletizing may have significant economic potential if incorporated in the biorenewables production chain.

Properties and applications of torrefied biomass

Appearance. Biomass undergoes a change in color during the torrefaction process that corresponds to changes in, both chemical and physical characteristics. Since the torrefaction temperature range is relatively wide (200-300 °C), the color of raw biomass can be altered to different extents, ranging from shades slightly darker than the original material to black, depending mainly on the temperature. Even though torrefied biomass retains the shape and dimensions of raw biomass, it has a lower bulk density due to devolatilization and drying. Moreover, it can appear as friable to the touch as original biomass or significantly more, depending on the treatment temperature.

Grindability. One of the most important benefits of the torrefaction process is the enhancement of biomass brittleness, which translates into its improved grindability. Biomass grindability is an important property not only for direct co-firing in existing coal-fired power plants but also for gasification and pyrolysis, especially in pulverized and fluidized bed systems. The tenacious, fibrous structure of biomass makes size reduction very energy intensive and a cost ineffective process. In addition, ground raw biomass includes a combination of spherical particles and fibers that encumber proper dispersion and fluidization [75]. In order to be suitable for utilization in existing power production systems, biomass has to have properties similar to coal. Bergman et al. [51] have found that grinding torrefied biomass required only 10-30% of energy needed for comminution of untreated

biomass (Figure 6). Moreover, equipment capacity increased about 7-15 times, depending on the torrefaction temperature, when torrefied biomass was ground.

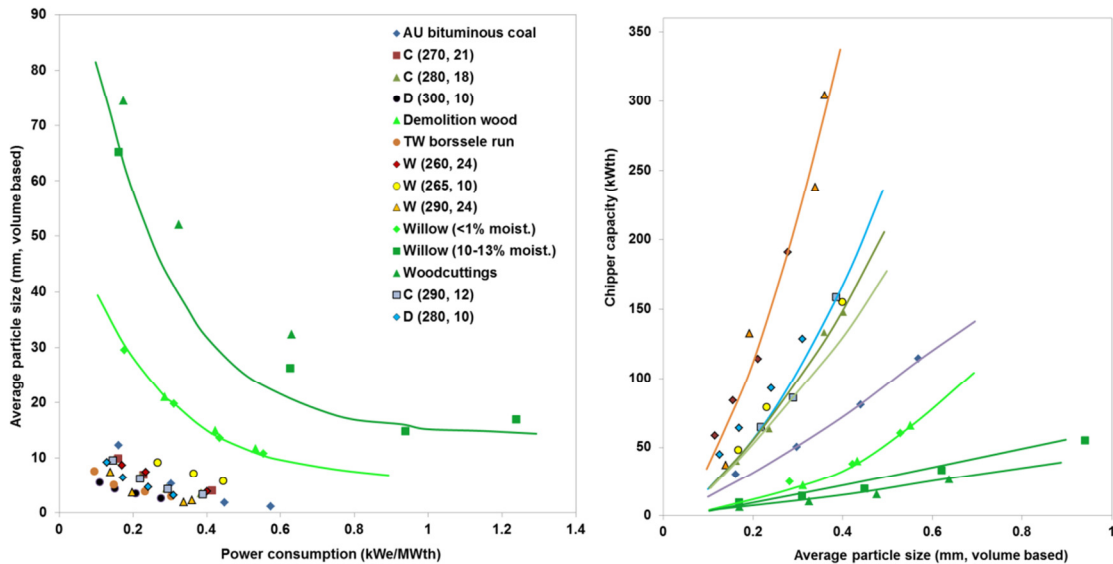


Figure 6. Power consumption and mill capacity during raw and torrefied biomass size reduction [51]

Ground torrefied biomass shows a particle size distribution similar to coal (Figure 7), which is another crucial parameter for the correct operation of combustion and thermochemical conversion facilities. It affects combustion efficiency, the quantity of residual carbon in the ash, and stability of combustion [74].

Heavy duty equipment, such as a hammer mill, traditionally used in pelletizing systems can be substituted for smaller, simpler, and less expensive cutting mills or jaw crushers, due to the improved physical characteristics of torrefied biomass [88]. This can the lower capital and operational cost of the whole production chain.

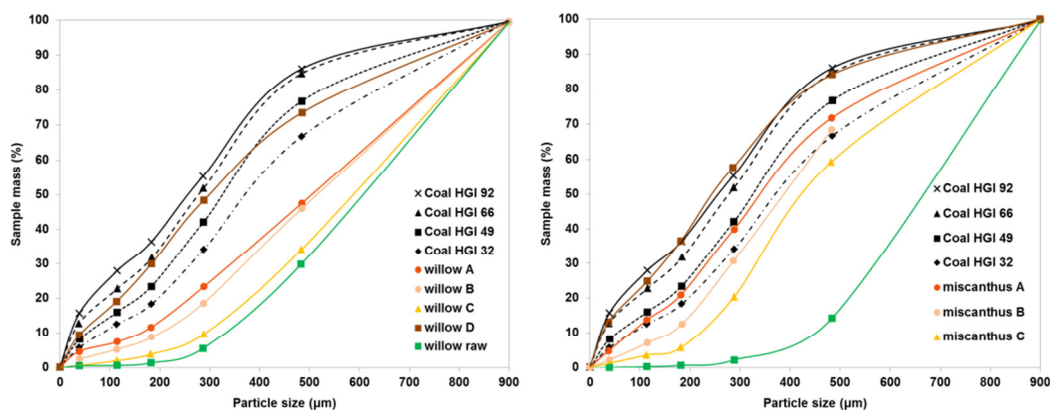


Figure 7. Particle size distribution of coal, raw and torrefied willow & miscanthus [74]

Hydrophobicity. Hydrophobicity plays an important role in the storage of biomass feedstock, since a large amount of biomass needs to be stored to support year-round biorefinery, or power plant operation. Hydrophobicity decreases the quantity of excess water that needs to be transported and removed in the combustion or upgrading steps, thus increasing overall cost. Furthermore, extra water makes biomass a suitable medium for microorganism growth [51, 89, 90]. Torrefaction improves the water repelling characteristics of biomass through the elimination of hydroxyl groups responsible for hydrogen bonding with water molecules, and the generation of a non-polar, hydrophobic compound [90, 91].

According to Acharjee et al. [90], the equilibrium moisture content of biomass dropped from 15 (raw biomass) to about 5% after wet torrefaction at 260 °C. Bergman et al. [88] conducted a 15 hour water uptake test on pelletized, torrefied biomass by submerging it in the water. The condition of the pellets was observed, while water uptake was determined gravimetrically. They concluded that torrefied pellets did not change significantly (swelling, disintegration) compared to raw biomass pellets, and absorbed about 7-20% moisture on a weight basis. Hydrophobicity of torrefied biomass briquettes was assessed by Felfli et al. [92]. They have found that water uptake decreased 73% after torrefaction, compared to

untreated biomass, probably due to tar condensation in the biomass particle and the formation of a hydrophobic chemical species. However, hydrophobicity decreased with an increase in torrefaction temperature most likely because of an increase in porosity. Felfli et al. investigated nature of torrefied pellets in regards to water uptake and reported findings similar to Bergman et. al. [51]. Torrefied pellets were more durable than raw biomass pellets, as justified by the absence of crumbling and excessive swelling.

Energy density. Chemical species rich in oxygen and hydrogen, such as water, acetic acid, methanol, and carbon dioxide are released via devolatilization of the raw biomass during the torrefaction process. Since these compounds contain more oxygen and hydrogen than carbon, the O/C and H/C ratio of torrefied biomass decreases. The change in the biomass O/C and H/C ratio upon torrefaction is depicted and compared to coal by van Krevelen diagram (Figure 8).

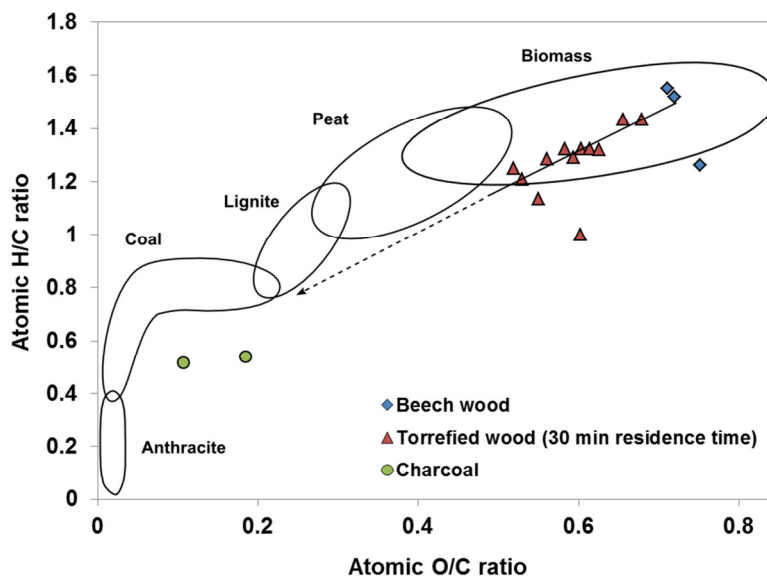


Figure 8. Van Krevelen diagram showing change in the biomass O/C and O/H ratio after torrefaction [64]

This change in the chemical properties of biomass is valuable for gasification, since organic material with high oxygen content causes excessive oxidation and reduces process thermal efficiency [64, 67]. Moreover, the energy density of biomass increases as a consequence of oxygen loss during torrefaction. This increase can be in the range between 102-120%, depending on reaction conditions [42]. Energy and bulk density of torrefied biomass can be further improved via pelletizing.

Combustion properties. The combustion conversion of torrefied woody biomass (about 95%) was found to be comparable to untreated wood and considerably higher than high- and low-volatile bituminous coal (about 80 and 60%, respectively). The high fixed carbon content of torrefied biomass indicates high reactivity. Moreover, complete carbon conversion can be expected. This implies that complete conversion can be reached in co-firing systems [51]. Bridgeman et al. [69] investigated combustion properties of torrefied biomass and concluded that there exists numerous differences between untreated and torrefied biomass. Moreover, combustion of the volatiles released during torrefied biomass combustion took place over the shorter temperature range and generated a higher heat of combustion. Torrefied biomass created a greater heat of combustion due to a higher fixed carbon content. In addition, the ignition time of volatiles and char decreased as a consequence of torrefaction, which could be an advantage during combustion.

Gasification properties. Prins et al. [64] assessed the properties of torrefied biomass for gasification using several reactor systems: air-blown gasification of wood, air-blown gasification of torrefied wood in a circulating fluidized-bed, and oxygen-blown gasification of torrefied wood in an entrained-flow gasifier. They concluded that the overall efficiency of the air-blown gasification of torrefied wood was lower than the gasification of untreated

wood. However, upon integration of torrefaction and gasification processes, overall efficiency increases to a level comparable to gasification of raw wood. Svoboda et al. [93] have found that torrefaction with grinding below 0.2 mm can be beneficial for gasification due to the minimization of overall loss, ease of feeding, and high specific energy of torrefied biomass. The gasification of torrefied biomass can be done at elevated pressures, which may be useful for downstream energy production in turbines or for production of chemicals. Nonetheless, this cannot be achieved with raw biomass due to issues with its feeding in pressurized systems [94].

References

1. Demirbas A. *Biofuels*. Springer: London, UK, 2009.
2. Montross M., Crofcheck C. Energy Crops for the Production of Biofuels. In *Thermochemical Conversion of Biomass to Liquid Fuels and Chemical*. Croker M., Ed. RSC Publishing: Cambridge, UK, 2010, pp 26-45.
3. Huber G.W., Corma A. Synergies between Bio- and Oil Refineries for the Production of Fuels from Biomass. *Angew. Chem. Int. Ed.* 2007, 46, 7184-7201.
4. Brown R. C. *Biorenewable Resources: Engineering New Products from Agriculture*. Blackwell Publishing Professional: Ames, IA, 2003.
5. Hohenstein W.G., Wright L.L. Biomass energy production in the united states: An overview. *Biomass Bioenerg.* 1994, 6, 161-173.
6. Graham R.L. An analysis of the potential land base for energy crops in the conterminous United States. *Biomass Bioenerg.* 1994, 6, 175-189.
7. Demirbas A. Conversion of Corn Stover to Chemicals and Fuels. *Energy Sciences, Part A* 2008, 30, 788-796.
8. Ganjyal G.M., Reddy N., Yang Y.Q., Hanna M.A. Biodegradable Packaging Foams of Starch Acetate Blended with Corn Stalk Fibers. *J. Appl. Ploy. Sci.* 2004, 93, 2627-2633.

9. Reddy N. Structure and properties of natural cellulose fibres obtained from cornhusks, cornstalks, rice, wheat, soybean straw and sorghum stalks and leaves. Ph.D. Dissertation, University of Nebraska, Lincoln, NE, 2006.
10. Pordesimo L.O., Hames B.R., Sokhansanj S., Edens W.C. Variation of corn stover composition and energy content with crop maturity. *Biomass Bioenerg.* 2005, 28, 366-374.
11. Kadam K.L., McMillan J.D. Availability of corn stover as a sustainable feedstock for bioethanol production. *Bioresour. Technol.* 2003, 88, 17-25.
12. Perlack R.D., Wright L.L., Turhollow A.F., Graham R.L., Stokes B.J., Erbach D.C. Biomass as feedstock for bioenergy and bioproducts industry: the technical feasibility of a billion-ton annual supply. DOE/GO-102995-2135 and ORNL/TM-2005/66. NTIS, Springfield, VA, 2005.
13. Lau M.W., Dale B.E. Cellulosic ethanol production from AFEX-treated corn stover using *Saccharomyces cerevisiae* 424A(LNH-ST). *Proc. Natl. Acad. Sci. U. S. A.* 2009, 106, 1368-1373.
14. Hettenhaus J.R., Wooley R., Wiselogel A. Biomass Commercialization Prospects in the Next 2-5 Years. NREL report no. NREL/SR-580-28886, DOE-AC36-99-GO10337, NREL, Golden, CO, 2000.
15. Gold S., Seuring S. Supply chain and logistics issues of bio-energy production. *J. Clean Prod.* 2011, 19, 32-42.
16. Ramos L.P. The chemistry involved in the steam treatment of lignocellulosic materials. *Qui. Nova* 2003, 26, 863-871.
17. Goyal C.G., Fischer J.J., Krohn M.J., Packwood R.E., Olson J.R. Variability in pulping and fiber characteristics of hybrid poplar trees due to their genetic makeup, environmental factors, and tree age. *TAPPI J.* 1999, 82, 141-147.
18. Sjorstrom E. *Wood Chemistry: Fundamental and Applications*. Academic Press: London, UK, 1981.
19. Mandre M. Responses of Norway spruce (*Picea abies L.*) to wood ash application. *For. Stud.* 2005, 42, 34-47.

20. Basu P. *Biomass Gasification and Pyrolysis: Practical Design*. Academic Press: Burlington, MA, 2010.
21. Klass D.L. *Biomass for Renewable Energy, Fuels, and Chemicals*. Academic Press: San Diego, CA, 1998.
22. Erbingerova A., Hromadkova Z., Heinze T. Hemicellulose. *Adv. Polym. Sci.* 2005, 186, 1-67.
23. Ramos L.P., Fontana J.D. Enzymatic Saccharification of Cellulosic Materials. *Methods Biotechnol.* 2004, 16, 219-233.
24. Girio F.M., Fonseca C., Carvalheiro F., Duarte L.C., Marques S., Bogel-Lukasik R. Hemicelluloses for fuel ethanol: A review. *Bioresour. Technol.* 2010, 4775-4800.
25. Sedorf R.R., MacKey J.J., Ralph J., Hatfield R.D. Unexpected variation in lignin. *Curr. Opin. Plant. Biol.* 1999, 2, 145-152.
26. Brebu M., Vasile C. Thermal degradation of lignin-A review. *Cellulose Chem. Technol.* 2010, 44, 353-363.
27. Lora J.H., Glasser W.G. Recent Industrial Applications of Lignin: A Sustainable Alternative to Nonrenewable Materials. *J. Polym. Environ.* 2002, 10, 39-48.
28. Boudet A.M., Lapierre C., Grima-Pettenati J. Biochemistry and molecular biology of lignification. *New Phytol.* 1995, 129, 203-236.
29. Whetten R.W., MacKey J.J., Sederoff R.R. Recent advances in understanding lignin biosynthesis. *Annu. Rev. Plant Physiol.* 1998, 49, 585-609.
30. Adler E., Lunquist K., Miksche G.E. The Structure and Reactivity of Lignin. *Adv. Chem. Ser.* 1996, 59, 22-35.
31. El Hage R., Brosse N., Chrusciel L., Sanchez C., Sannigrahi P., Ragauskas A. Characterization of milled wood lignin and ethanol organosolv from *miscanthus*. *Plym. Degrad. Stab.* 2009, 94, 1632-1638.
32. Buranov A.U., Mazza G. Lignin in straw of herbaceous crops. *Ind. Crop. Prod.* 2008, 28, 237-259.
33. Hatfield R., Vermerris W. Lignin Formation in Plants. The Dilemma of Linkage Specificity. *Plant Physiol.* 2001, 126, 1351-1357.

34. Whitmore F.W. Lignin-protein complex in cell walls of *pinus elliottii*: amino acid constituents. *Phytochemistry* 1982, 21, 315-318.
35. Iiyama K. Lam T.B.T. Covalent cross-links in the cell wall. *Plant. Physiol.* 1994, 104, 315-320.
36. Khanam L.A.M., Talukder D., Hye M.A. Toxic and repellent action of sugarcane bagasse-based lignin against some stored grain insect pests. *Univ. J. Zool. Rajshahi Univ.* 2006, 25, 27-30.
37. Ferguson L.R., Chavan R.R., Harris P.J. Changing concepts of dietary fibre: Implications for carcinogens. *Nutr. Cancer.* 2001. 39, 155-169.
38. Grabber J.H. How Do Lignin Composition, Structure, and Cross-Linking Affecting Degradability? A Review of Cell Wall Model Studies. *Crop Sci.* 2005, 45, 820-831.
39. Holladay J.E., Bozell J.J., White J.F., Johnson D. Top Value-Added Chemicals from Biomass. Volume II-Results of Screening for Potential Candidates from Biorefinery Lignin. PNNL-16983, DE-AC05-76RL01830, 2007.
40. Rowell R.M., Pettersen R., Han J.S., Rowell J.S., Tshabalala M.A. Cell Wall Chemistry. In *Hanbook of Wood Chemistry and Wood Composites*. Rowell R.M., Ed. CRC Press: Boca Raton, FL, 2005, pp. 35-76.
41. Biomass feedstock composition and property database.
<http://www.eere.energy.gov/biomass/progs/search1.cgi>.
42. Ciolkosz D., Wallace R. A review of torrefaction for bioenergy feedstock production. *Biofuels, Bioprod. Biorefin.* 2011, 5, 317-329.
43. Antal, M.J., M. Gronli. The art, science and technology of charcoal production. *Industrial and Engineering Chemistry Research*, 42, 1619-1640, 2003.
44. Bell, M.J., F. Worrall. Charcoal addition to soils in NE England: A carbon sink with environmental co-benefits? *Sci. Total Environ.* 2011, 409, 1704-1714.
45. Rousset, P., C. Figueiredo, M. De Souza, W. Quirino. Pressure effect on the quality of eucalyptus wood charcoal for the steel industry: A statistical approach. *Fuel Process. Technol.*, 92, 1890-1897, 2011.
46. Mohan D., C.U. Pittman, P.H. Steele. Pyrolysis of wood/biomass for bio-oil: A critical review, *Energ. Fuel.* 2006, 20, 848-889.

47. Huber G.W., S. Iborra, A. Corma. Synthesis of transportation fuels from biomass: chemistry, catalysis and engineering. *Chemical Reviews*, 106, 4044-4096.
48. Neathery, J.K. Biomass gasification. In *Thermochemical Conversion of Biomass to Liquid Fuels and Chemical*. Croker M., Ed. RSC Publishing: Cambridge, UK, 2010, pp. 68-94, 2006.
49. Savage P.E., Levine R.B., Huelsman C.M. Hydrothermal Processing of Biomass. In *Thermochemical Conversion of Biomass to Liquid Fuels and Chemical*. Croker M., Ed. RSC Publishing: Cambridge, UK, 2010, pp. 192-221.
50. Van der Stelt M.J.C., Gerhauser H., Kiel J.H.A., Ptasinski K.J. Biomass upgrading by torrefaction for the production of biofuels: A review. *Biomass Bioenerg.* 2011, 35, 3748-3762.
51. Bergman, P. C., Boersma, A. R., Zwart, R. W. R., Kiel, J. H. A. *Torrefaction for biomass co-firing in existing coal-fired power stations (Biocoal)*. ECN-C--05-013, Energy Research Centre of the Netherlands: Petten, NL, 2005.
52. Bourgeois, J. P., Doat, J. Torrefied Wood from Temperate and Tropical Species. *Bioenergy* 1984, 3, 153-159.
53. Enviva. <http://www.envivabiomass.com/press-releases/conocophillips-enviva-lp-partner-to-develop-torrefied-wood-pellet-business/>
54. Yang H., Yan R., Chen H., Zheng C., Lee D.H., Liang D.T. In-Depth Investigation of Biomass Pyrolysis Based on Three Major Components: Hemicellulose, Cellulose and Lignin. *Energy Fuels* 2006, 20, 388-393.
55. Di Blasi C., Lanzetta M. Intrinsic kinetics of isothermal xylan degradation in inert atmosphere. *J. Anal. Appl. Pyrolysis* 1997, 40-41, 287-303
56. Prins M.J., Ptasinski K.J., Jansen F.J.J.G. Torrefaction of wood. Part 1. Weight loss kinetics. *J. Anal. Appl. Pyrolysis* 2006, 77, 28-34.
57. Muller-Hagedorn M., Bockhorn H., Krebs L., Muller U. A comparative study on the pyrolysis of three different wood species. *J. Anal. Appl. Pyrolysis* 2003, 68-69, 231-249.
58. Chew J.J., Doshi V. Recent advantages in biomass pretreatment – Torrefaction fundamentals and technology. *Renew. Sust. Energ. Rev.* 2011, 15, 4212-4222.

59. Repellin V., Govin A., Rolland M., Guyonnet R. Modelling anhydrous weight loss of wood chips during torrefaction in a pilot kiln. *Biomass Bioenerg.* 2010, 34, 602-609.
60. Orfao J.J.M., Antunes F.J.A., Figueiredo J.L. Pyrolysis kinetics of lignocellulosic materials – three independent reaction models. *Fuel* 1999, 78, 349-358.
61. Varhegyi G., Antal M.J., Jakab E., Szabo P. Kinetic modelling of biomass pyrolysis. *J. Anal. Appl. Pyrolysis* 1997, 42, 73-87.
62. Varhegyi G., Antal M.J., Szekeley T., Szabo P. Kinetics of the Thermal Decomposition of Cellulose, Hemicellulose, and Sugar Cane Bagasse. *Energy Fuel* 1989, 3, 329-335.
63. Rousset P, Turner I, Donnot A, Perre' P. The choice of a low-temperature pyrolysis model at the microscopic level for use in a macroscopic formulation. *Ann. For. Sci.* 2006, 63, 213–229.
64. Prins M.J., Ptasiński K.J., Janssen F.J.J.G. More efficient biomass gasification via torrefaction. *Energy* 2006, 31, 3458-3470.
65. Pach M, Zanzi R, Bjørnbom E. Torrefied biomass a substitute for wood and charcoal. In *Proceedings of the 6th Asia-Pacific International Symposium on Combustion and Energy Utilization*, Kuala Lumpur, Malaysia, 2002. (I 34 U TABELI 1)
66. Prins M.J., Ptasiński K.J., Jansen F.J.J.G. Torrefaction of wood. Part 2. Analysis of products. *J. Anal. Appl. Pyrolysis* 2006, 77, 35-40.
67. Couhert C., Salvador S., Commandre J. Impact of torrefaction on syn-gas production from wood. *Fuel* 2009, 88, 2286–2290. (33 U TABELI 1)
68. Zanzi R., Ferro D., Torres A., Soler P.B., Bjornbom E. Biomass torrefaction,. In *Second World Conference and Technology Exhibition on Biomass for Energy, Industry and Climate Protection*, Rome, Italy, 2004. (32 u tabeli 1).
69. Bridgeman T.G., Jones, J.M., Shield, I., Williams, P.T. Torrefaction of reed canary grass, wheat straw and willow to enhance solid fuel qualities and combustion properties. *Fuel* 2008, 87, 844–856.
70. Pimchuai, A., Dutta, A., Basu, P. Torrefaction of agriculture residue to enhance combustible properties. *Energy and Fuel* 2010, 24, 4638–4645.

71. Ferro, D. T., Vigouroux, V., Grimm, A., Zanzi, R., Torrefaction of agricultural and forest residues. In *Proceedings of Cubasolar International Conference*, Guantanamo, Cuba, 2004.
72. Kargbo F.R., Xing J., Zhang Y., . Pretreatment for energy use of rice straw: A review. *African Journal of Agricultural Research* 200, 94, 1560-1565.
73. Nimlos, M.N., Brooking, E., Looker, M.J., Evans, R.J. Biomass torrefaction studies with a molecular beam mass spectrometer. *Prep. Pap.-Am. Chem. Soc., Div. Fuel Chem.* 2003, 48, 590-591.
74. Bridgeman T.G., Jones, I., Williams, P.T., Waldron D.J. An investigation of the grindability of two torrefied energy crops. *Fuel* 2010, 89, 3911-3918.
75. Arias B, Pevida C., Feroso J., Plaza M.G., Rubiera F., Pis J.J Influence of the torrefaction on grindability and reactivity of woody biomass. *Fuel Process. Technol.* 2008, 89, 169-175.
76. Yan W, Hastings J, Acharjee T, Coronella C and Vasquez V, Mass and energy balances of wet torrefaction of lignocellulosic biomass. *Energ. Fuel* 2010, 24, 4738-4742.
77. Lipinsky RS, Arcate JR and Reed T, Enhanced wood fuels via torrefaction. *Am. Chem. Soc. Div. Fuel Chem.* 2002, 47, 408-410.
78. Turner, I., Rousset, P., Remond, R., Perre, P., . An experimental and theoretical investigation of the thermal treatment of wood (*Fagus sylvatica* L.) in the range 200-260 °C. *Int. J. Heat Mass Trans.* 2010, 53, 715-725.
79. Medic D, Darr M, Potter B, Shah A. Effect of torrefaction process parameters on biomass feedstock upgrading. *Fuel* 2012, 91, 147-154.
80. Li H., Liu X., Legros L., Bi X.T., Lim C.J., Sokhansanj S. Torrefaction of sawdust in a fluidized bed reactor. *Bioresource. Technol.* 2012, 103, 453-458.
81. Budarin, V.L., Milkowski, K.J., Shuttleworth, P., Lanigan, B., Clark, J.H., Macquarrie, D.J., Wilson, A., Microwave torrefaction of biomass, US Patent US 2011/021979 A1, 07.01.2010.
82. Ren S., Lei H., Julson J., Wnag L., Bu Q., Ruan R. Microwave Torrefaction of Corn Stover. Paper 1110765. Annual International Meeting of the ASABE, Louisville, KN, 2010.

83. Yan W, Hastings J, Acharjee T, Coronella C and Vasquez V, Mass and energy balances of wet torrefaction of lignocellulosic biomass. *Energ. Fuel* 2010, 24, 4738–4742.
84. Allen S, Kam L, Zemann A and Antal M, Fractionation of sugar cane with hot, compressed, liquid water. *Ind. Eng. Chem. Res* 1996, 35, 2709–2715.
85. Petchpradab P, Yoshida T, Charinpanitkul T and Matsumura Y, Hydrothermal pre-treatment of rubber wood for the saccharification process. *Ind. Eng. Chem. Res.* 2009, 48, 4587–4591.
86. Uslu A., Faaij A., Bergman P. Pre-treatment technologies, and their effect on international bioenergy supply chain logistics. Techno-economic evaluation of torrefaction, fast pyrolysis and pelletisation. *Energy* 2008, 33, 1206 –1223.
87. Magalhaes A., Petrovic D., Rodriguez A., Putra Z., Thielemans G. Techno-economic assessment of biomass pre-conversion processes as a part of biomass-to-liquids line-up. *Biofuels, Bioprod. Biorefin.* 2009, 3, 584–600.
88. Bergman, P. C., Boersma, A. R., Zwart, R. W. R., Kiel, J. H. A. *Combined torrefaction and pelletisation. The TOP process.* ECN-C--05-073, Energy Research Centre of the Netherlands: Petten, NL, 2005.
89. Sadaka, S., Negi, S. Improvements of biomass physical and thermochemical characteristics via torrefaction process. *Environ. Prog. Sustainable Energy* 2009, 28, 427–434.
90. Acharjee T.C., Coronella C.J., Vasquez V.R. Effect of thermal pretreatment on equilibrium moisture content of lignocellulosic biomass. *Bioresour. Technol.* 2011, 102, 4849-4854.
91. Kobayashi, N., Okada, N., Hirakawa, A., Sato, T., Kobayashi, J., Hatano, S., Itaya, Y., Mori, S.,. Characteristics of solid residues obtained from hot-compressed-water treatment of woody biomass. *Ind. Eng. Chem. Res.* 2009, 48, 373–379.
92. Felfli, F.F., Luengo, C.A., Suarez, J.A., Beaton, P.A. Wood briquette torrefaction. *Energy Sustainable Dev.* 2005, 9, 19-22.
93. Svoboda K, Pohorely M, Hartman M and Martinec J. Pre-treatment and feeding of biomass for pressurized entrained flow gasification. *Fuel Process. Technol.* 2009, 90, 629–635

94. Deng J, Wang G, Kuang J, Zhang U and Luo Y. Pre-treatment of agricultural residues for co-gasification via torrefaction. *J. Anal. Appl. Pyrol.* 2009, 86, 331–337.

Chapter 3. Effects of torrefaction process parameters on biomass feedstock upgrading

A paper published in *Fuel*

D. Medic *, M. Darr, A. Shah, B. Potter, and J. Zimmerman

Department of Agricultural and Biosystems Engineering, Iowa State University, 100 Davidson Hall, Ames, IA 50011, USA

* Corresponding author. E-mail address: dmedic@iastate.edu (D. Medic)

Abstract

Biomass is a primary source of renewable carbon that can be utilized as a feedstock for biofuels or biochemicals production in order to achieve energy independence. The low bulk density, high moisture content, degradation during storage and low energy density of raw lignocellulosic biomass are all significant challenges in supplying agricultural residues as a cellulosic feedstock. Torrefaction is a thermochemical process conducted in the temperature range between 200 and 300 °C under an inert atmosphere, which is currently being considered as a biomass pretreatment. Competitiveness and quality of biofuels and biochemicals may be significantly increased by incorporating torrefaction early in the production chain, while further optimization of the process might enable its autothermal operation. In this study, torrefaction process parameters were investigated in order to improve biomass energy density, and reduce its moisture content. The biomass of choice (corn stover) was torrefied at three moisture content levels (30, 45 and 50%), three different temperatures (200, 250 and 300 °C), and three unique reaction times (10, 20 and 30 min).

Solid, gaseous, and liquid products were analyzed, and the mass and energy balance of the reaction was quantified. An overall increase in energy density (2-19%) and decrease in mass and energy yield (3-45% and 1-35% respectively) was observed with the increase in process temperature. Mass and energy losses also increased with an increase in the initial biomass moisture content.

Keywords. Biomass; corn stover; torrefaction; pretreatment.

Introduction

Energy has always played an important role in life, survival, and the development of mankind. Even though it has been superseded by more potent fossil energy sources during the last 200 years, biomass has played a major role in supplying energy since the beginning of civilization, and still plays an important role in economies of developing countries.

Biomass recently has received renewed attention worldwide, mainly as a consequence of high and volatile oil prices, and global climate changes caused by increased fossil fuel consumption. Moreover, rapid economic growth in developing countries, high dependence on global and local transportation, pollution, depletion of sources, and endangered national security of energy importing countries have raised the awareness of the need for non-fossil based renewable energy sources [1-3]. Among renewable energy sources, such as wind, solar, geothermal, wave, tidal and ocean thermal, biomass is the most likely short term energy source, with mature and readily applicable conversion technologies for the production of transportation compatible liquid fuels. Although in the long term other forms of renewable energy may supersede biomass it will still remain as the only source of renewable carbon needed for chemicals and synthetic materials production.

According to the Renewable Fuel Standard (RFS) from the Energy Independence and Security Act of 2007, the minimum annual quantity of renewable fuel in the US transportation sector should be increased from 9 billion in 2008 to 36 billion gallons in 2022, where after 2016 most of renewable fuel must be advanced biofuel derived from cellulosic feedstocks instead of food crops [4]. In order to sustain production demanded by the RFS significant amounts of lignocellulosic biomass has to be collected, stored, and converted into biofuels.

The low bulk density, high moisture content, and low energy density of biomass feedstocks have a negative effect on the feasibility of long distance feedstock transportation. Moreover, in order to supply a feedstock for continuous operation of biorefineries year round, biomass has to be collected from large and often distant areas and hauled either to local storage facilities, or to a refinery where it would be stored until conversion. Unfavorable physical properties of biomass dictate utilization of large storage facilities, which would further compromise economical use of biomass feedstock. In addition, storing such large amounts of wet biomass will further increase expenses through the high rate of dry matter loss due to microbial activity and the hazard of self-heating/combustion [5-8].

Thermochemical conversion technologies, such as pyrolysis, gasification and hydrothermal processing, along with biomass co-firing in existing coal fired power plants, might have an important role in the production of heat energy, advanced energy carriers, chemicals, solvents, and materials. However, all aforementioned technologies have strict demands regarding the physical condition of biomass feedstocks, such as particle size and shape which are conducive to optimal processing. Additionally the final end product characteristics and yields are also influenced by feedstock quality and composition [2].

Moreover, due to the recalcitrant nature of biomass it is difficult to grind it in a continuous and cost effective manner [7]. Heterogeneity of feedstocks can also influence refinery operation considering not only different types of biomass, for example demolition wood, agricultural residues, and dedicated energy crops, or different plant species, but also the same plant species grown in different areas [9, 10].

Torrefaction, sometimes also referred to as mild-pyrolysis, is a thermochemical process conducted in the temperature range between 200 and 300 °C, under an inert atmosphere and low heating rate. Torrefaction is currently being considered as a biomass feedstock pretreatment particularly for thermal conversion systems. During torrefaction various permanent gases and condensables, with high oxygen content, are formed mainly due to hemicellulose degradation. As a consequence the final solid product, so called torrefied biomass, will be composed mainly of cellulose and lignin, and characterized by increased brittleness, hydrophobicity, microbial degradation resistance, and energy density. Thus torrefaction can play a significant role in decreasing transportation and storage costs of large quantities of biomass needed to sustain biofuels production. In addition, torrefaction may have positive effect on pyrolysis, gasification, and co-firing units operation by lowering power consumption and cost for biomass grinding, eliminating compounds responsible for high acidity of pyrolysis oil, and by increasing the uniformity of biomass feedstocks [9-12].

About 30 years ago, the process of torrefaction was first utilized and operated commercially for the production of a reducing agent for the metallurgical industry, but since then it has received little attention. There have been several studies that investigated the effects of torrefaction on biomass properties and the composition of different fractions released during the process, but the majority of these have focused on dry woody biomass

which was finely ground before torrefaction. These experiments were conducted by utilizing either thermogravimetric analysis equipment (TGA) or small scale reactors [7, 10, 13, 14]. Since agricultural residues will play an important role in the production of advanced biofuels more research is needed to investigate the optimum torrefaction conditions for such feedstock.

The potential for torrefaction of agricultural residues immediately after the harvest, without drying and before significant size reduction should be investigated in order to incorporate torrefaction early in the supply chain, and maximize the benefit of the physical property changes induced through torrefaction. In this research the influence of torrefaction reaction time, temperature, and moisture content on the quantity and composition of torrefied corn stover was investigated. Quantitative and qualitative data from the analysis of solids, permanent gases, and condensable volatiles were used to investigate mass and energy flows in the torrefaction process. A Box-Behnken design of experiments was utilized in this research to statistically model the torrefaction process in terms of mass and energy yields, and evaluate the significance of temperature, time, and untreated corn stover moisture content as predictors of response variables. The results from this work will provide knowledge not only related to the influence of process parameters (time and temperature), but also related to the effect of moisture content of an untreated feedstock on the torrefied biomass characteristics.

Methods

Samples

Corn stover samples, harvested during the fall 2009, were obtained from Department of Agricultural and Biosystems Engineering at Iowa State University, Ames, Iowa. Corn stover biomass is a highly available agricultural residue in the Midwest, and has been proposed as a feedstock for advanced biofuels production. After harvest samples were stored in a cooling chamber at 3-5 °C to prevent feedstock degradation and minimize moisture loss.

Field harvested corn stover at 22 and 41% moisture content were selected as the medium and high test moisture levels. Additional corn stover was dried to provide a suitable low moisture test level. The size of samples was reduced in a hammer mill equipped with 25 mm screen.

Torrefaction Reactor

Torrefaction experiments were conducted in 2 liters stainless steel fixed bed reactor with 0.1m diameter and 0.25m height, heated by three ceramic heaters in close contact with the reactor wall and separately controlled by PID controllers. This setup was used for coarse control of temperature, while fine temperature control was performed through circulation of preheated nitrogen gas. Figure 9 shows the position of four thermocouples inside the torrefaction reactor used for the temperature control. Thermocouples were immersed in the biomass at four different heights (0.05, 0.1, 0.15 and 0.2m from the bottom of reactor). They were positioned along the circumference (diameter of 0.08m and origin at the axis of reactor) and shifted by 90°, as shown in Figure 9, top view. Nitrogen purge gas was used for maintaining an inert atmosphere during the experiments. For each experiment 4.5 L min⁻¹

($0.000075 \text{ m}^3 \text{ s}^{-1}$) of nitrogen was purged through the reactor. Outlet tubing was maintained at an elevated temperature of about $200 \text{ }^\circ\text{C}$ to prevent condensation of released volatiles.

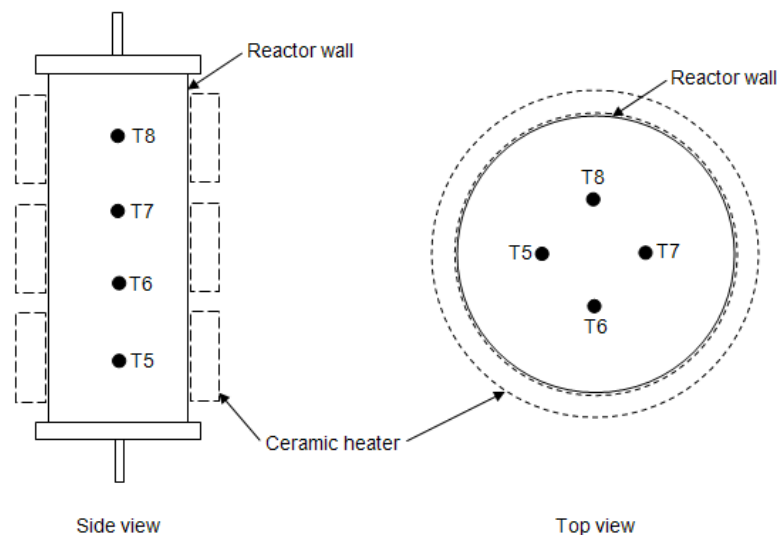


Figure 9. Position of four thermocouples (T5, T6, T7 and T8) utilized for controlling the temperature inside the reactor (not to scale)

For the purpose of comprehensively characterizing the torrefaction of corn stover the final torrefied solid product was recovered from the process and analyzed, while the volatiles released during the process as torrefaction gas were first separated into permanent gases and condensable volatiles (liquid), and then analyzed separately.

Gas Analysis

Volatiles and permanent gases released from the process were cooled immediately following release from the reactor, by means of glass impingers submerged in an ice bath. This facilitated removing the majority of the condensables and water from the gas sample. The remaining permanent gasses were then passed through desiccant columns before they

were analyzed by a Varian 490-GC micro-gas chromatograph (Varian, Palo Alto, CA) equipped with a Molsieve 5A and Poraplot U columns.

Liquids Analysis

Liquid fraction developed during the torrefaction process and collected in glass impingers was stored in the cooling chamber at 3-5 °C until it was analyzed. The water content in the condensed phase was analyzed according to the Karl-Fischer method by a moisture titrator (KEM MKS-500, Kyoto Electronics, Tokyo, Japan) and ASTM E 203–08 standard method [15]. Quantitative and qualitative analysis of organics present in condensed phase was conducted by a gas chromatograph equipped with Restek Stabilwax-DA column (Varian, Palo Alto, CA).

Proximate Analysis

Torrefied biomass samples were analyzed in a thermogravimetric analyzer TGA/DSC Star System (Mettler Toledo) according to a modified ASTM D 5142–04 method, in order to determine the content of moisture, volatiles, ash and fixed carbon [16]. Analysis was done under an inert atmosphere, obtained by purging nitrogen gas at flow rate of 100mL/min. Initially samples were heated to 105 °C at the heating rate of 10 °C/min. After retaining the samples at 105 °C for 40 min, these were further heated at the rate of 10 °C/min to 900 °C, and maintained at this temperature for 20 min. Subsequently the environment was changed to oxidative by purging 100mL/min of air for 30 min. The moisture content is determined by the mass loss after the heating period at 105 °C. Mass evolved between 105 °C and 900 °C represented volatile content, while the remaining was the fixed carbon content. The

remaining after heating the sample in oxidative atmosphere at 900 °C was considered to be ash.

Ultimate Analysis

Ultimate analysis of the solid fraction was done with PerkinElmer 2400 Series II CHNS/O Analyzer (PerkinElmer, Waltham, MA), according to ASTM D 5373–08 method [17]. Biomass samples were dried in an oven at 103 °C for 24 h before the ultimate analysis was conducted. Combustion was conducted at 925 °C under a helium atmosphere, while reduction was conducted at 650 °C.

High Heating Value Determination

The higher heating value of raw and torrefied biomass samples was computed using Equation 1 developed by Sheng and Azevedo [18].

$$\text{HHV (MJ/kg)} = -1.3675 + 0.3137 \cdot \text{C} + 0.7009 \cdot \text{H} + 0.0318 \cdot \text{O} \quad (1)$$

Where: C=percentage of carbon in biomass as determined by ultimate analysis; H=percentage of hydrogen in biomass as determined by ultimate analysis; O=percentage of oxygen determined by difference on dry and ash free basis, i.e. O (db, ash free)=100-C-H-N.

Design of Experiments

The set of torrefaction experiments conducted to meet the objectives of this project was based on a Box-Behnken experimental design, which is a three level design based on the combination of a two level factorial design and incomplete block design. It is useful for statistical modeling and optimization of a response variable of interest, which is a function of three or more independent variables. Moreover, Box Behnken design allows estimating coefficients in a second degree polynomial regression and modeling of a quadratic response

surface. The response surface can be further used for process optimization, identification of maximum or minimum responses, and significance of each involved factor or their combination. Furthermore, response surfaces can be used for calculating responses not only at experimentally investigated points, but also at any point on the surface [19-21]. Three factor-three level Box Behnken design, with 5 replicates at the center point and 17 runs in total was used in the experiments (Table 2). JMP statistical package from SAS (SAS Institute, Cary, NC) was used for the statistical analysis of experimental data.

Table 2. Box Behnken experimental design matrix generated by JMP

No.	Pattern	Moisture	Temperature	Time
1	--0	3	200	20
2	-0-	3	250	10
3	-0+	3	250	30
4	-+0	3	300	20
5	0--	22	200	10
6	0-+	22	200	30
7	000	22	250	20
8	000	22	250	20
9	000	22	250	20
10	000	22	250	20
11	000	22	250	20
12	0+-	22	300	10
13	0++	22	300	30
14	+ - 0	41	200	20
15	+ 0 -	41	250	10
16	+ 0 +	41	250	30
17	+ + 0	41	300	20

Results and Discussion

Process time and temperature were defined such that the torrefaction process temperature was the average of temperatures measured by four thermocouples within the torrefaction reactor during the experiment. The torrefaction start time was measured from the point when the temperature first reached the temperature proposed by the experimental

design. Figure 10 depicts an average temperature profile for one of the experiments at 250 °C.

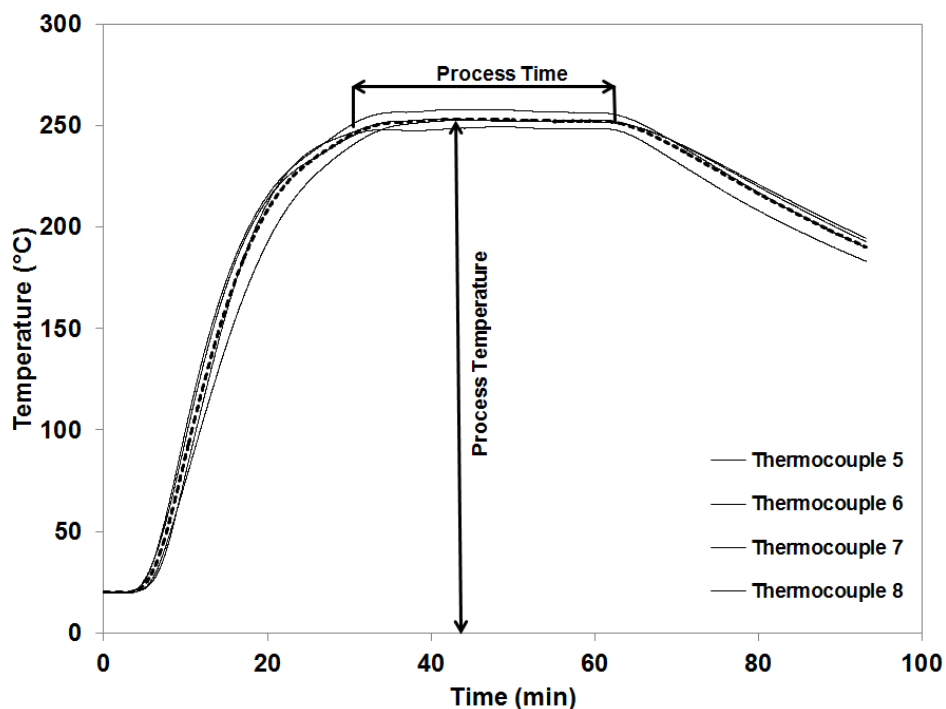


Figure 10. Temperature profiles for four thermocouples and average temperature profile (denoted by dashed line) used to determine process temperature and time

Mass balances for the torrefaction process were computed based on the results from the solid, liquid and gas analysis, and expressed on dry basis in the Table 3. Mass balances for torrefaction experiments conducted at low temperatures proved accurate, regardless of moisture content and time. However, at 300 °C errors in mass balance occurred mainly due to the lower yield of directly weighable torrefied solids, and an increased yield of volatiles that condensed throughout the exhaust system, and were hard to recover completely. Additionally, a high amount of aerosols formed at this temperature would require either electrostatic precipitators or filters to accurately account for their mass.

Table 3. Total mass balance for torrefaction experiments

Sample ID	Raw Biomass Moisture Content (%)	Process Parameters		Torrefied Biomass Yield (%)	Yield of Condensables (%)	Yield of Permanent Gases (%)
		Temp. (°C)	Time (min)			
3-200-20	3.2	200	20	97.1	0.02	0.4
3-250-10	3.2	250	10	86.6	1.79	1.1
3-250-30	3.2	250	30	84.4	4.07	1.4
3-300-20	3.2	300	20	57.4	13.30	2.7
22-200-10	22.1	200	10	98.1	0.39	0.5
22-200-30	22.1	200	30	98.4	0.40	0.6
22-250-20	22.1	250	20	86.2	4.32	1.3
22-250-20	22.1	250	20	85.3	4.37	1.3
22-250-20	22.1	250	20	83.4	4.39	1.5
22-250-20	22.1	250	20	83.5	4.26	1.4
22-250-20	22.1	250	20	83.4	4.09	1.4
22-300-10	22.1	300	10	58.0	11.52	2.0
22-300-30	22.1	300	30	53.9	18.39	3.3
41-200-20	41.0	200	20	91.2	0.66	0.6
41-250-10	41.0	250	10	80.0	3.79	1.2
41-250-30	41.0	250	30	78.7	6.11	1.3
41-300-20	41.0	300	20	56.3	18.59	2.9

There was an overall trend toward a decrease in yield of solids, and increase in yield of permanent gases and condensable products as both temperature and reaction time increased (Table 3). Loss of solids was much more pronounced between 250 and 300 °C, than between 200 and 250 °C, regardless of moisture content of samples. This was likely due to higher reactivity or more extensive devolatilization and carbonization of hemicellulose fraction above 250 °C. Along with degradation of hemicellulose, initial reactions of cellulose decomposition might occur in this temperature regime, as proposed by other researchers [22]. The same trend was observed for the yield of condensables and permanent gases. However, at 300 °C, regardless of moisture content of raw feedstock, yield of condensables was much higher than yield of permanent gases, which might be evidence of more intensive

decomposition of not only hemicellulose, but also other polymer fractions. This would support the production of heavier compounds responsible for tar formation observed in condensed phase. There was an evident influence of moisture content on dry matter loss at 250 °C and especially at 200 °C, where mass loss of samples with 45% moisture content was 3 times higher than that of samples with 3 and 22% raw biomass moisture content (Figure 11).

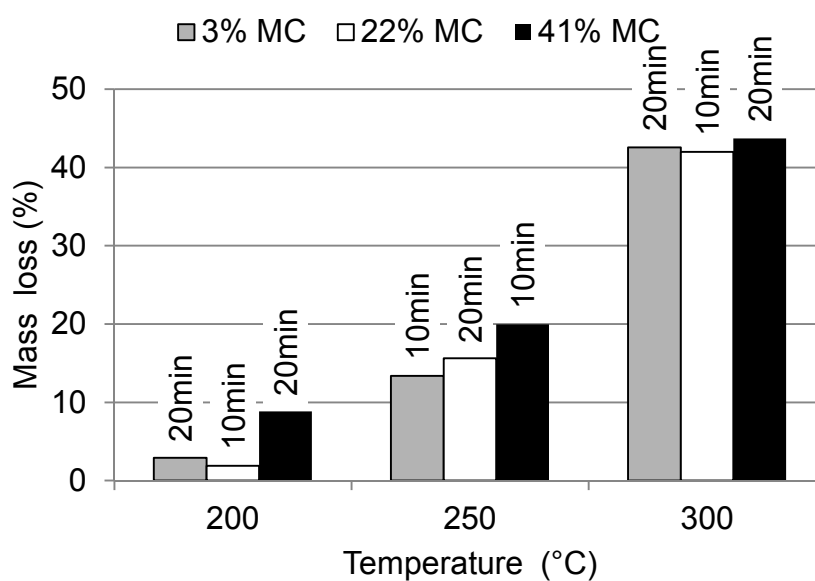


Figure 11. The effect of untreated biomass moisture content on mass loss of torrefied samples.

This interaction of mass loss and moisture content of the feedstock has not previously been reported in scientific journals, and is of high importance for designing a commercial scale torrefaction system. A possible reason for this might be the expansion of water vapor inside the plant polymer matrix during the ramping stage of biomass heating. This expansion loosens the material and makes it less resistive to heat transfer. Since water has a higher heat conduction coefficient than both air and nitrogen it enhances heat transfer through samples

with high moisture content. Prins [23] has proposed that at heating rates lower than 50 °C/min the parameter that restricts torrefaction reaction is reaction kinetics rather than heat transfer through the particle. Nevertheless, this might not be true since the particle size in these experiments were relatively large and representative of a real agricultural residue feedstock.

Moreover, since a packed bed reactor was used in this project a higher specific heat of water vapor than nitrogen gas might increase the amount of heat delivered to the zones closer to the top of reactor and enhance degradation of biomass. Another cause might be probability of close contact between released acids with biomass polymers, especially hemicellulose, as a result of increased specific area caused by expansion of water vapor. According to Huber et al. [24], short chain organic acids may act as a catalyst, thus promoting mainly hemicellulose degradation at this reaction condition, but also to a lesser extent, degradation of other polymers. As a consequence of a more aggressive environment during the processing of high moisture biomass, milder conditions (temperature/time) might be used to achieve the same effect as in the case of lower moisture content biomass torrefied at more extreme conditions. Nevertheless, there was almost no difference between mass losses of different samples at the most extreme time/temperature combinations regardless of sample moisture content. This might be due to accelerated thermal degradation of cellulose and lignin, in this temperature zone, after the total amount of hemicellulose was decomposed at lower temperatures, which would ultimately eliminate any initial difference between the samples.

Experimentally obtained mass loss data were analyzed using JMP statistical software and fitted into response surface quadratic model. The reduced model, containing only significant terms is shown in Equation 2.

$$\text{Predicted Mass Loss} = 95.68 - 1.0396 * \text{Temperature} + 0.2491 * \text{Moisture} + 0.00284 * (\text{Temperature})^2 \quad (2)$$

Where: Temperature = °C and Moisture = wt%db.

The summary of fit and analysis of variance are included in Table 4 and Table 5 respectively. As can be seen from Table 4 the mass loss response surface model is in good agreement with actual data obtained in experiments.

Table 4. Summary statistics for the mass loss response surface model with three predictors: moisture, temperature and time

R ²	0.993
R ² adjusted	0.985
Root Mean Square Error	1.807

Table 5. ANOVA for the mass loss response surface model with three predictors: moisture, temperature and time

Source	DF	Sum of	Mean	F Ratio	Prob. > F
Model	9	3465.10	385.01	117.82	<0.0001*
Error	7	22.87	3.268		
Corrected	16	3487.97			

* Significant

According to the model, temperature, moisture, and temperature squared were the only significant parameters (Table 6). The strength of effect of two significant process parameters on the dry matter mass loss is better revealed by surface plot in Figure 12. The effect of the moisture content of the raw biomass on dry matter loss is depicted in the plot by the more pronounced curvature in the temperature region below 260 °C and moisture content above 20%.

Table 6. List of all terms used to obtain mass loss and energy yield models and their respective p -values

Term	Mass loss model Prob.> t	Energy yield model Prob.> t
Intercept	< 0.0001*	< 0.0001*
Time	0.1964	0.3783
Temperature	< 0.0001*	< 0.0001*
Moisture	0.0069*	0.0025*
Time*Temperature	0.2630	0.4481
Time*Moisture	0.8106	0.8937
Temperature*Moisture	0.2260	0.4481
(Time) ²	0.8546	0.6227
(Temperature) ²	< 0.0001*	0.0002*
(Moisture) ²	0.0848	0.0211*

*Significant terms (as determined by JMP statistical package)

As revealed by Figure 13, water represents the largest portion of condensables released during the torrefaction process, followed by acetic acid, furfural, methanol, and hydroxyacetone, but in much smaller quantities. The water represented in Figure 13 is only reaction water and does not include water associated with the initial moisture content of the biomass. Water is formed in the process of polymer dehydration through the release of hydroxyl groups, while acetic acid and methanol are formed from acetoxy and methoxy groups attached to hemicellulose sugar monomers and lignin. Other compounds are generated at high temperatures by thermal decomposition of monomers [11].

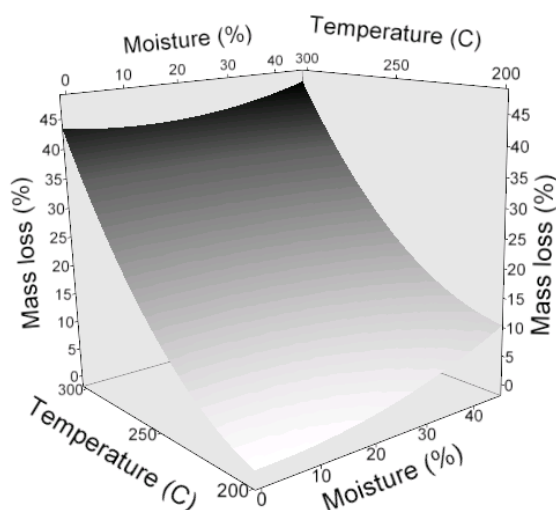


Figure 12. Surface plot of the effect of temperature and moisture content of raw biomass on predicted mass loss (time = 20 min)

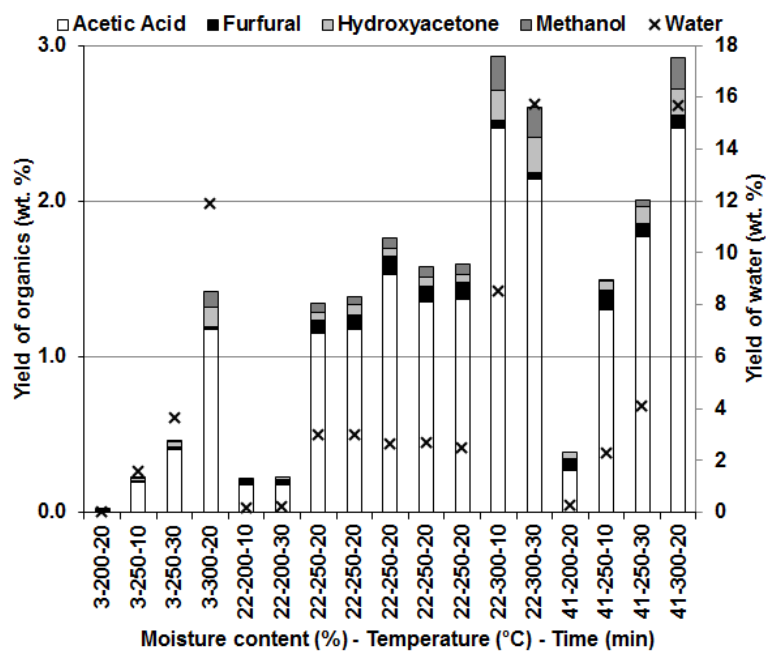


Figure 13. Composition of condensable volatiles released during torrefaction (The amount of water produced in torrefaction reaction and condensed together with organics was determined as a difference between the total water content in condensable phase and initial biomass moisture content. Only the reaction water is shown in Figure 13.)

As can be seen in Figure 13, the amount of condensables released during torrefaction of biomass samples with initial moisture content of 22 and 41% are not significantly different. However, they are two times higher than in the case of torrefaction of samples with 3% initial moisture content.

Figure 14 shows the composition of permanent gas phase released during the torrefaction of biomass with different initial moisture contents and at various combinations of process parameters. In Figure 14, only carbon monoxide and carbon dioxide are shown, since these are the main gas components, even though traces of methane and hydrogen were present at high reaction temperature.

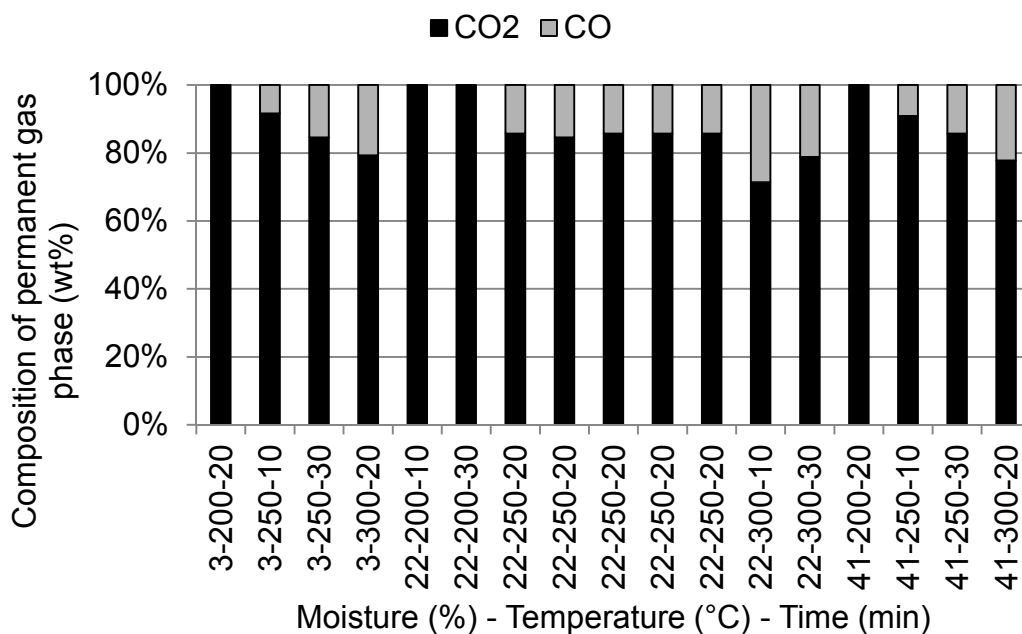


Figure 14. Change in permanent gas composition with process parameters and raw biomass moisture content

As can be seen in Figure 14, the ratio of carbon monoxide and carbon dioxide increases with the increase in both temperature and time. This is different from the influence

of time on mass yield which does not have a significant effect. The composition of the permanent gas phase is not affected significantly by moisture content of raw feedstock. Production of carbon dioxide during the process might be explained by decarboxylation of acid groups attached to hemicellulose, while carbon monoxide may be produced in the reaction of carbon dioxide and steam with char at high temperatures [25].

Figure 15 shows the results of the proximate analysis of corn stover torrefied at different treatment conditions. As can be seen in Figure 15, temperature has the strongest effect on torrefied biomass composition. Moreover, as the temperature increases the amount of fixed carbon follows the same trend and rises from about 1.5 up to 3 times, at 250 °C and 300 °C respectively, relative to untreated biomass. This is a consequence of the more extensive removal of hydrogen and oxygen from biomass, although some carbon will be released in the form of hydrocarbons. There is a trend in the reduction of volatiles content by about 30% at the highest temperature as a result of aforementioned changes in biomass composition. This torrefied material will produce less organic compounds and aerosols during combustion, and has a higher heating value. Water content of torrefied corn stover determined during proximate analysis was water adsorbed by biomass while it was waiting for the analysis in the TGA's auto-sampler.

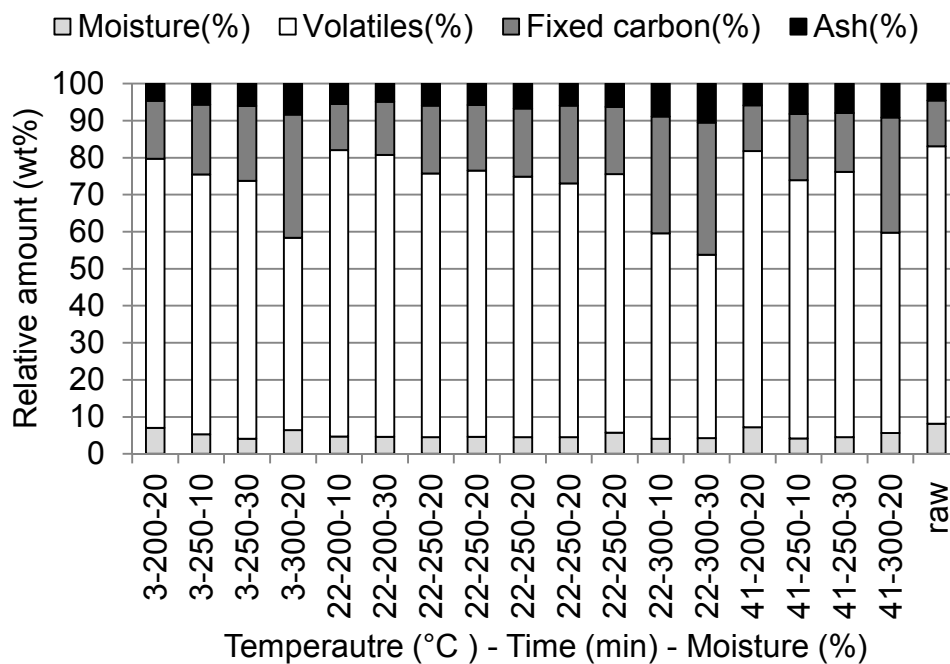


Figure 15. Proximate analysis of torrefied and raw corn stover

Torrefaction increases the amount of atomic carbon while decreases the amount of atomic hydrogen and oxygen as shown in Table 7. A consequence of this change in the chemical composition was a decrease in the O/C and H/C ratio of torrefied biomass in comparison to raw biomass. This is due to the release of volatiles rich in hydrogen and oxygen, such as water and carbon dioxide. The decrease in O/C, regardless of the moisture content in the raw biomass, can be up to about 7, 15 and 45% at 200, 250 and 300 °C respectively. This change in the chemical composition of biomass improves its quality as an energy source through an increase in energy density, since more oxygen than carbon is lost in the form of volatiles.

Table 7. Ultimate analysis and computed energy density of torrefied samples^a

Sample	C	H	N	O ^b	HHV ^c
3-200-20	45.8	5.5	0.5	48.2	18.4
3-250-10	47.7	5.3	0.6	46.4	18.8
3-250-30	49.1	5.4	0.6	45.0	19.2
3-300-20	58.7	4.7	0.7	35.8	21.5
22-200-10	45.7	5.7	0.7	47.9	18.5
22-200-30	45.8	5.5	0.6	48.1	18.4
22-250-20	49.1	5.4	0.7	44.8	19.2
22-250-20	48.3	5.5	0.6	45.6	19.1
22-250-20	49.2	5.4	0.7	44.7	19.3
22-250-20	49.4	5.4	0.6	44.5	19.3
22-250-20	48.7	5.4	0.6	45.3	19.1
22-300-10	56.6	4.9	0.9	37.6	21.0
22-300-30	59.0	4.7	1.0	35.4	21.6
41-200-20	45.6	5.4	1.0	48.0	18.2
41-250-10	48.2	5.3	0.9	45.6	18.9
41-250-30	48.8	5.2	0.9	45.1	19.0
41-300-20	55.8	4.8	1.1	38.2	20.8
Raw	44.2	5.8	0.5	49.5	18.2

^aSulfur levels for all analyzed samples were at levels lower than analyzer's precision level and were discarded as uncertain.

^bDetermined by difference

^cCalculated

Another important characteristic of torrefied corn stover is its increase in energy density when compared to raw biomass. This is the result of a decrease in mass of torrefied samples through the release of compounds rich in oxygen and hydrogen. It can be seen in Figure 16 that temperature has strongest impact on energy density of torrefied biomass, while the effect of time and moisture is much less expressed.

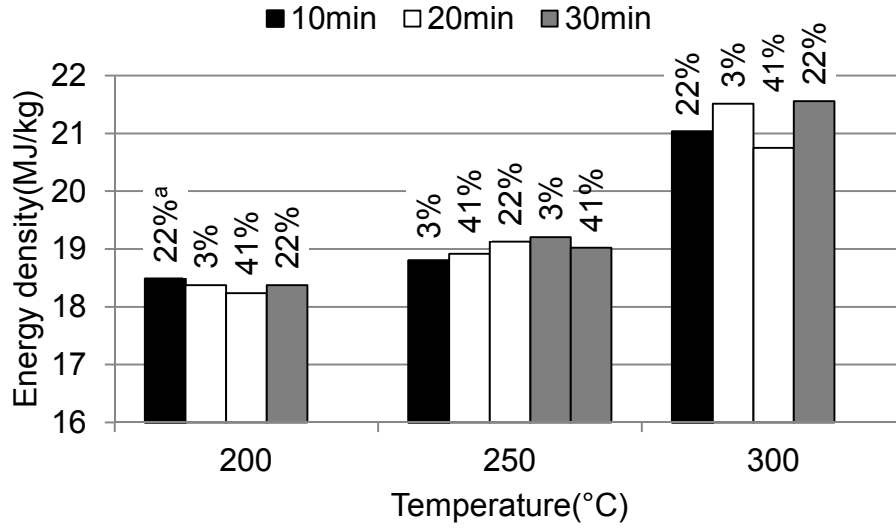


Figure 16. Effect of process parameters and raw biomass moisture content on energy density of torrefied material

Energy yield per dry raw biomass indicates the total energy preserved in the torrefied biomass. It was computed from mass yield and higher heating values using Equation 3 and expressed as a percentage of energy content of untreated dry biomass.

$$E_{\text{yield}} (\%) = (m_{\text{torrefied}} / m_{\text{initial}})_{\text{dry basis}} * (E_{\text{torrefied}} / E_{\text{initial}})_{\text{dry basis}} * 100 \quad (3)$$

Where: $m_{\text{torrefied}}$ = mass of biomass feedstock measured after torrefaction expressed on dry basis; m_{initial} = mass of untreated (raw) biomass feedstock measured before torrefaction expressed on dry basis; $E_{\text{torrefied}}$ = specific energy content of biomass feedstock after torrefaction expressed on dry basis; $E_{\text{initial-dry basis}}$ = specific energy content of biomass feedstock before torrefaction expressed on dry basis

Energy yields computed using Equation 3 are shown in Figure 17.

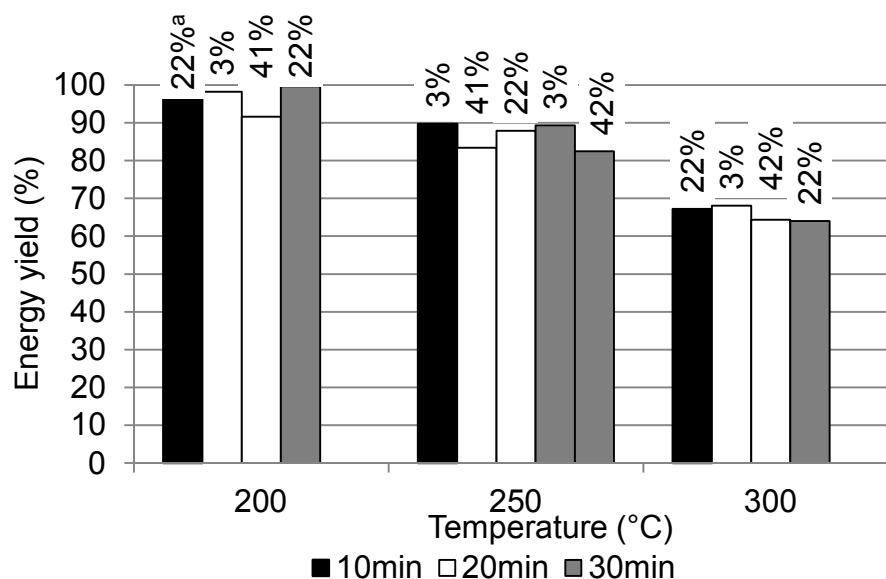


Figure 17. Effect of process parameters and initial moisture content of untreated biomass on energy yield (^araw biomass moisture content on a wet basis)

These values were fitted to response surface model represented by Equation 4, in order to analyze the effect of process parameters on energy yield.

$$\text{Predicted Energy Yield} = 10.0379 - 0.0144 * \text{Moisture} + 0.9278 * \text{Temperature} \\ 0.00721 * (\text{Moisture})^2 - 0.002461 * (\text{Temperature})^2 \quad (4)$$

Where: Temperature = °C and Moisture = wt%db.

As shown in Table 8 and Table 9, the model (Equation 4) was in good correlation with the actual data as justified by relatively high R^2 values (a measure of the amount of deviation around mean explained by the model). The small p-value in the ANOVA indicates high model significance.

Table 8. Summary statistics for the energy yield response surface model with three predictors: moisture, temperature and time

R ²	0.989
R ² adjusted	0.977
Root Mean Square Error	1.804

Table 9. ANOVA for the for the energy yield response surface model with three predictors: moisture, temperature, and time

Source	DF	Sum of	Mean Square	F Ratio	Prob. > F
Model	9	2253.06	250.341	76.88	< 0.0001*
Error	7	22.79	3.256		
Corrected	16	2275.86			

*Significant

In this model (Equation 4) the significant parameters are temperature, temperature squared, moisture and moisture squared (Table 6). As revealed in Figure 18, biomass torrefied at lower temperatures has the highest energy yield, which was expected since this parameter was strongly dependent on mass yield which was significantly affected by process temperature. Moisture has much less influence on energy yield than temperature as seen in Figure 18.

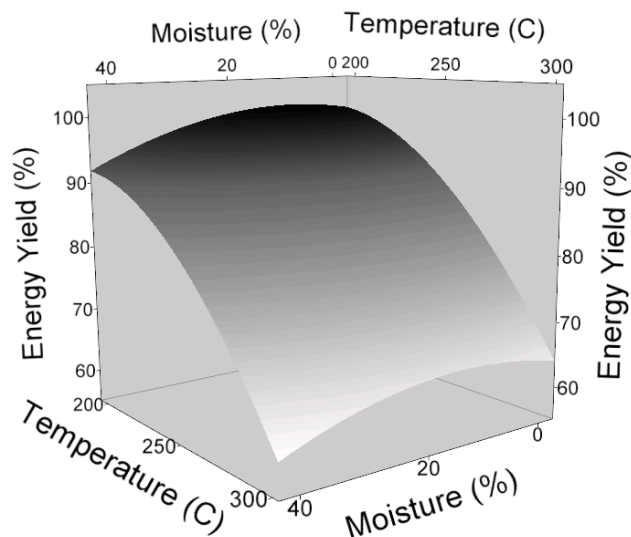


Figure 18. Surface plot of the effect of temperature and moisture content of raw biomass on predicted energy yield (time = 20 min)

However, the initial moisture content induced up to 10% more energy loss at temperatures below 220 °C and raw biomass moisture content higher than 20%. This was correlated with mass loss and justified by the similar contour plot curvature in Figure 12. Moreover, as displayed in Figure 18, moisture had a stronger influence on energy yield than on mass loss, even at 300 °C. This might be due to the loosening effect of water on fibrous matrix, its role in polymer hydrolysis, and formation of organic acids that promotes more extensive cellulose and lignin degradation through high energy volatile compounds, such as tar.

Conclusions

Corn stover undergoes changes in chemical composition, mass, and energy content during the torrefaction process. As expected these changes were more extensive at high temperatures and characterized by mass loss of up to 45% as well as a decrease in the O/C

ratio from 1.11 to 0.6 and an increase in the energy density of about 19%. However, high mass loss offset gain in energy density and significantly reduced overall energy yield. Moisture content had a significant effect on energy density, mass and energy yield, and generally induced a reduction in each of these parameters. Moreover, the effect of moisture is more pronounced at lower temperatures, where if moisture content in raw biomass is increased from 22% to 44%, energy yield could be reduced by about 10%. Nevertheless, there is a raw biomass moisture content window between 3% and approximately 20% that can allow for the use of corn stover feedstock directly from the field without any negative effect on energy yield.

Despite inevitable losses in energy yield during the process, additional research in the future might justify the use of torrefaction as a biomass pretreatment or upgrading step, by obtaining data that will prove savings in torrefied biomass particle size reduction, improvements in storage stability, hydrophobicity, and chemical properties important for thermochemical processes, such as pyrolysis, gasification, and co-firing.

Acknowledgements

Funding for this project was provided by the ConocoPhillips Company. Additional technical support was provided by CSET (Center for Sustainable Energy, Iowa State University, Ames) and BCRF (Biocentury Research Farm, Iowa State University, Ames). We would like to thank Andy Suby, Samuel Jones, Patrick Johnston and Marge Rover for their contribution to this work.

References

1. Demirbas A. Biofuels. London: Springer; 2009.

2. Klass D. L. Biomass for Renewable Energy, Fuels and Chemicals. San Diego: Academic Press; 1998.
3. WEC, World Energy and Climate Policy: 2009 Assessment. 2009, World Energy Council: London, UK.
4. The Energy Independence and Security Act of 2007, Pub. L. No. 110-40 H.R. 6, 121 Stat. 1492 (January 7. 2007)
5. BRDI, Roadmap for Bioenergy and Biobased Products in the United States. Biomass Research and Development Initiative, October 2007.
6. Bridgeman T. G., Jones J. M., Shield I., Williams P.T. Torrefaction of reed canary grass, wheat straw and willow to enhance solid fuel qualities and combustion properties. Fuel 2008;87:844-56.
7. Arias B., Pevida C., Feroso J., Plaza M. G., Rubeira F., Pis J. J. Influence of torrefaction on the grindability and reactivity of woody biomass. Fuel Processing Technology 2008;89:169-75.
8. Lipinsky E. S., Arcate J. R., Reed T. B. Enhanced Wood Fuels via Torrefaction. Inovative Thinking, Inc.: Fuel Chemistry Division Preprints 2002;47:408-10.
9. Yan W., Acharjee T. C., Coronella C. J., Vaquez R. V. Thermal Pretreatment of Lignocellulosic Biomass. Environmental Progress and Sustainable Energy 2009;28:435-40.
10. Bergman P. C. A., Boersma A. R., Zwart R. W. R., Kiel J.H.A. Torrefaction for Biomass Co-firing in Existing Coal-Fired Power Stations, The Netherlands: ECN: Petten; 2005.
11. Prins M. J., Ptasinski K. J., Janssen F. J. J.G. Torrefaction of wood. Part 2. Analysis of products, J Anal Appl Pyrol 2006;77:35-40.
12. Bergman P. C. A. Combined Torrefaction and Pelletization: The TOP Process, The Netherlands: ECN: Petten; 2005.
13. Couhert C., Salvador S., Commandre J-M. Impact of torrefaction on syngas production from wood. Fuel 2009;88:2286-90.
14. Prins M. J., Ptasinski K. J., Janssen F. J. J.G. Torrefaction of wood. Part 1. Weight Loss Kinetics, J Anal Appl Pyrol 2006;77:28-34.

15. ASTM E 203 – 08: Standard Test Method for Water Using Volumetric Karl Fischer Titration. 2008, ASTM Standards, Vol. 15.05.
16. ASTM D 5142 – 04: Standard Test Method for Proximate Analysis of the Analysis Sample of Coal And Coke by Instrumental Procedures. 2008, ASTM Standards, Vol. 05.06.
17. ASTM D 5373 – 08: Standard Test Method for Instrumental Determination of Carbon, Hydrogen and Nitrogen in Laboratory samples of Coal. 2008, ASTM Standards, Vol. 05.06.
18. Sheng C., Azevedo J. L. T. Estimating the higher heating value of biomass fuels from basic analysis data. *Biomass Bioenerg* 2005;28:499-507.
19. Box G. E. P., Behnken D. W. Some New Three Level Design for the Study of Quantitative Variables. *Tehcnometrics* 1960;2:455-75.
20. Carlborn K., Matuana L. M. Modeling and Optimization of Formaldehyde-Free Wood Composites Using a Box-Behnken Design. *Polym Composites* 2006;27:497-503.
21. Muthukumar M., Mohan D., Rajendran M. Optimization of Mix Properties of Mineral Aggregates Using Box Behnken Design of Experiments. *Cement Concrete Comp* 2003;25:751-8.
22. Koukious E. G., Mavrokoukoulakis J., Abatzoglou N. Energy densification of biomass. *Proceedings of 1st. National Conference on Soft Energy Forms; 1982; Thessaloniki, Greece.*
23. Prins M. J. *Thermodynamic analysis of biomass gasification and torrefaction.* The Netherlands: Technische Universiteit Eindhoven: Eindhoven; 2005
24. Huber G. W., Iborra S., Corma A. Synthesis of Transportation Fuels from Biomass: Chemistry, Catalysis and Engineering. *Chem Rev* 2006;106:4044-98.
25. White R. H., Dietenberger M. A. Wood Products: thermal degradation and fire. In: Buchow K. H. J., Cahn R. W., Flemings M. C., Ilschner B., Kramer E. J., Mahajan S., editors. *The Encyclopedia of Materials: Science and Technology.* Amsterdam, the Netherlands: Elsevier; 2001.

Chapter 4. Effect of torrefaction on water vapor adsorption properties and resistance to microbial degradation of corn stover

A paper published in *Energy & Fuels*

D. Medic^{*}, M. Darr, A. Shah, S. Rahn

Department of Agricultural and Biosystems Engineering, Iowa State University, 100

Davidson Hall, Ames, IA 50011, USA

* Corresponding author. E-mail address: dmedic@iastate.edu (D. Medic)

Abstract

The equilibrium moisture content (EMC) of biomass affects transportation, storage, downstream feedstock processing, and the overall economy of biorenewables production. Torrefaction is a thermochemical process conducted in the temperature regime between 200 and 300 °C under an inert atmosphere that, among other benefits, aims to reduce the innate hydrophilicity and susceptibility to microbial degradation of biomass. The objective of this study was to examine water sorption properties of torrefied corn stover. The EMC of raw corn stover, along with corn stover thermally pretreated at three temperatures, was measured using the static gravimetric method at equilibrium relative humidity (ERH) and temperature ranging from 10 to 98% and from 10 to 40 °C, respectively. Five isotherms were fitted to the experimental data to obtain the prediction equation which best describes the relationship between the ERH and the EMC of lignocellulosic biomass. Microbial degradation of the samples was tested at 97% ERH and 30 °C. Fiber analyses were conducted on all samples. In general, torrefied biomass showed an EMC lower than that of raw biomass, which implied an

increase in hydrophobicity. The modified Oswin model performed best in describing the correlation between ERH and EMC. Corn stover torrefied at 250 and 300 °C had negligible dry matter mass loss due to microbial degradation. Fiber analysis showed a significant decrease in hemicellulose content with the increase in pretreatment temperature, which might be the reason for the hydrophobic nature of torrefied biomass. The outcomes of this work can be used for torrefaction process optimization, and decision-making regarding raw and torrefied biomass storage and downstream processing.

Keywords: equilibrium moisture content, torrefaction, microbial degradation, corn stover, hydrophobicity

Introduction

Lignocellulosic biomass has recently gained renewed attention in developed countries as a sustainable, abundant, and readily available energy and carbon source. Furthermore, public concern about the negative environmental impacts of fossil fuels use, energy dependence on foreign petroleum, and volatile oil prices have promoted the use of biomass feedstock in energy, fuel, and chemical production. Biomass has characteristics distinct from traditional, fossil energy/carbon sources that make its application more costly and complex than traditional fossil fuels. A number of factors increase the cost of biorenewables production, including the high oxygen content of biomass and products derived from it, the low energy and bulk density of biomass, a recalcitrant and heterogeneous nature, and high moisture content [1]. Unlike other unfavorable biomass characteristics, high moisture content is the parameter that affects multiple steps in a biorenewables production chain, such as transportation, storage, and upgrading of lignocellulosic biomass. Moisture increases the cost

of transportation by increasing the amount of superfluous material that has to be transported [2]. Dry matter loss of wet biomass can be up to 30% depending on pretreatment and storage type, which increases overall production cost [1-3]. Furthermore, storage of large quantities of high moisture biomass represents a fire hazard due to spontaneous ignition [4,5]. The energy requirement for size reduction increases significantly as a consequence of the increase in moisture content of biomass [6,7]. Gasification of high moisture feedstock causes an increase in tar yield, a decrease in thermal efficiency of the system, and a decrease in operation temperature [8]. Moisture increases char yield and has a mixed effect on bio-oil yield and composition, depending on temperature and mineral matter content [9]. Moreover, the high water content decreases the heating value of biomass, causes ignition issues, demands large process equipment to handle large flue gas volume, and affects the overall combustion quality [10].

Adsorption is a process of gas, liquid or dissolved solid uptake by the surface of solid phase, driven by minimization of the surface free energy. Desorption is a process opposite to adsorption. Adsorbed atoms or molecules leave the surface of the solid phase, and return to gas or liquid phase as a result of desorption. It depends on temperature and pressure, so as adsorption [11,12]. Equilibrium moisture content (EMC) is established when the moisture content of material in question is in thermodynamic equilibrium with the relative humidity of the surrounding atmosphere at a particular temperature and pressure [13]. Therefore, change in the relative humidity of the environment affects the moisture content of any biological material at constant pressure and temperature [7]. The relationship between the EMC and the equilibrium relative humidity (ERH) at a constant temperature is expressed by moisture sorption isotherms [14]. The shape of isotherms gives insight into the mechanism of water

adsorption and depends on structure and composition of material, in addition to pressure and temperature [15]. Desorption isotherm does not necessarily have to be the same as adsorption isotherm. The former usually has higher values than adsorption isotherm in the midrange levels of relative humidity. This is referred to as sorption hysteresis. Several theories have been developed to explain occurrence of hysteresis, such as capillary condensation, phase change of non-porous solids and structural changes of non-rigid solids [11]. Understanding the relationship between EMC and ERH helps in designing drying, combustion, and thermochemical conversion systems; making decisions regarding storage methods for different biomass types; and improving product quality in general [16].

More than 270 models have been used in the literature to predict water vapor sorption characteristics in materials of biological origin. According to Van der Berg and Bruin [17], these models can be broadly classified into three categories: theoretical, semi-empirical, and empirical. Theoretical models are based on a monolayer/multilayer sorption and a condensed film, and employ constants that have physical meaning. This is the opposite of empirical models, whose constants are not related to material properties [18]. Moreover, there is no single model that is capable of representing sorption behavior of every biological material over a wide range of temperatures and relative humidity levels [19]. Five isotherm equations: modified Henderson, modified Chung-Pfost, modified Halsey, modified Oswin and Guggenheim-Anderson-deBoer (GAB) are accepted by the American Society of Agricultural and Biological engineers as standard models for describing the relationship between the ERH and the EMC of agricultural products [20].

Torrefaction is a thermochemical process conducted in the temperature range between 200 and 300 °C under an inert atmosphere and low heating rate. It is currently being

considered as a biomass feedstock pretreatment, particularly for thermal conversion systems. The final solid product, referred to as torrefied biomass, is composed mainly of cellulose and lignin. It is characterized by increased brittleness, hydrophobicity, microbial degradation resistance, and energy density. Thus, torrefaction can play a significant role in decreasing the costs of transportation and storage of biomass in the large quantities needed to sustain biofuels production [6,21].

A lot of research on the EMC-ERH relationship has been dedicated to fruits and vegetables, dairy, forage, grain, agricultural residues, and wood [22-27]. Several researchers investigated the water sorption of charcoal, coals, and activated carbon [28-30]. However, there have been only a few studies that investigated water adsorption properties of torrefied biomass [21,31].

The objective of this work was to assess the hydrophobic nature of thermally treated biomass. Therefore, water adsorption characteristics of raw and torrefied corn stover were determined experimentally at four temperatures and five relative humidity levels. In addition, the suitability of five models for fitting ASABE accepted isotherms was evaluated. A microbial degradation test was conducted to assess dry matter loss due to microbial growth at high ERH. Furthermore, fiber analysis test was performed to explain the lower water vapor adsorption onto torrefied corn stover.

Methods

Sample preparation

Corn stover biomass was harvested in the fall 2010 from Iowa State University research fields located in Story County, IA. The bulk wet samples were stored in a cooling

chamber at a temperature below 5 °C to preserve their original qualities and to prevent the microbial degradation.

Subsamples of the wet material were dried at 60 °C for 72h and stored in a desiccator until torrefaction or water vapor sorption experiments were conducted. The moisture content of samples before and after experiments was determined according to the ASAE standard for forage moisture measurement D358.2 [32]. All samples were ground and sifted before experiments to obtain physically uniform samples with a particle size less than 2mm. Ground corn stover biomass was torrefied at 200, 250 and 300 °C according to the method employed by Medic and co-workers [33] with the modifications that all samples were dried before the processing and were torrefied for 20 minutes.

Water vapor adsorption experiments

The EMC of biomass was determined at 10, 20, 30 and 40 °C using the static gravimetric method [34]. For this, 2g (0.0001g resolution) of samples were spread in a thin layer in Petri dishes and placed in hygrostats, which were sealed plastic containers. Duplicates of raw corn stover, and corn stover samples torrefied at 200, 250 and 300 °C were set in each hygrostat. Five saturated solutions of inorganic salts were used to control the ERH in the hygrostats as shown in Table 10 [35].

Table 10. ERH of saturated solutions at four temperature levels

Salt	Chemical formula	ERH (decimal)			
		10 °C	20 °C	30 °C	40 °C
Lithium chloride	LiCl	0.113	0.113	0.113	0.112
Magnesium chloride	MgCl ₂	0.335	0.331	0.324	0.316
Magnesium nitrate	Mg(NO ₃) ₂	0.574	0.544	0.514	0.484
Sodium chloride	NaCl	0.757	0.755	0.751	0.747
Potassium sulfate	K ₂ SO ₄	0.982	0.976	0.970	0.964

All salts were reagent grade (Fischer Scientific, Pittsburgh, PA). Solutions were prepared at 50 °C with excess salt to ensure a saturation condition. Remote data loggers to continuously measure and record temperature and relative humidity (HOBO U23 Pro v2, Onset Computer Corporation, Pocasset, MA) were placed in each hygrostat. An incubator with refrigeration capability (Isotemp incubator, Fischer Scientific, Pittsburgh, PA) was utilized to maintain different temperature levels (± 1 °C) during experiments. Samples EMC were assumed to be in equilibrium with the ERH when there was no difference (≤ 0.001 g) in three subsequent weight measurements. The weights of the biomass samples were measured every two days. The samples were covered with the lids immediately after removing them from the hygrosats. Only one sample at a time was outside the hygrostat. The duration of the whole process was less than 60 seconds per sample. Tukey-Kramer Honestly Significant Difference procedure, available in JMP pro 9 statistical package (SAS Institute, Cary, CA) was used for pairwise comparison of all EMC means.

Adsorption modeling

Relationships between ERH and EMC of raw and torrefied corn stover at four different temperatures and five different ERH levels were determined by fitting the experimental data using five isotherm models (Equations 1-5) suggested in ASAE standard D245.6 [20]. The GAB model is used in its adapted form to account for temperature influence [13, 36].

1. Modified Henderson model:

$$\text{EMC} = \left[\frac{\ln(1-\text{ERH})}{-A \cdot (t+B)} \right]^{\frac{1}{C}} \quad (1)$$

2. Modified Chung-Pfost model:

$$EMC = -\frac{1}{C} \ln \left[\frac{\ln(ERH)(t+B)}{-A} \right] \quad (2)$$

3. Modified Halsey model:

$$EMC = \left[\frac{-\exp(A+B \cdot t)}{\ln(ERH)} \right]^{\frac{1}{C}} \quad (3)$$

4. Modified Oswin model:

$$EMC = (A+B \cdot t) \left[\frac{ERH}{1-ERH} \right]^{\frac{1}{C}} \quad (4)$$

5. Modified GAB (Guggenheim-Anderson-deBoer) model:

$$EMC = \frac{A \cdot B_0 \cdot C_0 \cdot ERH}{(1-B_0 \cdot ERH)(1-B_0 \cdot ERH + B_0 \cdot C_0 \cdot ERH)} \quad (5)$$

$$B_0 = B \cdot \exp\left(\frac{H_1}{R \cdot T}\right)$$

$$C_0 = C \cdot \exp\left(\frac{H_2}{R \cdot T}\right)$$

Where: EMC = equilibrium moisture content (%_{db}); ERH = equilibrium relative humidity (decimal); A, B, C, B₀, C₀, H₁, H₂ = empirical constants (Note: Their values are specific to particular model.); t = temperature (°C); T = absolute temperature (K); R = universal gas constant (kJ kmol⁻¹ K⁻¹).

Non-linear regression was used to fit the aforementioned models into experimental results and obtain unknown coefficients. Regression analysis was done using JMP pro 9 statistical package (SAS Institute, Cary, CA). The procedure employed the Gauss-Newton algorithm to minimize the residual sum of squares between predicted and observed data in an iterative way. The adequacy of tested models was evaluated using different statistical criteria,

including mean percent relative error (MRE), residual sum of squares (RSS), root mean square error (RMSE), coefficient of determination (R^2), and plot of residuals [19, 37].

Relations 6-8 were used to determine MRE, RSS RMSE, and residuals, respectively.

$$\text{MRE} = \frac{100}{n} \sum_{i=1}^n \frac{|\text{EMC}_{\text{exp.}} - \text{EMC}_{\text{pred.}}|}{\text{EMC}_{\text{exp.}}} \quad (6)$$

$$\text{RSS} = \sum_{i=1}^n (\text{EMC}_{\text{exp.}} - \text{EMC}_{\text{pred.}})^2 \quad (7)$$

$$\text{RMSE} = \sqrt{\frac{\text{RSS}}{\text{df}}} \quad (8)$$

$$\text{Residual} = \text{EMC}_{\text{exp.}} - \text{EMC}_{\text{pred.}} \quad (9)$$

Where: n = number of observations; $\text{EMC}_{\text{exp.}}$ = experimentally obtained equilibrium moisture content; $\text{EMC}_{\text{pred.}}$ = equilibrium moisture content predicted by the model; df = degree of freedom.

The model with the smallest values of MRE, RMSE and RSS, as well as the largest value of R^2 was considered to be the best fit for the experimental data, and the most accurate description for the relationship between sample's EMC and ERH. Furthermore, a model was considered acceptable only if its plot of residual vs. predicted EMC showed no systematic spread or pattern [19].

Microbial degradation experiment

The microbial degradation test was conducted using the same equipment and experimental set up that was used for water vapor adsorption tests. The duration of the test was 30 days. During the experiment, temperature was maintained at 30 °C with the help of incubator. Relative humidity was maintained at 97% (saturated solution of K₂SO₄ salt). These parameters were chosen to promote natural microbial growth without any attempt to inoculate material by specific fungi species. Dry matter content of samples was determined before and after the experiment, according to ASAE standard method D358.2 [32].

Fiber analysis

Fiber analysis was done according to the National Renewable Energy Laboratory procedure [38]. In short, carbohydrates present in the biomass were dissolved in two stage sulfuric acid hydrolysis and the resulting monomers were analyzed by means of high performance liquid chromatography with refractive index detector (Varian ProStar 355/356, Varian Inc., Palo Alto, CA) and a column (Bio-Rad Aminex HPX-87P, Hercules, CA). Solid residual was weighed and considered to be acid insoluble lignin, while acid soluble lignin in hydrolysate was determined spectrometrically.

Results and discussion

Experimental results

The EMCs of raw and corn stover torrefied at 200 (T200), 250 (T250) and 300 °C (T300) are included in Table 11. EMC of all four types of biomass decreased with an increase in temperature during water adsorption experiments. The minimum and maximum EMC, with temperature in parentheses, of raw, T200, T250 and T300 were 1.77 (40 °C) and

45.38 (10 °C) %db; 1.63 (40 °C) and 42.88 (10 °C) %db; 1.18 (40 °C) and 25.68 (10 °C) %db; and 1.54 (40 °C) and 30.44 (20 °C) %db; respectively. This phenomenon is typical for biological products, and might be a consequence of the enhanced excitation states of water molecules at higher temperatures, which lowers cohesive forces between them [36].

Clausius-Clapeyron equation predicts shift of adsorption isotherms downwards due to increase in temperature, which is a consequence of more energy available for water vaporization and decrease in moisture binding energy [39,40]. As expected, EMC of biomass increased with an increase in ERH and, with no exception, samples exposed to the lowest and highest ERH also respectively had the lowest and highest EMC, regardless of pretreatment temperature. Dry raw corn stover had the highest EMC values at all temperatures for ERH above 0.4. There was no significant difference between samples below 0.4, according to Tukey-Kramer HSD test, regardless of environmental temperature. Furthermore, EMC of thermally treated samples decreased with the increase in torrefaction process temperature. This is mainly a consequence of a decrease in the number of water adsorption sites and changes in the material structure due to cleavage of hydroxyl groups from biomass polymers and the formation of non-polar unsaturated structures [6,41,42]. Moreover, hemicellulose fraction in biomass is degraded to different extents during torrefaction, depending on temperature [21]. Since the main mechanism of water adsorption onto biomass is binding to polar sites, such as hydroxyl groups in sugar molecules, elimination of hemicellulose also increases hydrophobicity [43]. The difference between hydrophobicity of corn stover torrefied at 250 and 300 °C is not statistically significant. Tukey-Kramer HSD test revealed that differences between ERH levels for the same sample and environmental temperature are all significant (not shown in Table 11). This is true regardless of sample type. If the samples

of the same kind and ERH, but different environmental temperature, are compared to each other no straightforward conclusion could be established. Moreover, the only exception is the highest ERH value at which all samples were significantly different. Therefore, hydrophobicity of thermally treated material was clearly expressed only at the highest ERH level, regardless of environmental temperature, with raw and samples torrefied at 250 °C having highest and lowest EMC, respectively.

Table 11. EMC of raw and torrefied corn stover

RH (decimal)	T (°C)	Sample	EMC (%db)	S.D. (%db)	Sample	EMC (%db)	S.D. (%db)	Sample	EMC (%db)	S.D. (%db)	Sample	EMC (%db)	S.D. (%db)
0.113	10	Raw	2.35	0.02	T200	2.13	0.19	T250	1.73	0.16	T300	1.86	0.04
0.335	10	Raw	5.75	0.10	T200	4.98	0.14	T250	3.84	0.21	T300	4.34	0.04
0.574	10	Raw	9.93	0.00	T200	8.53	0.16	T250	6.80	0.14	T300	6.84	0.13
0.757	10	Raw	15.50	1.07	T200	12.35	0.45	T250	9.95	0.04	T300	9.76	0.01
0.982	10	Raw	45.38	1.53	T200	42.88	0.91	T250	25.68	0.10	T300	26.13	0.86
0.113	20	Raw	2.06	0.05	T200	2.03	0.04	T250	1.51	0.14	T300	1.67	0.19
0.331	20	Raw	5.04	0.13	T200	4.31	0.05	T250	3.32	0.07	T300	3.90	0.01
0.544	20	Raw	8.04	0.02	T200	6.76	0.14	T250	5.20	0.08	T300	5.87	0.02
0.755	20	Raw	13.11	0.03	T200	11.20	0.04	T250	8.62	0.00	T300	8.90	0.06
0.976	20	Raw ^F	41.48	0.94	T200	33.14	0.02	T250	24.00	1.03	T300	30.34	0.27
0.113	30	Raw	1.99	0.02	T200	2.00	0.02	T250	1.70	0.09	T300	1.82	0.20
0.324	30	Raw	4.86	0.00	T200	4.01	0.03	T250	3.25	0.03	T300	3.66	0.09
0.514	30	Raw	7.41	0.05	T200	6.23	0.05	T250	4.84	0.01	T300	5.44	0.03
0.751	30	Raw	12.22	0.10	T200	10.68	0.05	T250	8.34	0.13	T300	8.65	0.01
0.97	30	Raw ^F	24.81	0.44	T200 ^F	23.24	1.45	T250 ^F	16.44	0.12	T300	15.57	0.06
0.112	40	Raw	1.77	0.27	T200	1.63	0.13	T250	1.18	0.00	T300	1.54	0.06
0.316	40	Raw	4.66	0.26	T200	3.79	0.25	T250	2.92	0.05	T300	3.62	0.06
0.484	40	Raw	6.41	0.08	T200	5.35	0.05	T250	4.07	0.00	T300	4.74	0.21
0.747	40	Raw	10.94	0.40	T200	9.25	0.15	T250	7.30	0.09	T300	7.99	0.09
0.964	40	Raw	18.17	2.38	T200	13.78	0.21	T250	10.16	0.47	T300	11.06	0.27

^F Fungi growth observed

Growth of fungi colonies was observed at the highest ERH values on raw samples at 20 °C and 30 °C, and on T200 and T250 samples only at 30 °C. This might affect EMC of the samples. However, samples with mold contamination did not show any abnormally high EMC values caused by dry matter loss due to microbial degradation. Hence, the aforementioned samples were also included in the statistical analysis and fitting of water adsorption isotherms.

Fitting sorption models to experimental results

Five water sorption isotherms, selected according to the ASABE standards, were used to fit experimental data presented in Table 11. Non-linear regression was used for fitting yielded unknown model parameters that are shown in Table 12. Statistical criteria for model performance characterization (MRE, RMSE, RSS, and R^2) are also given in Table 12. These were used for the selection of the model that described the relationship between ERH and EMC most accurately. Lowest MRE, RMSE and RSS values are used to indicate the best model for fitting experimental data. The modified Oswin model represented the best model for fitting raw and torrefied biomass, as with this model lowest values of the aforementioned three parameters were obtained. The modified Henderson was the second best performing model.

In addition to previously discussed statistical parameters used for model performance characterization, a residual plot is often used as a main criterion for model acceptance or rejection. Residual plots for all five selected models are shown in Figure 19. As can be seen in the figure 19, modified Chung-Pfost, modified Henderson, and modified GAB models show a systematic distribution of residuals.

Table 12. Water vapor adsorption parameters for the raw and torrefied corn stover

Sample	Model	A	B	C	H ₁	H ₂	R ²	MRE (%)	RSS	RMSE
Raw	Modified Chung-Pfost	80.3430	12.9223	0.1395			0.8942	44.01	3.028	0.0422
	Modified Halsey	4.7831	-0.0358	2.1794			0.9645	31.39	1.017	0.0245
	Modified Oswin	10.6784	-0.1340	2.4557			0.9766	20.02	0.671	0.0199
	Modified Henderson	0.0018	26.4117	1.0734			0.9686	17.99	0.899	0.0230
	GAB	3.8848	0.3849	47.3216	2090.335	45000	0.9594	30.14	1.162	0.0278
	T200	Modified Chung-Pfost	70.4461	9.3173	0.1601			0.8740	48.19	2.835
Modified Halsey		4.4186	-0.0420	2.1203			0.9783	25.45	0.489	0.0170
Modified Oswin		9.3512	-0.1311	2.3795			0.9875	15.44	0.281	0.0129
Modified Henderson		0.0027	20.9265	1.0297			0.9748	22.72	0.568	0.0183
GAB		3.2719	0.3362	47.6590	2427.192	42356.11	0.9749	25.37	0.565	0.0194
T250		Modified Chung-Pfost	93.4331	13.4685	0.2416			0.9106	32.11	0.836
	Modified Halsey	4.1963	-0.0353	2.3710			0.9548	29.51	0.423	0.0158
	Modified Oswin	6.9828	-0.0826	2.6851			0.9712	18.92	0.270	0.0126
	Modified Henderson	0.0022	26.6979	1.1954			0.9661	14.32	0.317	0.0137
	GAB	2.6351	0.3527	61.0000	2256.327	41223.2	0.9529	27.73	0.440	0.0171
	T300	Modified Chung-Pfost	107.560	18.4000	0.2239			0.8551	31.15	1.663
Modified Halsey		4.2505	-0.0321	2.3463			0.9076	27.49	1.060	0.0250
Modified Oswin		7.3975	-0.0848	2.6590			0.9223	18.38	0.891	0.0229
Modified Henderson		0.0019	32.5443	1.1756			0.9072	19.47	1.064	0.0250
GAB		2.7887	0.3993	39.1527	1965.523	44322	0.9016	24.27	1.129	0.0274

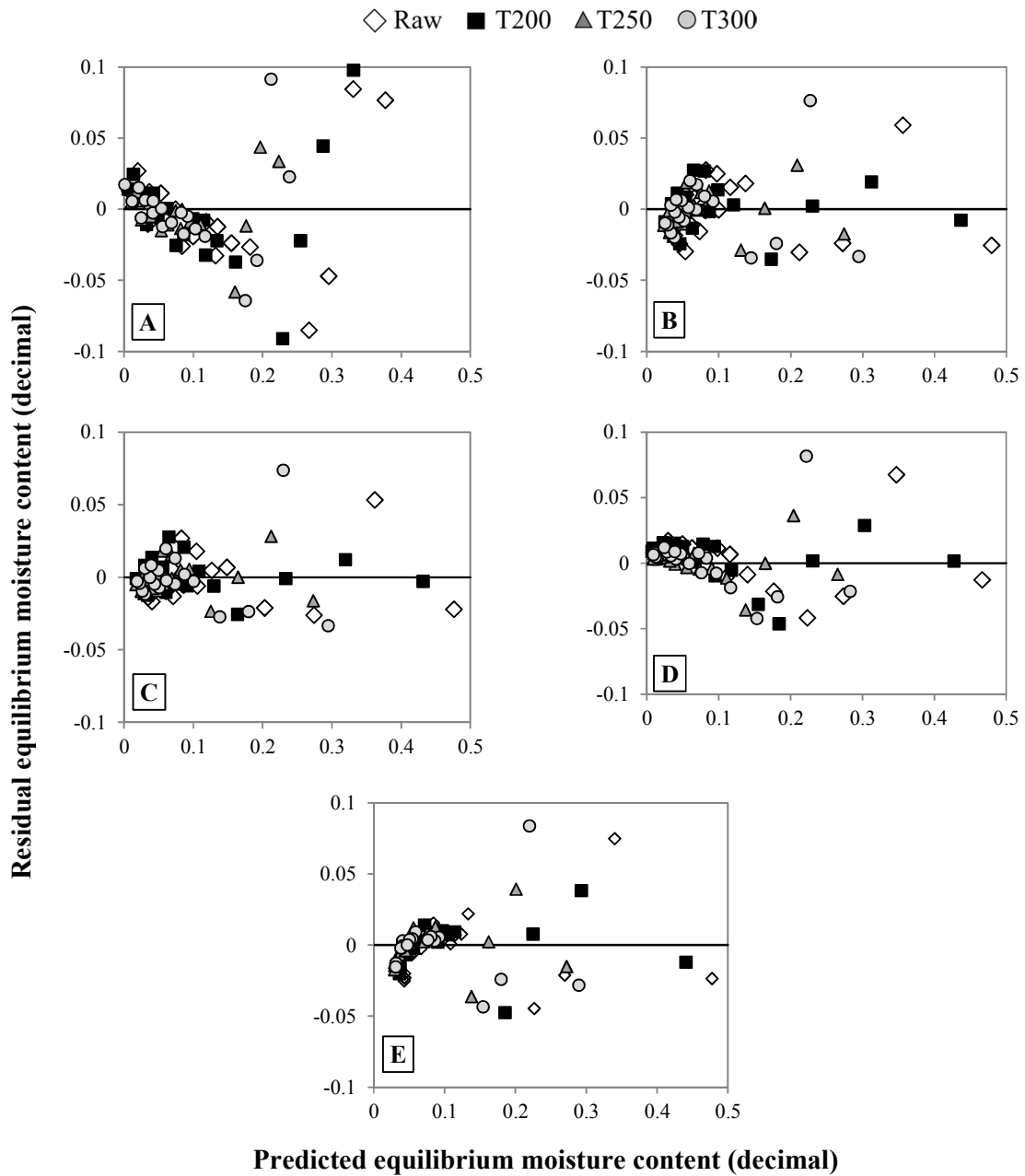


Figure 19. Residual plots of the water vapor adsorption isotherms for raw and torrefied corn stover (A – Modified Chung-Pfost, B – Modified Halsey, C - Modified Oswin, D - Modified Henderson, E – GAB)

Therefore, these were poor models for describing the correlation of ERH and EMC of corn stover and had to be rejected. Modified Oswin and Halsey models had a random distribution of residuals, but since the former one has better statistical parameters it has been accepted as the best among five investigated models. The modified Oswin model provided the best fit not only for raw corn stover, but also for torrefied corn stover. Igathinathane and co-workers [27] investigated the EMC of three corn stover components and concluded that the modified Oswin and Halsey isotherm models performed best based on prediction capabilities and randomized residuals.

As can be seen in Figure 20, 21, 22, and 23, the fitted modified Oswin equation shows that EMC data of raw and torrefied corn stover follow a sigmoidal curve, typical for the most agricultural products [44]. This type of curve represents a type II isotherm, according to Brunauer and Emmet's classification [45]. This family of isotherms describes multilayer adsorption with an asymptotic trend as water activity approaches 1.0. Type II isotherm is concave downward in the low and concave upward in the high RH region. It represents isotherms typical for BET adsorption mechanism that allows infinite adsorption for RH values close to 1. The concavity in the low RH range is considered to represent the end of formation of monomolecular layer, and the beginning of the development of the multilayer of water molecules [46]. In case of lignocellulosic material the monolayer is created via strong hydrogen bonding of single molecules in amorphous regions of plant fiber matrix. Almost linear mid-portion of the isotherm corresponds to weak bonds between multiple layers of water molecules or to filling of the fine capillaries. The steep portion of the isotherm beyond concavity in the high RH region is consequence of the swelling of the cellulose, and condensation of free water in coarse capillaries where they exist in a bulk state [47,48]. The previously discussed trend of decrease in EMC with increase in environmental temperature, regardless of sample type,

is clearly depicted in these figures. However, this trend is less expressed in the case of corn stover torrefied at 250 (T250) and 300 °C (T300). It can be seen in the figures that increase in ERH causes increase in EMC of all samples. This is especially pronounced at ERH values above 0.9. The abrupt increase in EMC at ERH above 0.9 is larger for raw (45% db) and T200 (40% db) than for T250 (25% db) and T300 (25% db). As already stated, the difference between raw and corn stover torrefied at higher temperatures may be due to degradation of hemicellulose. Moreover, the elimination of hemicellulose leads to the elimination of monosaccharide and hydroxyl moieties that served as water binding sites. Curves show a sharp increase at about 0.8-0.9 ERH, which is characteristic for type II isotherms [49].

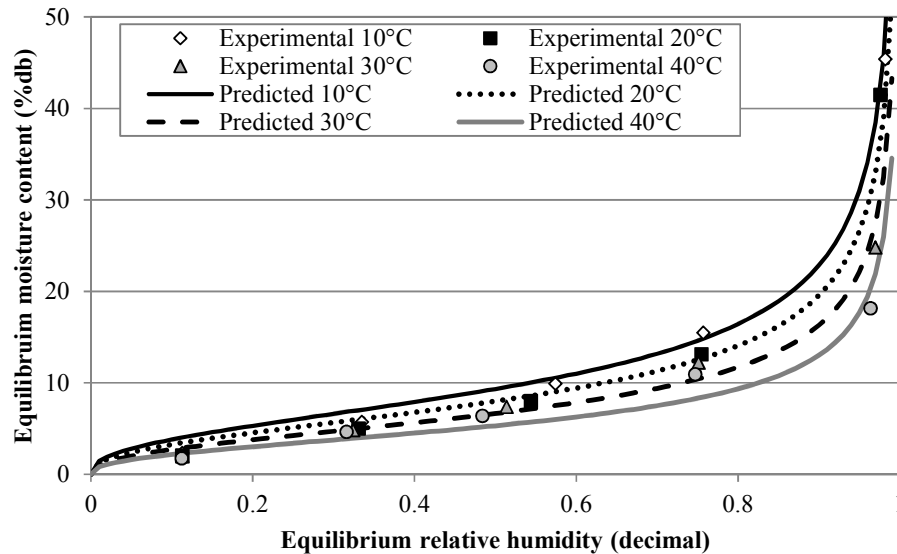


Figure 20. Experimental and isotherms predicted by Modified Oswin model of raw corn stover

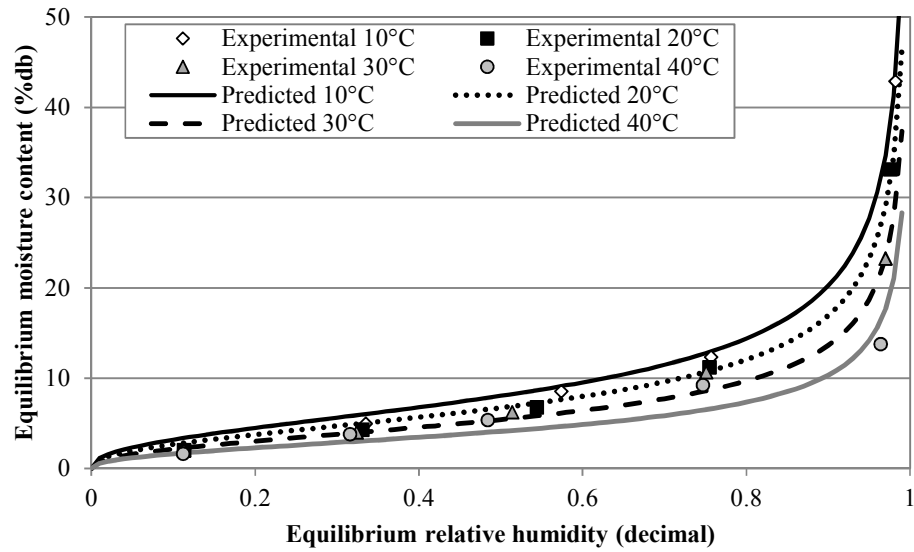


Figure 21. Experimental and isotherms predicted by Modified Oswin model of corn stover torrefied at 200 °C

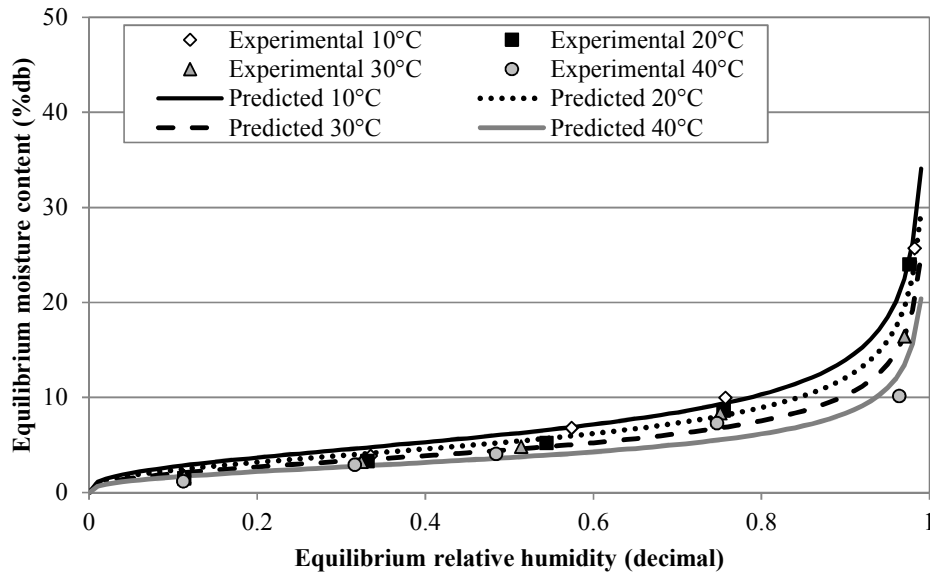


Figure 22. Experimental and isotherms predicted by Modified Oswin model of corn stover torrefied at 250 °C

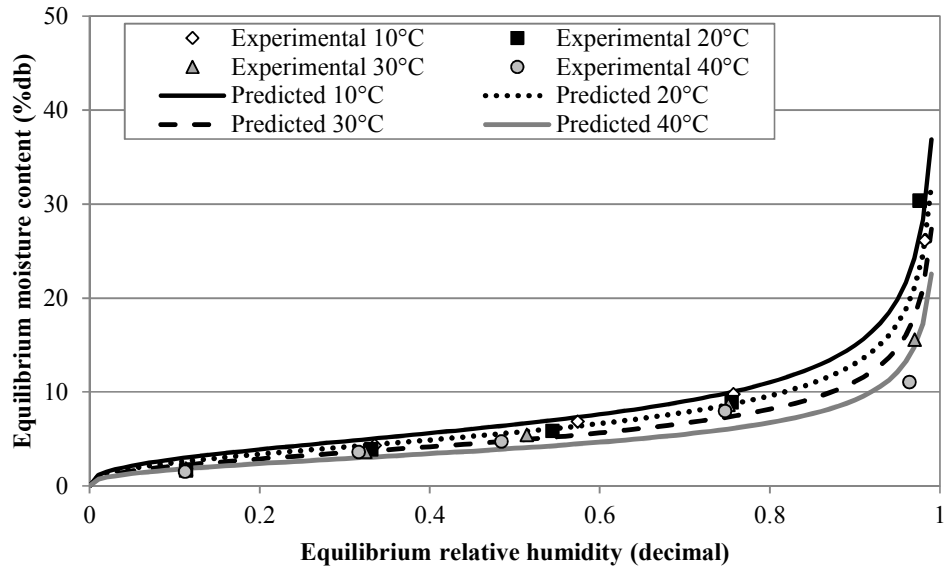


Figure 23. Experimental and isotherms predicted by Modified Oswin model of corn stover torrefied at 300 °C

As can be seen in Figure 24, torrefied biomass has distinct water vapor adsorption properties from raw biomass. Therefore, all predicted isotherms of torrefied samples are grouped together at 40 °C. However, raw corn stover at 10 °C and corn stover torrefied at 200 °C had a similar predicted EMC, but they were significantly different from samples torrefied at 250 and 300 °C, which had similar behavior at this environmental temperature.

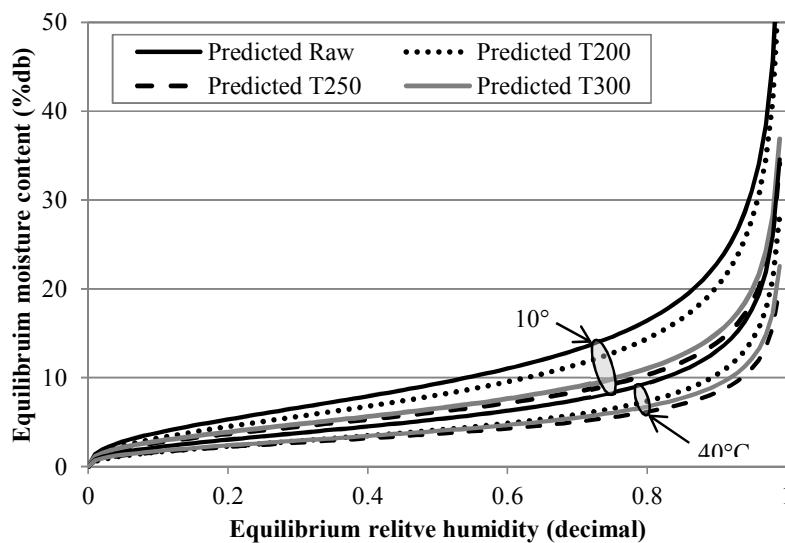


Figure 24. Comparison of raw and torrefied corn stover isotherms at 10 and 40 °C

Microbial degradation results

Microbial degradation tests were conducted at 30 °C and 0.97 ERH. These values were chosen as they were the only conditions that sustained fungi growth on all four samples. The results are presented in Figure 25. Dry matter loss (DML) of the raw corn stover sample was about 17% after 30 days, and was the highest among all samples (Figure 25).

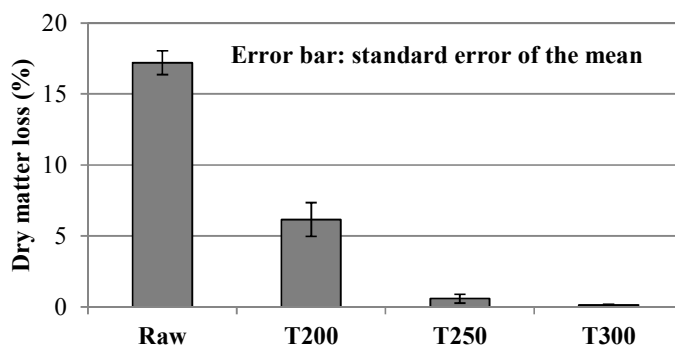


Figure 25. Dry matter loss due to microbial degradation at 0.97 ERH and 30 °C

This value was about 3 times higher than the dry matter mass loss of T200 sample. DML for corn stover torrefied at 250 and 300 °C were less than 1%.

As discussed in the section 3.1 and 3.2, even though torrefied biomass is comparatively more hydrophobic in nature than raw biomass, it still adsorbs a relatively significant amount of water vapor. At the temperature and ERH used in the microbial degradation experiment, raw and T200, and T250 and T300 samples had EMC values of about 25 and 15%_{db}, respectively. However, DML was significantly lower in the case of corn stover torrefied at 250 °C and 300 °C than in the case of raw biomass. This might be not only due to the elimination of hemicellulose and an increase in hydrophobicity, but also the formation of sugar and lignin degradation products toxic to microorganisms, such as furan and phenol derivatives that are trapped in the pores of torrefied material [50-53].

Fiber analysis results

Results of the fiber analysis are shown in Table 13. There was an overall trend of decrease in both xylan and arabinan quantity with increase in torrefaction temperature. In this work, these two compounds are considered to represent hemicellulose fraction of corn stover, since other minor components, such as galactan and mannan were registered only in traces. As expected, raw and biomass pretreated at 300 °C had respectively the highest (28%) and the lowest (4%) amount of hemicellulose. Similar trend was also observed by several other researchers [6, 22]. Increase in the torrefaction temperature from 250 to 300 °C caused cellulose degradation and decrease in its contents from about 45 to 20%, respectively. Nevertheless, there was no significant difference between raw, T200, and T250 in regards to cellulose content, which was expressed as a glucan percentage. Relative total lignin content increased from 20 to 75% with the temperature

increase, probably due to carbohydrate elimination and conversion to acid insoluble products during the thermal pretreatment.

Table 13. Fiber analysis of raw and torrefied corn stover

Sample	ASL (%)	AIL (%)	Glucan (%)	Xylan (%)	Arabinan (%)
Raw	2.6 ± 0.14 ^a	19.4 ± 0.37 ^a	45.7 ± 0.14 ^a	27.8 ± 0.07 ^a	4.6 ± 0.01 ^a
T200	2.6 ± 0.14 ^a	22.9 ± 0.25 ^b	44.9 ± 0.31 ^a	25.5 ± 0.04 ^b	4.0 ± 0.23 ^b
T250	2.7 ± 0.21 ^a	33.3 ± 0.55 ^c	46.0 ± 0.41 ^a	15.8 ± 0.70 ^c	2.3 ± 0.05 ^c
T300	1.0 ± 0.04 ^b	75.1 ± 0.49 ^d	19.9 ± 0.27 ^b	3.6 ± 0.27 ^d	0.4 ± 0.01 ^d

ASL = acid soluble lignin

AIL = acid insoluble lignin

Note: Values are given as mean ± standard deviation of two measurements. Samples marked with different letters in superscript are significantly different at $\alpha = 0.05$ according to the Tukey-Kramer pair-wise mean comparison test. Different fiber categories were not compared to each other.

Conclusion

The EMC of raw and thermally pretreated corn stover was measured at ERH and temperature ranging from 10 to 98% and 10 to 40 °C, respectively. Except at the highest ERH value, sample torrefied at 200 °C did not have water adsorption properties different from the raw biomass. However, the adsorption properties of samples torrefied at 250 and 300 °C were significantly different from the raw biomass. Torrefaction may have increased hydrophobicity of biomass through the elimination of the hydrophilic carbohydrate fraction and its partial conversion into non-polar, hydrophobic degradation products. Five isotherms were fitted to the experimental data to obtain the EMC-ERH prediction equations. Isotherms of all samples belong to type II. Modified Oswin model, followed by modified Halsey model, showed the best performances and were recommended for the characterization of water vapor sorption behavior of raw and torrefied corn stover. Modified Chung-Pfost, modified Henderson and GAB models were not recommended since their residual plots were systematic. Degradation test at highest ERH and 30 °C showed that raw biomass had about 17% dry matter loss due to microbial

degradation. Samples torrefied at 250 and 300 °C had negligible dry matter loss when compared to raw and samples torrefied at 200 °C. This might be predominantly due to higher hydrophobicity and probably the formation of degradation products toxic to fungi. Fiber analysis showed a significant decrease in hemicellulose content and a relative increase in the lignin content of torrefied corn stover. Optimal torrefaction temperature was found to be 250 °C, since higher process temperatures cause excessive dry matter loss during the torrefaction process without significantly enhancing hydrophobicity and resistance to microbial degradation of torrefied corn stover.

Acknowledgements

Funding for this project was provided by the ConocoPhillips Company. Additional technical support was provided by Center for Sustainable Energy (CSET) and Biocentury Research Farm (BCRF) of Iowa State University, Ames, IA. We would also like to thank Andy Suby and Patrick Johnston for their contribution to this work.

References

1. Brown, R. C. *Biorenewable Resources: Engineering New Products from Agriculture*, 1th ed.; Blackwell Publishing Professional: Ames, IA, 2003; pp 3-12.
2. Jenkins, B. M.; Sumner, H. R. T. *ASABE* **1986**, 29 (3), 824-836.
3. Shinnars, J. K.; Binversie, J. B.; Muck, E. R.; Weimer, J. P. *Biomass Bioenerg.* **2007**, 31, 211-221.
4. Nurmi, J. *Biomass Bioenerg.* **1999**, 17, 41-47.
5. Wadsö, L. *Fire Mater.* **2007**, 31, 241-255.
6. Bergman, P. C.; Boersma, A. R.; Zwart, R. W. R.; Kiel, J. H. A. *Torrefaction for biomass co-firing in existing coal-fired power stations (Biocoal)*; ECN-C--05-013; Energy Research Centre of the Netherlands: Petten, NL, July 2005.
7. Igathinathane, C.; Womac, A. R.; Sokhanasanj, S.; Narayan, S. *Biomass Bioenerg.* **2009**, 33, 547-557.

8. Neathery, J. K. Biomass gasification. In *Thermochemical Conversion of Biomass to Liquid Fuels and Chemicals*, 1st ed.; Crocker, M., Ed.; Royal Society of Chemistry: Cambridge, UK, 2010; pp 67-94.
9. Gray, M. R.; Corcoran, W. H.; Gavalas, G. R. *Ind. Eng. Chem., Process Des. Dev.* **1985**, *24*, 646-651.
10. Khan, A. A.; De Jong, W.; Jansens, P. J.; Spliethoff, H. *Fuel Process. Technol.* **2009**, *98*, 21-58.
11. Mantell, C. L. *Adsorption*. McGraw Hill: New York, NY, 1951; pp 1-19.
12. Crittenden, B.; Thomas, W. J. *Adsorption Technology & Design*. Butterworth-Heinemann: Oxford, UK, 1998; pp 31-65.
13. Cordeiro, D. D.; Raghavan, G. S. V.; Oliveira, W. P. *Biosyst. Eng.* **2006**, *94* (2), 221-228.
14. Nurhan A.; Hasan T. J. *Stored Prod. Res.* **2006**, *42*, 112-135.
15. Mayor L.; Moreira R.; Chenlo F.; Sereno A. *Eur. Food Res. Technol.* **2005**, *220*, 163-167.
16. Singh, R. N. *Biomass Bioenerg.* **2004**, *26*, 251-253.
17. Van der Berg, C.; Bruin, S. *Water Activity and Its Estimation in Food Systems: Theoretical Aspects*. In *Water activity: Influences on Food Quality*; Rockland, L. B., Steward, G. F., Eds.; Academic Press: New York, NY, 1981; pp 1-61.
18. Labuza T. P.; Altunakar B. *Water Activity Prediction and Moisture Sorption Isotherms*. In *Water Activity in Foods: Fundamentals and Application*, 1st ed.; Barbosa-Canovas, G. V., Fontana, A. J., Jr., Schmidt, S. J., Labuza, T. P., Eds.; Blackwell Publishing Professional: Ames, IA, 2007; pp 109-154.
19. Chen, C. C.; Morey, R. V. T. *ASAE* **1989**, *32*, 983-990.
20. *ASAE standard D245.6. Moisture Relationships of Plant-Based Agricultural Products*. St. Joseph, MI, 2007.
21. Yan, W.; Acharjee, T. C.; Coronella, C. J.; Vasquez, V. R. *Environ. Prog. Sustainable Energy* **2009**, *28*, 435-440.
22. Greig, S. J.; Sing, K. S. *Adsorption, Surface Area and Porosity*, 2nd ed., Academic Press: New York, NY, 1982.
23. Chirife, J.; Fontan F. C.. *J. Food Sci.* **1982**, *47*, 661-663.
24. Rüegg, M. *Water in Dairy Products Related to Quality, with Special Reference to Cheese*. In *Properties of water in foods in relation to quality and stability*; Simatos, D.,

- Multon J. L., Eds.; NATO ASI Series E 90; Martinus Nijhoff Publishers: Dordrecht, NL, 1985; pp 603-625.
25. Sakaar, C. Wood-Water Relations, 1st ed.; Springer-Verlag: Berlin, DE, 1988.
 26. Fasina, O. O.; Sokhansanj, S. J. Agr. Eng. Res. **1993**, 55, 51-63.
 27. Igathinathane, C.; Womac, A. R.; Sokhansanj, S.; Pordesimo, L. O. T. ASAE **2005**, 48 (4), 1449-1460.
 28. Wiig, E. O.; Juhola A. J. J. Am. Chem. Soc. **1949**, 71, 516-568.
 29. Monzam, E. R.; Shadle, L. J.; Evans, R.; Schroeder, K. Energy Fuels **1998**, 12, 1299-1304.
 30. Bedia J.; Rodriguez-Mirasol J.; Cordero T. J. Chem. Technol. Biotechnol. **2007**, 82, 548-557.
 31. Acharjee , T. C.; Coronella , C. J.; Vasquez , V. R. Bioresour. Technol. **2011**, 102, 4849-4854.
 32. ASAE standard D358.2 (R2008). Moisture Measurement - Forages. St. Joseph, MI, 1998.
 33. Medic, D.; Darr, M.; Shah, A.; Potter, B.; Zimmermann, J. **Fuel** 2011, 91, 147-154.
 34. Spiess, W. E. L.; Wolf, W. Water activity. In Water Activity: Theory and Application to Food; Rockland, L. B., Beuchat, L. R., Eds.; IFT Basic Symposium Series 664; Marcel Dekker: New York, NY, 1987; pp 215-233.
 35. Greenspan, L. J. Res. Natl. Bur. Stand. Sec. A **1977**, 81, 89-96.
 36. Mohamed, L. A.; Kouhila, M.; Jamali, A.; Lahsani, S.; Mahrouz, M. J. Food Eng. **2005**, 67, 491-498.
 37. Osborn, G. S.; White, G. M.; Sulaiman, A. H.; Walton, L. R. T. ASAE **1989**, 32, 2109-2113.
 38. Sluiter, J.; Hames, B.; Ruiz, R.; Scarlata, C.; Sluiter, J.; Tempelton, D.; Croker, D. Determination of Structural Carbohydrates and Lignin in Biomass; Technical report NREL/TP-510-42618; National Renewable Energy Laboratory: Golden, CO, July 2011.
 39. Okos, M. R.; Narsimhan, G.; Singh, R. K.; Weitnauer, A. C. Food Dehydration. In Handbook of Food Engineering; Heldman, D. R., Lund, D. B., Eds.; Marcel Dekker: New York, NY, 1992; pp 437-562.
 40. Barbosa-Canovas G. V.; Juliano P. Desorption Phenomena in Food Dehydration Process. In Water Activity in Foods: Fundamentals and Application, 1st ed.; Barbosa-

- Canovas, G. V., Fontana, A. J., Jr., Schmidt, S. J., Labuza, T. P., Eds.; Blackwell Publishing Professional: Ames, IA, 2007; pp 109-154.
41. Olsson A-M.; Salmen, L. *Carbohydr. Res.* **2004**, 339, 813-818.
 42. Taniguchi, T.; Harada, H.; Nakato, K. *Nature* **1978**, 272, 230-231.
 43. Bjork, H.; Rasmunson, A. *Fuel* **1995**, 74, 1887-1890.
 44. Lewicki, P. P. Data and Models of Water Activity. II: Solid Foods. In *Food properties handbook*, 2nd ed.; Shafiur, R., M., Ed.; CRC Press: Boca Raton, FL, 2009; pp 66-151.
 45. Brunauer, S.; Deming, L. S.; Dming W. E.; Troller, E. J. *Am. Chem. Soc.* **1940**, 62, 1723-1732.
 46. Rouqu?rol, F.; Rouquerol, J.; Sing, K. S. W. *Adsorption by Powders & Porous Solids: Principles, Methodology and Applications*; Academic Press: New York, NY, 1998; pp 19-20.
 47. Assaf, A. G.; Haas R. H.; Purves, C. B. *J. Am. Chem. Soc.* **1944**, 66, 66-73.
 48. Inagaki, T.; Yonenbou, H.; Tsuchikawa, S. *App. Spectrosc.* **2008**, 62, 860-865.
 49. Do, D. D. *Adsorption Analysis: Equilibrium and Kinetics*; Imperial College Press: London, UK, 1998; pp 49-148.
 50. Rivilli, P. L.; Alarcon, R.; Isasmendi, G. L.; Perez, J. D. *BioRes.* **2012**, 7, 112-117.
 51. Jung, K-H.; Yoo, S. K.; Moon, S-K.; Lee, U-S. *Mycobiology* **2007**, 35, 29-47.
 52. Gutierrez, T.; Buszko, M. L.; Ingram, L.O.; Preston J. F. *Appl. Biochem. Biotechnol.* **2002**, 98-100, 327-340.
 53. Voda, K.; Boh, B.; Vrtacnik, M.; Pohleven, F. *Int. Biodeterior. Biodegrad.* **2003**, 51, 51-59.

Chapter 5. Effect of particle size, different corn stover components and gas residence time on torrefaction of corn stover

A paper accepted with pending revisions by *Energies*

Dorde Medic *, Matthew Darr, Ajay Shah, and Sarah Rahn

Department of Agricultural and Biosystems Engineering, Iowa State University, 100 Davidson Hall, Ames, IA 50011, USA

* Corresponding author. E-mail address: dmedic@iastate.edu

Abstract

Large scale biofuel production will be possible only if significant quantities of biomass feedstock can be stored, transported, and processed in an economic and sustainable manner. Torrefaction has the potential to significantly reduce the cost of transportation, storage, and downstream processing through the improvement of physical and chemical characteristics of biomass. The main objective of this study was to investigate the effects of particle size, plant components, and gas residence time on the production of torrefied corn (*Zea mays*) stover. Different particle sizes included 0.85 mm and 20 mm. Different stover components included ground corn stover, whole corn stalk, stalk shell and pith, and corn cob shell. Three different purge gas residence times were employed to assess the effects of interaction of volatiles and torrefied biomass. Elemental analyses were performed on all of the samples, and the data obtained was used to estimate the energy contents and energy yields of different torrefied biomass samples. Particle density, elemental composition, and fiber composition of raw biomass fractions were also determined. Stalk pith torrefied at 280 °C and stalk shell torrefied at 250 °C had highest

and lowest dry matter loss, of about 44% and 13%, respectively. Stalk pith torrefied at 250 °C had lowest energy density of about 18-18.5 MJ/kg, while cob shell torrefied at 280 °C had the highest energy density of about 21.5 MJ/kg. The lowest energy yield, at 59%, was recorded for stalk pith torrefied at 280 °C, whereas cob and stalk shell torrefied at 250 °C had highest energy yield at 85%. These differences were a consequence of the differences in particle densities, hemicellulose quantities, and chemical properties of the original biomass samples. Gas residence time did not have a significant effect on the aforementioned parameters.

Keywords: torrefaction; corn stover; particle size; gas residence time

Introduction

Transportation fuels produced from lignocellulosic biomass have recently gained attention due to their positive effects on fossil fuel displacement, greenhouse gas emission reduction, rural development, and national security enhancement. The Energy Independence and Security Act (EISA) of 2007 mandates an increase in the minimum annual quantity of renewable fuels in the United States transportation sector, from 58 billion liters in 2012 to 136 billion liters in 2022. As per the EISA mandate, out of the total renewable fuels produced in 2022, 79 billion liters should be advanced biofuels derived mainly from cellulosic feedstock, which does not compete with food production [1]. Large amounts of lignocellulosic biomass have to be collected, stored, and processed to support biofuels production at levels demanded by EISA. There is a variety of conversion technologies available for the production of biofuels, such as fermentation, pyrolysis, gasification, and hydrothermal processing. Although thermochemical pathways employ higher temperatures and/or pressures than biochemical pathways, they have numerous advantages, such as higher reaction rates, fewer feedstock pretreatment

requirements, and an easier integration with the existing fossil fuel production infrastructure.

All conversion technologies are constrained by a narrow tolerance range for the physical characteristics of the converted biomass, such as particle size, shape, and moisture content. For example, a particle size larger than the accepted range will increase the amount of gas produced in the gasification process but, due to a slower gas diffusion speed, will decrease the quality of the gas produced, by reducing the amount of hydrogen and carbon monoxide present.[2-4]. A large particle size also gives rise to the inter-particle vapor-char interaction and increases the yield of undesirable, light bio-oil fractions [5-7]. The shape of particle can influence proper fluidization, interfere with reactor feeding, induce material bridging, and affect product distribution in thermochemical systems [8-10]. The gasification of biomass with high moisture content results in more tar formation, unreliable operation, and low process efficiency [11]. An increase in the moisture content could enhance char yield during pyrolysis [12, 13].

Size reduction and drying are energy intensive processes that significantly deteriorate the economy of biofuel production. A high heterogeneity of a lignocellulosic biomass, even among the same plant species, may degrade the quality of the final product produced by pyrolysis or gasification [14-17]. In addition, long distance feedstock transportation increases the cost of biorenewable production due to the feedstock's low bulk and energy densities. Large scale production requires large quantities of biomass to be stored in order to support the operation of biorefineries over the whole year. Biomass feedstock's susceptibility to microbial degradation during storage further compromises its economical utilization for fuel production [18, 19]. Torrefaction can be employed to significantly reduce the cost of transportation, storage, and downstream processing by

improving biomass brittleness, hydrophobicity, resistance to microbial degradation, energy density, homogeneity, and chemical characteristics [20, 21, 22].

Torrefaction is a thermochemical process conducted in a temperature regime between 200 and 300 °C under an inert atmosphere, with a low heating rate. It induces depolymerization and devolatilization of hemicellulose, the most reactive polymer under torrefaction reaction conditions [23 - A]. As a consequence, various volatile species with high oxygen contents are formed, along with a solid product composed of mainly cellulose and lignin [17, 20, 24]. The product distribution from the torrefaction process, as well as the characterization of different product streams has been conducted by several researchers [25, 26]. The suitability of many biomass feedstocks, including woody crops, agricultural residues, and dedicated energy crops, have been investigated. Most of the studies only assessed the torrefaction temperature and residence time as the variables influencing the quality and quantity of the solid product, permanent gases, and condensables produced [15-17, 19, 20, 24, 28-30]. Feedstock particle size and purge gas residence time are two other important parameters that has not yet been addressed. The positive effect of torrefaction on energy consumption during biomass size reduction can be captured only if the large particle size of biomass is utilized in the torrefaction process. A large particle size induces higher char production and lower liquid yield in the pyrolysis process [5-7]. However, how this affects the torrefaction process, or product yield and quality is not known. Purge gas residence times or volatile residence times have a strong impact on bio-oil and char yield in the pyrolysis process. Secondary reactions between char and volatiles in pyrolysis process enhance the yield of solids and decrease bio-oil yield. Prins *et al.* [24] concluded that formation of carbon monoxide during torrefaction can be explained by the reaction of carbon dioxide and steam with solid char. This confirms that there is indeed potential for solid-volatiles interaction in the

torrefaction process. Torrefaction, as a process that has some similarities to pyrolysis, also might be affected by the purge gas flow rate. The reduction of purge gas use may be important for reducing capital and operating costs. In addition, both factors are important for proper reactor design, scale up, and operation.

The objective of this study was to investigate the torrefaction behavior of two particle sizes, (< 0.85mm and 20mm) and three corn stover components (stalk shell, stalk pith, and cob shell). Three purge gas flow rates, i.e. gas residence times, (List the three rates here) were employed to assess potential interaction between volatiles and torrefied biomass that can influence biomass yield and quality, in the same manner as in the pyrolysis process. Torrefaction of the corn stover was conducted in a thermogravimetric analyzer (TGA) and a bench scale reactor. The dry matter loss (DML) during torrefaction experiments was recorded. All samples were analyzed for carbon, hydrogen, nitrogen, and sulfur contents, and the obtained data were used to calculate the energy content of torrefied samples and their energy yields. Results of the proximate analysis of raw biomass were used to determine ash content of the torrefied biomass. Particle density and the composition of raw biomass were determined as well.

Materials and Methods

Corn stover samples

Corn stover biomass was harvested Fall 2010 from Iowa State University research fields located in Story County, IA. The bulk wet samples were dried at 60 °C for 72 h immediately after the harvest. Dry samples were stored in a cooling chamber at a temperature below 5 °C to preserve their original quality and prevent microbial degradation.

A subsample of the bulk material was ground by hammer mill and sifted through an 850 μm sieve to obtain ground stover sample. Subsamples of corn stalk and cobs were handpicked from bulk corn stover samples. Stalks were cut into discs to enable separation of shell and pith. Cobs were also cut into discs and separated from the pith. Discs were cut further into 5x5x5 mm cubes by hand (Figure 26). Stalk shell samples were cut into 5x5x2 mm cuboid (Figure 26). The shape of cube was chosen for stalk pith and cob shell, because it is closest to a spherical shape. A spherical shape is preferable because it does not favor any dimension in the heat transfer process; however, since this shape is difficult to cut reliably, the cube was used. In addition, the natural geometry of stalk shell dictated its shape to be in a form of a cuboid prism. Finally, the largest sample size was obtained by handpicking stalks of about 20 mm diameter and cutting them into rods 100 mm long (Table 14).

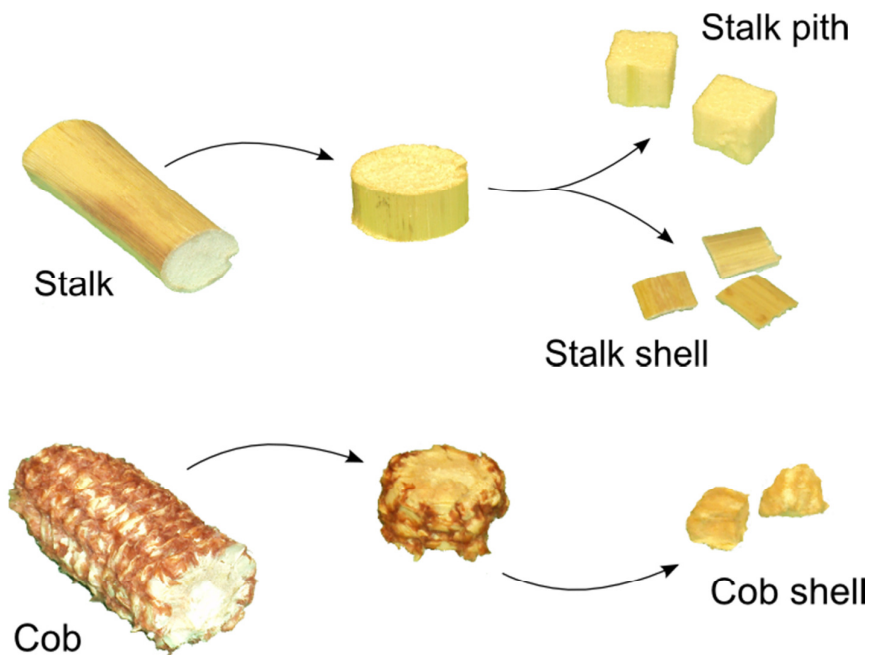


Figure 26. Different corn stover components

Table 14. Sample designation and basic properties

Factor	Level	Dimensions (mm)	Shape
Particle size	Ground stover	<0.85	Spherical
	Whole stalk	19x16x100	Elliptic cylinder
Corn stover component	Stalk shell	5x5x2	Prism
	Stalk pith	5x5x5	Cube
	Cob shell	5x5x5	Cube
Gas residence time	1.2 sec		
	12 sec		
	60 sec		

All samples were dried at 60 °C for 72 h and stored in a desiccator until the torrefaction experiments were conducted. The moisture contents of samples before and after the experiments were determined according to the ASAE standard D358.2 for forage moisture measurement [31].

Torrefaction experiments

Torrefaction of ground stover, stalk shell, stalk pith, and cob shell was conducted in a TGA (TGA/DSC Star System, Mettler-Toledo, Columbus, OH) equipped with an autosampler. Experiments were done at 250 and 280 °C using two temperature time programs and 900 µl pans (Figure 27).

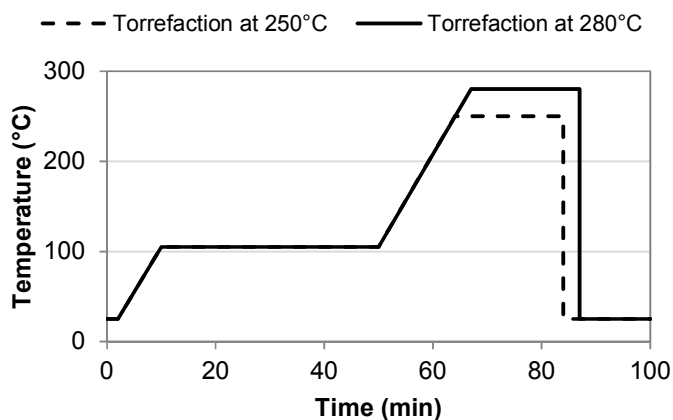


Figure 27. Temperature programs used to conduct torrefaction experiments in the TGA

The drying phase at 105 °C was employed before torrefaction to eliminate the influence of water evaporation on DML during torrefaction. Both ramping phases employed a 10 °C/min heating rate. Torrefaction was conducted for 20 min, regardless of the torrefaction temperature. In order to register the correct sample weight after torrefaction, a final isothermal step at 25 °C was utilized. An inert atmosphere was maintained by means of nitrogen purge gas.

A stainless steel bench scale reactor was constructed to accommodate the largest particle size samples. The reactor was 20 mm in diameter and 120 mm in length. It was heated indirectly by two heaters controlled independently by PID controllers (Figure 28). This setup enabled the formation of two distinct heating zones for stable temperature control. Two thermocouples were used to sense the reactor temperature. Furthermore, preheated nitrogen purge gas was used to supply additional heat to the system and prevent temperature fluctuations. Samples were loaded into the reactor through the end farther from the gas heater. The reactor was purged with nitrogen for 5 min at flow rate of 1L/min before every run. The samples were unloaded once the temperature in the reactor was below 100 °C, in the same manner as the loading procedure. The cooling phase from the torrefaction temperature to 200 °C took 7-9 min, depending on the torrefaction temperature. The torrefaction reaction is considered to start above 200 °C [23]. The reactor was purged with nitrogen at 1 L/min during the cooling phase to maintain a constant pressure, evenly cool the biomass, and terminate the torrefaction process. The weight of each whole stalk sample was about 1.5-1.6 g.

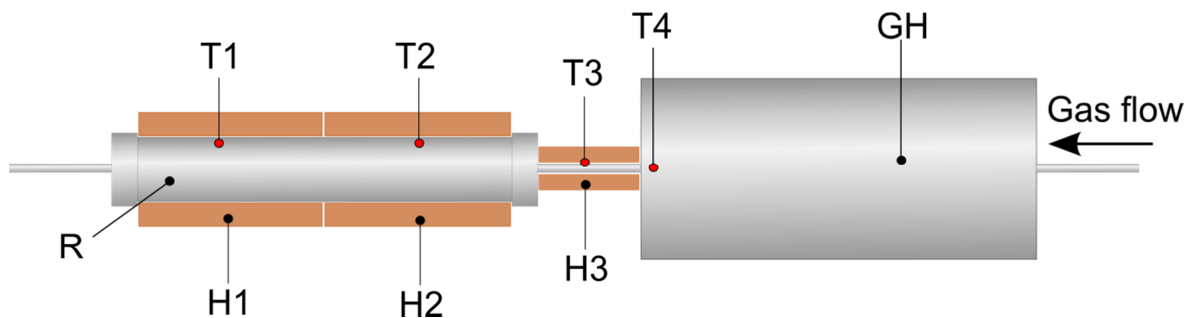


Figure 28. Bench scale reactor setup used in torrefaction experiments (R-reactor; GH – gas heater; H1, H2, H3-heaters; T1, T2, T3, T4 – thermocouples; all thermocouples were positioned inside the respective unit of the system, except T3, which was positioned between the metal gas line and the heater)

The temperature profiles recorded during torrefaction experiments in the bench scale reactor at 250 and 280 °C are shown in Figure 29.

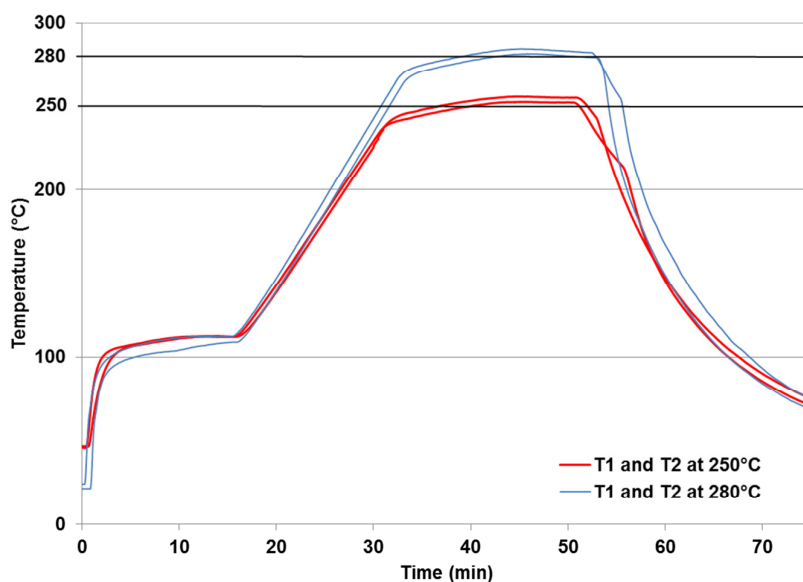


Figure 29. Temperature time profile of the bench scale reactor

Each experiment was conducted in triplicate. The final solid products were recovered and further analyzed while volatile gases were not collected.

Chemical analysis of raw and torrefied biomass

Moisture, volatiles, ash, and fixed carbon contents of the raw biomass samples were determined using the same TGA that was used for torrefaction experiments, according to the modified ASTM D 5142–04 method [32]. The analysis was done under a nitrogen atmosphere (100 mL/min). Initially samples were heated to 105 °C at the heating rate of 5 °C/min and retained at 105 °C for 40 min to determine the moisture content. They were further heated at the rate of 5 °C/min to 900 °C and maintained at this temperature for 20 min to determine the quantity of the volatiles. Subsequently the environment was changed to oxidative by purging 100mL/min of air for 30 min to determine the fixed carbon content. The remainder, after heating the sample under an oxidative atmosphere at 900 °C, was considered ash.

Elemental analyses of different raw and torrefied biomass samples were done using a CHNS/O analyzer (PerkinElmer 2400 Series II CHNS/O Analyzer, PerkinElmer, Waltham, MA), according to the ASTM D 5373–08 method [33]. Biomass samples were dried in an oven at 103 °C for 24 h before the elemental analysis. Combustion and reduction were conducted at 925 and 650 °C under a helium atmosphere, respectively.

The HHV of raw and torrefied biomass samples were computed using Eq. (1) developed by Sheng and Azevedo [34]. In Eq. (1), C and H are the percentages of carbon and hydrogen in the biomass as determined by the ultimate analysis, and O is the percentage of oxygen determined by the difference, on both a dry and ash free basis (i.e., $O(daf) = 100 - C - H - N - S$).

$$HHV (MJ/kg) = -1.3675 + 0.3137*C + 0.7009*H + 0.0318*O \quad (1)$$

Compositional analyses of raw corn stover fractions were conducted to obtain the content of neutral detergent fiber (NDF), acid detergent fiber (ADF), and acid detergent lignin (ADL). The analyses were done according to AOAC Standards 973.18. and 2002.04

[35, 36]. The hemicellulose and cellulose contents were calculated from the obtained NDF, ADF, ADL, and ash contents. The hemicellulose and cellulose contents were calculated as the difference between NDF and ADF, and ADF and ADL, respectively. Lignin was determined gravimetrically from ADL. The ash content was determined gravimetrically from the remainder after calcination of dry ADL in the muffle furnace.

Statistical analysis

The experimental design used to accomplish the objectives of this work consisted of 3 factors. The torrefaction temperature factor consisted of two levels: 250 and 280 °C. The feedstock factor consisted of three levels: stalk shell and pith, and cob shell (Table 14). The gas residence time factor consisted of three levels: 1.2, 12, and 60 seconds. A statistical analysis was done to determine the significant difference between average DML, O/C (oxygen to carbon ratio), H/C (hydrogen to carbon ratio) HHV, and energy yields of torrefied biomass at a 95% confidence interval. Ground stover and whole stalk samples were analyzed separately from stalk shell, pith, and cob shell samples. A Tukey-Kramer Honestly Significant Difference (Tukey-Kramer HSD) test was conducted after performing a One-Way Analysis of Variance (ANOVA). The JMP statistical package from SAS (SAS Institute, Cary, NC) was used for the statistical analysis of the experimental data.

Results and Discussion

The average DML of ground stover and whole stover samples torrefied at 250 and 280 °C are shown in Figure 30. DML of the samples torrefied at 250 °C did not differ significantly, according to a Tukey-Kramer HSD test (not shown). This was probably due to a limited devolatilization of hemicellulose at this process temperature. Under these conditions the torrefaction reaction might be localized in the stalk shell of whole stover,

but it is sufficient to cause DML similar to the smallest particle size. Products of the reaction in the pith of whole stover might condense and retain in the particle due to higher mass transfer resistance of the less porous stalk shell. At 280 °C there was a significant difference ($p < 0.0001$) between the ground stover and whole stover components' DML of 2-5 percentage points, regardless of residence time. Under these conditions, the differences in the physical characteristics of two sample types significantly influence the torrefaction reaction. Devolatilization of hemicellulose in the shell of the whole stalk sample may not be sufficient to offset the limited devolatilization of the pith. Volatile gases, developed during the process and condensed in the particle, further deteriorate both the heat and mass transfer properties of whole stover samples. These aforementioned constraints in the transfer phenomena were less expressed in ground stover samples, which is why they had higher DML. As per the Tukey-Kramer HSD test, there was no significant difference in DML of ground stover and whole stover induced by gas residence time, regardless of the torrefaction temperature.

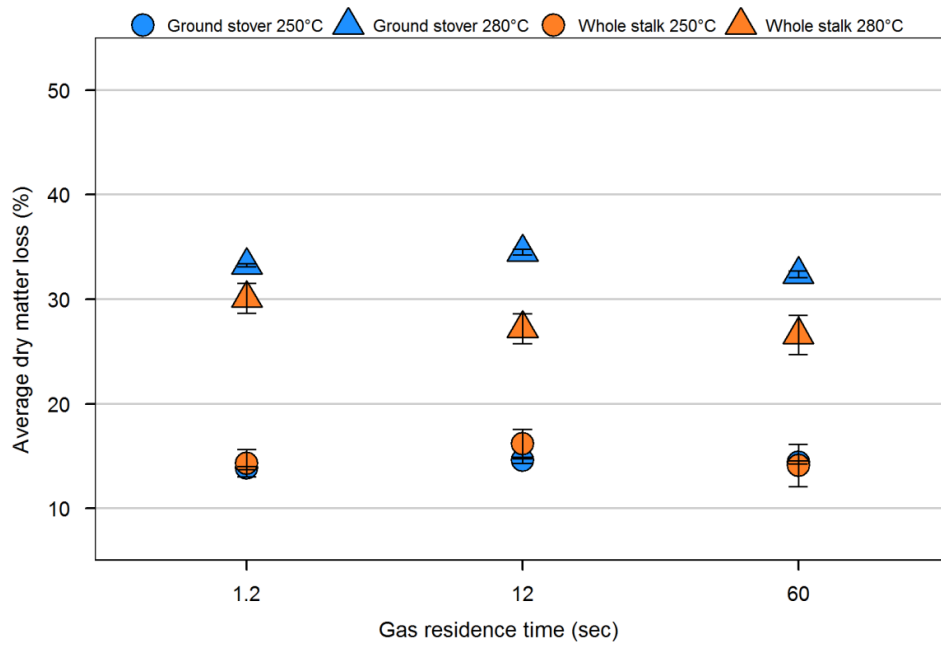


Figure 30. Average dry matter loss of torrefied ground stover and whole stalk samples (error bar=standard deviation)

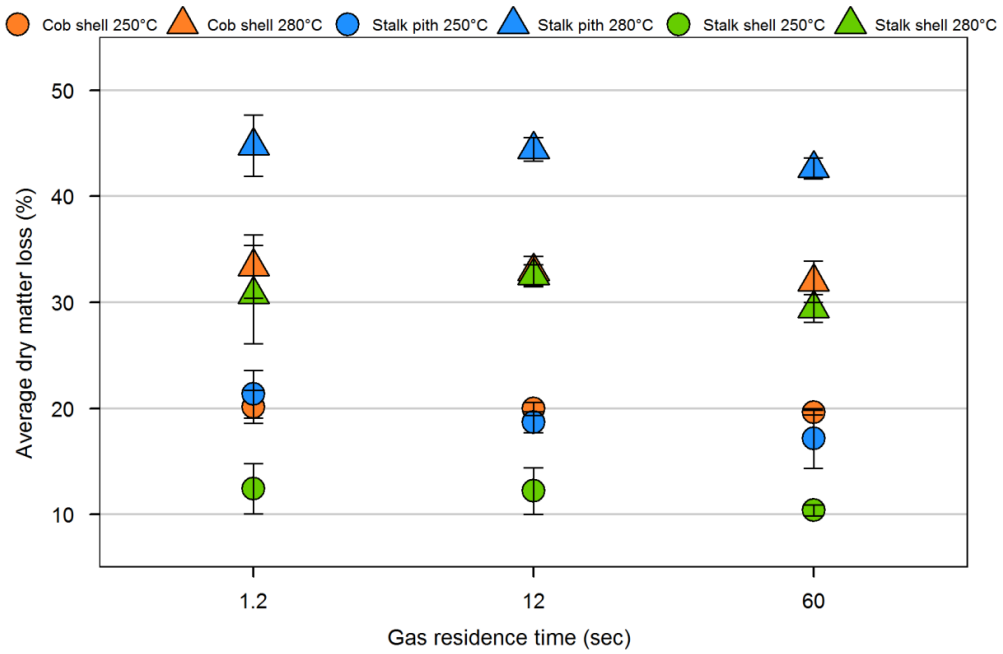


Figure 31. Average dry matter loss of torrefied stalk shell, stalk pith, and cob shell (error bar=standard deviation)

Table 15. Proximate analysis of raw corn stover biomass*

Sample	Volatiles (%)	Fixed carbon (%)	Ash (%)	Particle density (kg/m ³)	Fiber composition (%)			
					Cellulose	Hemicellulose	Lignin	Other
Ground stover	77.05±0.22	17.56±0.01	5.45±0.33	-	43.3±0.5	32.3±0.1	6.3±0.4	18.03±0.0
Stalk shell	75.43±0.20	21.31±0.00	3.18±0.06	444.61±48.39	56.6±0.2	15.2±1.0	13.5±0.1	15.62±1.3
Stalk pith	80.57±1.27	13.89±1.13	5.49±0.12	34.93±6.66	57.6±0.4	21.3±1.8	6.1±0.6	14.40±0.8
Cob shell	76.88±2.43	18.96±2.24	4.13±0.27	357.40±47.84	45.2±0.3	38.3±1.1	10.3±0.0	7.17±1.4
Whole stover	76.74±0.87	17.20±0.73	3.86±0.17	116.48±18.02	56.2±1.8	17.6±1.0	11.6±0.8	14.60±0.0

*All values are expressed on dry basis as a mean of two measurements ± standard deviation.

The two anatomical fractions of corn stalk and corn cob showed different behavior under torrefaction reaction conditions (Figure 31). At 250 °C there was no significant difference in DML between cob shell and stalk pith samples. However, these two samples differed significantly from the stalk shell sample. Corn cob and stalk shell have the highest and the lowest hemicellulose content, respectively, among all corn stover fractions (Table 15). The same findings have been reported by Krull *et al.* [37] and Garlock *et al.* [38]. Cob shell particle density, approximately 350 kg/m³, is comparable to stalk shell density, and much higher than stalk pith density, approximately 40 kg/m³, (Table 15). Therefore, the torrefaction reaction at 250 °C might not be intensive enough to cause significant devolatilization of stalk shell samples due to their lower hemicellulose content and high particle density. The high content of reactive hemicellulose in cob shell makes it prone to higher DML during torrefaction. Nonetheless, the high particle density of cob shell increases the resistance to heat and mass transfer, thus preventing excessive DML by limiting hemicellulose's exposure to high temperatures. Stalk pith, on the other hand, has a lower hemicellulose content and lower particle density. Therefore, even though the hemicellulose present in stalk pith is more exposed to high temperatures, its low content limits DML. The opposite effect of hemicellulose content and particle density might be the reason for the same DML of cob shell and stalk pith at 250 °C.

At 280 °C there was no significant difference between cob shell and stalk shell, but these two samples differed significantly from stalk pith. Heat and mass transfer might be more significant factors once most of the hemicellulose was degraded at 280 °C and devolatilization of cellulose and lignin had started. As can be seen in Figure 31, stalk pith, which offers less resistance to heat/mass transfer, has a DML approximately 15 percentage points higher than the other two corn stover fractions. Furthermore, there were

no significant differences in DML of stalk shell, stalk pith, and cob shell due to different gas residence times, regardless of torrefaction process temperatures.

Differences between the carbon, nitrogen, sulfur, hydrogen, and oxygen contents of biomass samples were not statistically analyzed. Instead the O/C ratio and HHV were analyzed using the Tukey-Kramer HSD test to determine their significant differences (not shown in Table 16). According to statistical analysis, the O/C ratio of ground stover and whole stalk were significantly different, ($p \leq 0.002$), regardless of the temperature. The difference was about 9 and 5 percentage points at 250 and 280 °C, respectively. Stalk pith had the highest O/C, 1.06 and 0.88 at 250 and 280 °C, respectively. Cob shell had the lowest O/C, 0.77 and 0.66 at 250 and at 280 °C, respectively. The reason for the decrease in the O/C ratio during torrefaction is the generation of volatiles rich in oxygen such as CO₂ and H₂O [20, 24]. Apart from the higher initial value of the O/C ratio, the highest O/C value of corn pith after torrefaction might be due to devolatilization of cellulose and lignin, in addition to hemicellulose. Therefore, the O/C ratio did not change significantly since both C and O were lost in comparable quantities through devolatilization.

Table 16. Elemental analysis and HHV of biomass samples

Sample	Torrefaction temperature (°C)	Gas residence time (sec)	C (wt %)	H (wt %)	N (wt %)	S (wt %)	O (wt %)	O/C	H/C	HHV (MJ/kg)	
Ground stover	250	1.2	45.76±0.37	5.99±0.13	0.62±0.06	0.36±0.10	47.28±0.43	1.03±0.02	0.13±0.01	18.68±0.14	
		12	45.78±1.08	5.27±1.20	0.46±0.08	0.32±0.08	48.17±2.42	1.05±0.08	0.11±0.00	18.85±1.10	
		60	46.27±0.22	5.81±0.24	0.63±0.06	0.56±0.03	46.73±0.13	1.01±0.01	0.12±0.02	18.70±0.11	
	280	1.2	49.59±0.25	5.56±0.08	0.65±0.10	0.33±0.08	43.86±0.31	0.88±0.02	0.11±0.00	19.48±0.07	
		12	50.21±0.10	5.57±0.07	0.70±0.07	0.39±0.05	43.13±0.09	0.86±0.00	0.13±0.00	19.66±0.02	
		60	50.35±0.31	5.45±0.08	0.71±0.05	0.36±0.03	43.14±0.29	0.85±0.01	0.11±0.00	19.61±0.10	
	Raw	-	44.84±0.70	6.32±0.07	0.46±0.15	0.12±0.03	48.26±0.67	1.08±0.03	0.14±0.00	18.66±0.24	
	Stalk shell	250	1.2	48.76±0.18	5.75±0.21	0.19±0.02	0.23±0.16	45.06±0.30	0.92±0.01	0.12±0.00	19.39±0.18
			12	48.35±0.68	5.77±0.20	0.19±0.01	0.31±0.17	45.38±1.00	0.94±0.03	0.10±0.00	19.45±0.30
60			48.60±0.37	5.67±0.06	0.14±0.02	0.36±0.44	45.22±0.83	0.93±0.02	0.12±0.00	19.29±0.12	
280		1.2	53.97±1.30	5.54±0.19	0.16±0.05	0.66±0.71	39.67±1.13	0.74±0.04	0.09±0.01	20.70±0.25	
		12	55.83±0.38	5.29±0.14	0.32±0.06	0.24±0.14	38.32±0.32	0.69±0.01	0.12±0.01	21.07±0.20	
		60	53.78±0.62	5.37±0.04	0.15±0.04	0.40±0.43	40.30±1.01	0.75±0.03	0.11±0.01	20.54±0.14	
Raw		-	47.87±0.06	6.28±0.07	0.04±0.03	0.10±0.04	45.72±0.15	0.95±0.01	0.13±0.00	19.50±0.05	
Stalk pith		250	1.2	46.40±0.06	5.48±0.05	0.33±0.12	0.15±0.02	47.64±0.04	1.03±0.00	0.12±0.00	18.54±0.06
			12	45.61±0.54	5.58±0.14	0.31±0.04	0.18±0.02	48.32±0.45	1.06±0.02	0.10±0.01	18.46±0.14
	60		45.18±0.08	5.34±0.09	0.26±0.05	0.08±0.05	49.14±0.08	1.09±0.00	0.12±0.01	18.10±0.08	
	280	1.2	49.99±0.67	4.77±0.18	0.46±0.07	0.11±0.07	44.67±0.57	0.90±0.02	0.10±0.01	19.07±0.12	
		12	51.27±1.31	5.02±0.29	0.47±0.23	0.12±0.03	43.13±1.41	0.84±0.05	0.12±0.00	19.60±0.53	
		60	49.89±0.40	4.75±0.12	0.54±0.30	0.02±0.01	44.79±0.57	0.90±0.02	0.10±0.01	19.04±0.03	
	Raw	-	44.69±0.77	5.93±0.12	0.12±0.01	0.16±0.07	49.10±0.83	1.10±0.04	0.13±0.00	18.36±0.30	
	Cob shell	250	1.2	52.74±0.13	5.80±0.01	0.51±0.25	0.18±0.03	40.77±0.26	0.77±0.01	0.11±0.00	20.54±0.04
			12	53.23±0.83	6.07±0.14	0.29±0.01	0.19±0.02	40.22±0.94	0.76±0.03	0.10±0.00	20.67±0.33
60			52.42±0.40	5.68±0.05	0.31±0.06	0.10±0.02	41.49±0.41	0.79±0.01	0.11±0.01	20.37±0.10	
280		1.2	56.52±0.30	5.48±0.09	0.40±0.04	0.05±0.03	37.56±0.20	0.66±0.01	0.10±0.01	21.39±0.03	
		12	56.44±0.69	5.86±0.10	0.41±0.03	0.18±0.04	37.11±0.62	0.66±0.02	0.11±0.00	21.62±0.15	
		60	56.12±0.48	5.41±0.05	0.37±0.07	0.05±0.04	38.05±0.54	0.68±0.02	0.10±0.01	21.23±0.14	
Raw		-	47.15±0.14	6.25±0.02	0.10±0.04	0.08±0.04	46.41±0.21	0.98±0.01	0.13±0.00	19.28±0.04	
Whole stover		250	1.2	47.96±0.41	5.83±0.35	0.30±0.08	0.26±0.04	45.65±0.67	0.95±0.02	0.12±0.01	19.21±0.33
			12	48.36±1.27	5.73±0.11	0.41±0.03	0.25±0.02	45.25±1.33	0.94±0.06	0.11±0.00	19.25±0.39
	60		47.78±1.00	5.98±0.12	0.30±0.04	0.29±0.12	45.65±0.93	0.95±0.04	0.12±0.00	19.26±0.34	
	280	1.2	52.57±0.95	5.42±0.23	0.40±0.11	0.32±0.10	41.30±0.95	0.79±0.03	0.11±0.00	20.23±0.22	
		12	51.83±0.82	5.68±0.14	0.35±0.01	0.23±0.03	41.90±0.94	0.81±0.03	0.12±0.01	20.20±0.31	
		60	50.94±0.31	5.72±0.13	0.29±0.04	0.27±0.04	42.77±0.35	0.84±0.01	0.11±0.01	19.98±0.17	
	Raw	-	47.95±0.23	6.18±0.02	0.14±0.06	0.16±0.02	45.63±0.25	0.95±0.01	0.13±0.00	19.45±0.08	

*All values are expressed on dry basis as a mean of two measurements ± standard deviation.

The differences between the O/C ratios due to gas residence time were not significant, regardless of temperature. According to statistical analysis, there was no significant difference ($p \geq 0.2766$) between the H/C ratios of ground stover and whole stalk, regardless of temperature. This is a consequence of the limited change in hydrogen content when compared to the change in carbon content. The former was less than 1 percentage point, while the latter was up to 6 percentage points. Cob shell had a significantly lower H/C ratio ($p < 0.0001$) than stalk pith and shell at 250 °C, which correlates to a higher loss of hydrogen than carbon, probably through the elimination of organics, such as acetic acid and methanol [20]. However, the absolute difference between the average C/H ratio of cob shell, and stalk shell and pith was only 0.008 percentage points. There was not any significant difference ($p > 0.3105$) between these samples at 280 °C, where the absolute difference was 0.003 percentage points. The gas residence time did not have any significant effect on H/C ratio, regardless of torrefaction temperature, particle size or corn stover component. The contents of nitrogen and sulfur remained almost constant and did not show any trend regardless of particle size, corn stover component, or gas residence time. Moreover, these two elements are present in very limited amounts and do not significantly contribute to the energy density of the biomass.

Ash content of the raw biomass samples (Table 15) was used to compute the ash content of torrefied biomass using Eq. (2). Furthermore, the ash content of torrefied biomass was used to compute HHV on an ash free basis (Table 16).

$$\text{Ash}_{\text{torrefied}}(\% \text{db}) = \frac{\text{Ash}_{\text{raw}}(\% \text{db})}{100 - \text{DML}(\% \text{db})} \cdot 100 \quad (2)$$

Where:

db= dry basis

HHV followed a trend opposite to the O/C ratio (Table 16). All samples were significantly different ($p \leq 0.0065$) regardless of torrefaction temperature. Whole stalk samples had a higher HHV than ground stover by approximately 0.7 and 0.5 MJ/kg at 250 and 280 °C, respectively. Cob shell had the lowest O/C ratio and consequently had the highest HHV of 20.6 and 21.5 MJ/kg at 250 and 280 °C, respectively. Stalk pith had the lowest values of 18.3 and 19.23 MJ/kg at 250 and 280 °C, respectively. The HHV of the samples at distinct gas residence time levels was not significantly different ($p \geq 0.5520$), regardless of the torrefaction temperature.

The average energy yields of the torrefied samples are shown in Figures 32 and 33. Yields were computed using Eq. (3):

$$\text{Energy yield (\%)} = \left(\frac{m_{\text{torrefied}}}{m_{\text{raw}}} \right)_{\text{db}} \left(\frac{\text{HHV}_{\text{torrefied}}}{\text{HHV}_{\text{raw}}} \right)_{\text{db}} \cdot 100 \quad (3)$$

The Tukey-Kramer HSD test was conducted to determine the significant differences between torrefied samples. According to the statistical analysis, the ground stover and whole stover samples torrefied at 250 °C were not significantly different; however, the samples did show a significant difference of approximately 6 percentage points at 280 °C (Figure 32). Energy yields followed a trend opposite to DML. This is probably due to a large change in DML that could not be offset by the change in HHV of torrefied samples. Gas residence times did not show any significant effect on the energy yield as revealed by statistical analysis. This is in accordance with the effect of gas residence time on DML and HHV.

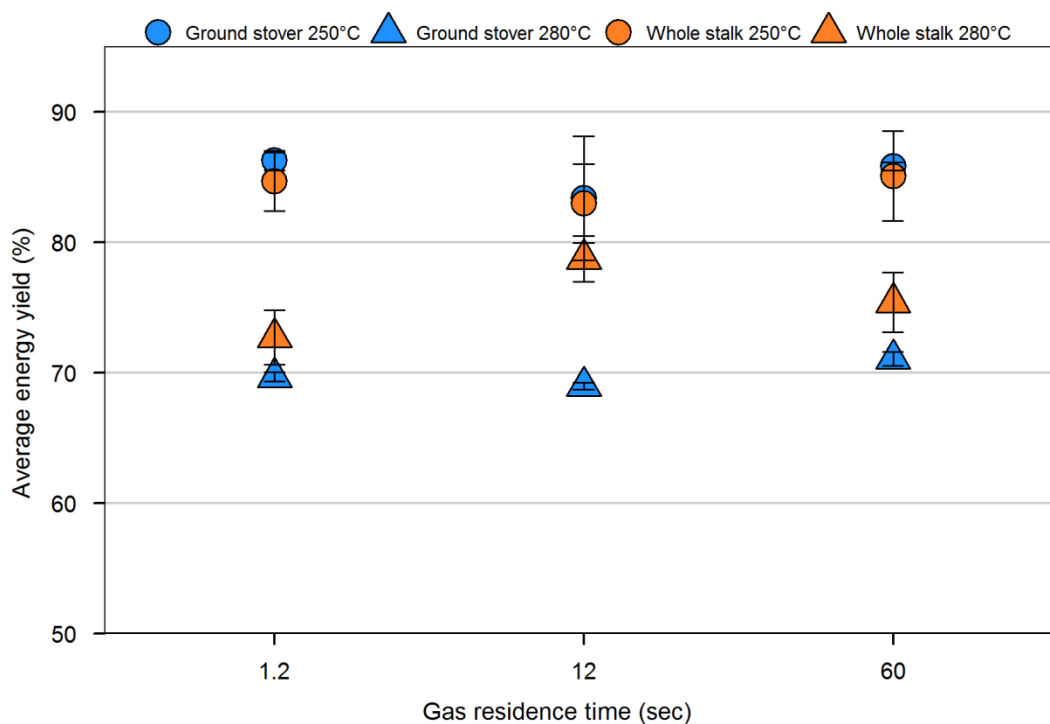


Figure 32. Average energy yield of torrefied ground stover and whole stalk samples (error bar=standard deviation)

Average energy yields of stalk shell and cob shell were not significantly different at both 250 and 280 °C (Figure 33). The absence of any difference between these two samples at 250 °C was caused by a larger HHV of cob shell than stalk shell, which offset the difference in DML. However, these two samples had energy yields different from stalk pith samples, regardless of temperature. The energy yield of stalk pith was approximately 6 and 15 percentage points lower than the energy yields of stalk shell and cob shell at 250 and 280 °C, respectively. There was no difference between average energy yields due to gas residence time, regardless of sample type.

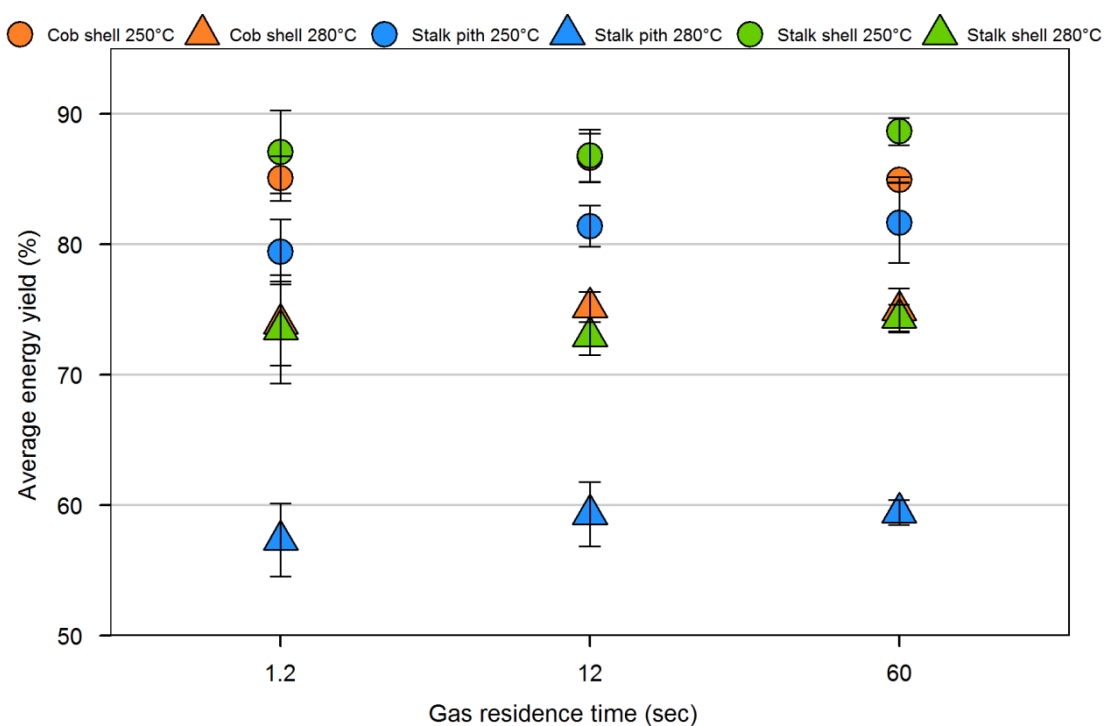


Figure 33. Average energy yield of torrefied stalk shell, stalk pith, and cob shell samples (error bar=standard deviation)

Conclusions

The effects of corn stover particle size and fraction type, as well as gas residence times on torrefaction were investigated through the analysis of DML, energy yield, and chemical properties of torrefied biomass. Torrefaction of ground corn stover at 280 °C induced higher DML than torrefaction of the whole stalk. The whole corn stalk had higher HHV and energy yield values, probably due to its different fiber composition and less energy lost through devolatilization. In general, stalk pith and stalk shell had respectively the highest and the lowest DML, regardless of the torrefaction temperature. Stalk pith and cob shell had the lowest and the highest HHV, respectively. The energy yield of stalk pith was the lowest at both 250 and 280 °C. Furthermore, the energy yield of stalk shell was the highest but not significantly different than cob shell, regardless of temperature. The difference in the

behavior of corn stover fractions was the consequence of different physical characteristics and fiber composition. Gas residence time did not have any significant effect on DML, HHV, and energy yield.

Acknowledgments

This research project was supported by funding provided by the ConocoPhillips Company. Additional technical support was provided by the Center for Sustainable Energy (CSET) and Biocentury Research Farm (BCRF) of Iowa State University, Ames, IA. We would also like to thank Patrick Johnston for his contribution to this work.

References

1. The Energy Independence and Security Act of 2007, Pub. L. No. 110-40 H.R. 6, 121 Stat. 1492; January 7, 2007.
2. Feng, Y.; Xiao, B.; Goerner, K.; Cheng, G.; Wang, J. Influence of particle size and temperature on gasification performance in externally heated gasifier. *Smart Grid Renewable Energy* **2011**, 2, 158-164.
3. Luo, S.; Xiao, B.; Guo, X.; Hu, Z.; Liu, S.; He, M. Hydrogen-rich gas from catalytic steam gasification of biomass in a fixed bed reactor: Influence of particle size on gasification performance. *Int. J. Hydrogen Energy* **2009**, 34, 1260-1264.
4. Moghiman, M.; Hashemi, T.; Zahmatkesh, I.; Daghighi, Y. Effects of particle size and equivalence ratio on cyclone gasification of wood powder. *J. Energy Inst.* **2007**, 80, 29-34.
5. Shen, J.; Wang, X-S.; Garcia-Perez, M.; Mourant, D.; Rhodes, M. J.; Li, C-Z. Effects of particle size on the fast pyrolysis of oil mallee woody biomass, *Fuel* **2009**, 88, 1810-1817.
6. Gaston, K. R.; Jarvis, M. W.; Pepiot, P.; Smith, K. M.; Frederick, W. J.; Nimlos, M. R. Biomass Pyrolysis and Gasification of Varying Particle Sizes in a Fluidized-Bed Reactor. *Energ. Fuel* **2011**; 25, 3747-3757.

7. Zhu, W.; Song, W.; Lin, W. Effect of the Coal Particle Size on Pyrolysis and Char Reactivity for Two Types of Coal and Demineralized Coal, *Energ. Fuel* **2008**, 22, 2482-2487.
8. Bergman, P. C. A.; Boersma, A. R.; Kiel, J.H.A.; Prins, M. J.; Ptasinski, K. J.; Janssen F. J. J. G. Torrefaction for entrained-flow gasification of biomass, ECN-C-05-067, ECN:Petten, The Netherlands, 2005.
9. Paulrud, S.; Mattson, J. E.; Nilsson, C. Particle and handling characteristics of wood fuel powder: effects of different mills. *Fuel Process. Technol.* **2002**, 76, 23-39.
10. Lu, H.; Ip, E.; Scott, J.; Foster, P.; Vickers, M.; Baxter, L. L. Effects of particle shape and size on devolatilization of biomass particle. *Fuel* **2010**, 89, 1156-1168.
11. Neathery, J. K. Biomass gasification. In *Thermochemical conversion of biomass to liquid fuels and chemicals*; Crocker, M., Ed.; Blackwell Publishing Professional: Ames, IA, USA, 2007; pp.67-94.
12. Antal, M. J.; Gronli, M. The art, science, and technology of charcoal production. *Ind. Eng. Chem. Res.* **2003**, 42, 1619-1640.
13. Antal, M. J.; Croiset, E.; Dai, X.; DeAlmeida, C.; Shu-lai Mok, W.; Norberg, N. High-yield biomass charcoal. *Energy Fuel.* **1996**, 10, 652-658.
14. Klass, D. L. *Biomass for Renewable Energy, Fuels and Chemicals*, Academic Press: San Diego, CA, 1998.
15. Arias, B.; Pevida, C.; Feroso, J.; Plaza, M. G.; Rubeira, F.; Pis, J. J. Influence of torrefaction on the grindability and reactivity of woody biomass. *Fuel Process. Technol.* **2008**, 89, 169-75.
16. Yan, W.; Acharjee, T. C.; Coronella, C. J.; Vaquez, R. V. Thermal Pretreatment of Lignocellulosic Biomass. *Environ. Prog. Sustainable Energy* **2009**, 28, 435-40.
17. Bergman, P. C. A.; Boersma, A. R.; Zwart, R. W. R.; Kiel, J.H.A. Torrefaction for Biomass Co-firing in Existing Coal-Fired Power Stations, ECN:Petten, The Netherlands, 2005.
18. BRDI, Roadmap for Bioenergy and Biobased Products in the United States. Biomass Research and Development Initiative, October 2007.

19. Bridgeman, T. G.; Jones, J. M.; Shield, I.; Williams, P.T. Torrefaction of reed canary grass, wheat straw and willow to enhance solid fuel qualities and combustion properties. *Fuel* **2008**, 87, 844-56.
20. Medic, D.; Darr, M.; Shah, A.; Potter, B.; Zimmermann, J. Effects of torrefaction process parameters on biomass feedstock upgrading. *Fuel* **2011**, 91, 147-154.
21. Shah A.; Darr, M.; Medic, D.; Anex, R.; Khanal, S.; Maski, D. Techno-economic analysis of a production-scale torrefaction system for cellulosic biomass upgrading, *Biofuels, Bioprod. Biorefin.* **2012**, 6, 45-57.
22. Medic D.; Darr, M.; Shah, A.; Rahn, S. Effect of torrefaction on water vapor adsorption properties and resistance to microbial degradation of corn stover, *Energy Fuels*, Available online February 2012. DOI: 10.1021/ef3000449
23. Chen, W-H.; Kuo, P-C. Torrefaction and co-torrefaction characterization of hemicellulose, cellulose and lignin as well as of some basic constituents in biomass. *Energy* **2011**, 36, 803-811.
24. Prins, M. J., Ptasinski, K. J.; Janssen, F. J. J.G; Torrefaction of wood. Part 2. Analysis of products, *J. Anal. Appl. Pyrol.* **2006**; 77:35-40.
25. Ciolkosz D.; Wallace R. A review of torrefaction for bioenergy feedstock production. *Biofuels, Bioprod. Biorefin.* **2011**, 5, 317-329.
26. Van der Stelt, M. J. C.; Gerhauser, H.; Kiel, J. H.A.; Ptasinski, K. J. Biomass upgrading by torrefaction for the production of biofuels: A review. *Biomass. Bioenerg.* **2011**, 35, 3748-3762.
27. Chen, W-H.; Kuo, P-C. Torrefaction and co-torrefaction characterization of hemicellulose, cellulose and lignin as well as of some basic constituents in biomass. *Energy* **2011**, 36, 803-81
28. Bergman, P. C. A. Combined Torrefaction and Pelletization: The TOP Process, ECN:Petten, The Netherlands, 2005.
29. Couhert, C.; Salvador, S.; Commandre, J-M. Impact of torrefaction on syngas production from wood. *Fuel* **2009**, 88, 2286-2290.
30. Prins, M. J.; Ptasinski, K. J.; Janssen, F. J. J.G. Torrefaction of wood. Part 1. Weight Loss Kinetics, *J. Anal. Appl. Pyrol.* **2006**, 77, 28-34.

31. ASAE standard D358.2 (R2008). *Moisture Measurement - Forages*. American Society of Agricultural Engineers: St. Joseph, MI, 1998.
32. ASTM D 5142 – 04: *Standard Test Method for Proximate Analysis of the Analysis Sample of Coal and Coke by Instrumental Procedures*. ASTM International: West Conshohocken, PA, 2008.
33. ASTM D 5373 – 08: *Standard Test Method for Instrumental Determination of Carbon, Hydrogen and Nitrogen in Laboratory samples of Coal*. ASTM International: West Conshohocken, PA, 2008.
34. Sheng, C.; Azevedo, J. L. T. Estimating the higher heating value of biomass fuels from basic analysis data. *Biomass Bioenerg.* **2005**, 28, 499-507.
35. AOAC Standard 973.18. Fiber (Acid Detergent) and Lignin in Animal Feeds; Association of Official Analytical Chemists: Gaithersburg, MD, USA, 1990.
36. AOAC Standard 2002.04. Gravimetric Determination of Amylase-Treated Neutral Detergent Fiber in Feeds Using Refluxing in Beaker or Crucibles; Association of Official Analytical Chemists: Gaithersburg, MD, USA, 2002.
37. Krull, L.H.; Inglett, G. E. Analysis of Neutral Carbohydrate in Agricultural Residues by Gas-Liquid Chromatography. *J. Agric. Food Chem.* **1980**, 28, 917-919.
38. Garlock, R. J.; Chundawat, S. P.; Balan, V.; Dale, B. E. Optimizing harvest of cont stover fractions based on overall sugar yields following ammonia fiber expansion pretreatment and enzymatic hydrolysis. *Biotechnol. Biofuels.* **2009**, 2:art. #29.

Chapter 6. General conclusions and future work

During torrefaction corn stover undergoes significant changes in chemical and physical properties which are responsible for increased energy density, reduced O/C ratio, improved hydrophobicity, increased resistance to microbial degradation, and increased grindability, as well as mass and energy losses in the process. It has been found that temperature has the most significant effect on changes in biomass properties during torrefaction, followed by initial feedstock moisture content and residence time. However, high mass loss due to extensive devolatilization at a high temperature offsets the gain in energy density, and significantly reduced the overall energy yield. Moisture content had a significant effect on energy density, mass and energy yield, and generally induced a reduction in each of these parameters. The effect of moisture is more pronounced in the low torrefaction temperature regime (200-250 °C) and initial moisture content above about 20%.

One of the most desired changes induced during the torrefaction process is an increase in brittleness of biomass. That is the reason why the majority of researchers studied this property and utilized it to determine optimal torrefaction conditions. Hydrophobicity and resistance to microbial degradation, although very important for transportation and storage of biomass, have not received the same attention. It has been found in this study that only samples torrefied above 250 °C had water sorption properties significantly different from the raw biomass. This might be due to the elimination of the hydrophilic carbohydrate fraction and its partial conversion into non-polar, hydrophobic degradation products. Five isotherms were fitted to the experimental data to obtain the EMC-ERH prediction equations. The modified Oswin model, followed by the modified Halsey model, showed the best performances. Samples torrefied above 250 °C had negligible dry matter loss due to

microbial degradation when compared to raw biomass and samples torrefied at 200 °C. This might be predominantly due to higher hydrophobicity and the formation of degradation products toxic to fungi. Fiber analysis showed a significant decrease in hemicellulose content and a relative increase in the lignin content of torrefied corn stover.

The effect of biomass' particle size and purge gas residence time on the final product characteristics have not been investigated in the torrefaction literature. It has been found in the current work that torrefaction of ground corn stover at 280 °C induced higher DML than torrefaction of the whole stalk. Whole corn stalk had higher HHV and energy yield values, probably due to the different fiber composition and less energy rich species lost through devolatilization. In general, stalk pith and stalk shell had respectively the highest and the lowest DML, regardless of the torrefaction temperature. Stalk pith and cob shell had the lowest and the highest HHV, respectively. The energy yield of stalk pith was the lowest at both torrefaction temperatures. Furthermore, energy yield of stalk shell was the highest, but not significantly different than cob shell, regardless of temperature. The difference in the behavior of corn stover fractions was the consequence of different physical characteristics and fiber composition. Gas residence time did not have any significant effect on DML, HHV, and energy yield.

This study provides knowledge about the effect of main reactor parameters (temperature, solids and volatiles residence time) and feedstock properties (particle size and initial moisture content) on final product characteristics. Insights on correlation between process and feedstock parameters, and final product characteristics can help optimization of torrefaction process parameters in a way that will favor most desired properties, such as energy density, fixed carbon content, acidity, hemicellulose content, hydrophobicity or

resistance to microbial degradation. According to the results of this study, optimum torrefaction temperature is 250 °C due to modest DML, significant decrease in hemicellulose content without negatively affecting cellulose content, increase in fixed carbon content and decrease in acidity of torrefied biomass. Moisture content of corn stover feedstock should be below 25%wb due to higher DML in at torrefaction temperatures lower than 250 °C.

However, this is not major concern at temperatures higher than 250 °C. Residence time of solids was not statistically significant factor and can be as short as 10 min. Gas residence time did not show any significant effect on DML or chemical properties, and can be as long as 60 sec. Corn stover particle size can be up to 20mm without any negative effect on DML, HHV or energy yield. Different corn stover components have distinct DML, HHV, energy yield and elemental composition after torrefaction. Therefore, grinding to particle size of about 5 mm can cause separation into fractions that yield heterogeneous torrefied product.

In general, the current work can help development and optimization of integrated, highly autonomous and robust thermochemical biomass upgrading systems to support sustainable and economic feedstock transportation, storage, and downstream processing.

Future work

In the recent literature, torrefaction has been recognized as a viable pretreatment option to reduce the cost of transportation, size, and storage of lignocellulosic feedstock. It has been proposed that torrefaction should be optimized to achieve maximum brittleness of biomass [1-3]. However, torrefaction also enhances other biomass properties, such as fixed carbon content, hydrophobicity, acidity, and oxygen-to-carbon ratio that are relevant for co-firing, pyrolysis, and gasification. Optimizing torrefaction for specific end use of torrefied

biomass might deteriorate final product characteristics important for other purposes, as well as process economy, and decrease profit by narrowing market for the end product. For example, process optimized to yield high energy density feedstock suitable for co-fining purpose might not be the best one for producing feedstock for downstream processing in pyrolysis or gasification. Torrefaction process optimized to increase biomass hydrophobicity might not be severe enough to significantly increase biomass brittleness. Therefore, comprehensive torrefaction optimization work should be conducted to select proper operating conditions that would yield feedstock suitable for not only one, but multiple downstream processes. Such feedstock would have the best chemical and physical properties, without sacrificing efficiency and yield of the torrefaction process.

Traditional methods, such as proximate, ultimate, compositional analysis, and calorimetry, have been routinely applied in research to assess chemical changes in torrefied biomass [1-4]. Nevertheless, these methods are slow, time consuming, and sometimes technically demanding. Therefore, rapid methods for process and quality control must be developed and applied in both research and production systems to enable quick adjustments to fluctuations in the torrefaction process parameters, feedstock composition, and final product utilization. Rapid analytical methods for characterization of torrefied and untreated biomass, such as infra-red (IR) spectroscopy, would enable frequent sampling and consequently greater flexibility and agility in process and quality control. Thus far, there has been very limited literature available on the application of IR spectroscopy to torrefied woody biomass [4], but none on herbaceous torrefied biomass characterization.

Additional resources should be directed toward the development of reactor designs that would utilize feedstock with as few pretreatment requirements as possible. This is a

crucial step for justification of the importance of torrefaction for the economy of biorenewables production. Potential for volatiles combustion should be experimentally confirmed. Success of this work would eliminate waste treatment and management issues, and increase overall process efficiency.

References

1. Bergman P. C., Boersma A. R., Zwart R. W. R., Kiel J. H. A. *Combined torrefaction and pelletisation. The TOP process*. ECN-C--05-073, Energy Research Centre of the Netherlands: Petten, NL, 2005.
2. Bridgeman T.G., Jones, I., Williams, P.T., Waldron D.J. An investigation of the grindability of two torrefied energy crops. *Fuel* 2010, 89, 3911-3918.
3. Arias B., Pevida C., Feroso J., Plaza M.G., Rubiera F., Pis J.J Influence of the torrefaction on grindability and reactivity of woody biomass. *Fuel Process. Technol.* 2008, 89, 169-175.
4. Rousset P., Davireux F., Macedo L., Perre P. Characterisation of the torrefaction of beech wood using NIRS: Combined effects of temperature and duration. *Biomass Bioenerg.* 2011, 35, 1219-1226.